Investigating the Mechanisms of Hepatocyte or Biliary Epithelial Cell-Mediated Liver Regeneration

by

Jacquelyn Olivia Russell

B.A., Rutgers University, 2014

Submitted to the Graduate Faculty of

School of Medicine in partial fulfillment

of the requirements for the degree of

Doctor of Philosophy

University of Pittsburgh

2019

UNIVERSITY OF PITTSBURGH

SCHOOL OF MEDICINE

This thesis was presented

by

Jacquelyn Olivia Russell

It was defended on

May 3, 2019

and approved by

Kari Nejak-Bowen, Assistant Professor, Department of Pathology

George Michalopoulos, Professor and Chair, Department of Pathology

Donghun Shin, Associate Professor, Department of Developmental Biology

Alejandro Soto-Gutiérrez, Associate Professor, Department of Pathology

Bryan Brown, Assistant Professor, Department of Bioengineering

Dissertation Director: Satdarshan P. S. Monga, Professor and Vice Chair, Division of Experimental Pathology, Department of Pathology

Investigating the Mechanisms of Hepatocyte or Biliary Epithelial Cell-Mediated Liver Regeneration

Jacquelyn Olivia Russell, PhD

University of Pittsburgh, 2019

The liver performs a wide array of functions such that it is indispensable for survival. Uniquely, the liver is the only human internal organ capable of regeneration. Failure of liver regeneration is thought to induce progression of chronic liver disease (CLD) to cirrhosis and end-stage liver disease, which is currently the 12th leading cause of death in the U.S. The only current treatment for end-stage liver disease is a liver transplant, for which there is a major dearth of donor organs. Therefore, understanding the molecular mechanisms underlying liver regeneration could lead to the development of desperately needed new therapies for liver disease. There are two main epithelial cell types in the liver: hepatocytes and biliary epithelial cells (BECs). Typically, liver regeneration after an acute injury is mediated by proliferation of hepatocytes. This is the case after partial hepatectomy (PHx), where 2/3 of the liver is surgically removed. We identified a role for bromodomain and extraterminal (BET) proteins in driving hepatocyte proliferation after PHx. BET proteins are a family of chromatin readers that interact with the basic transcriptional machinery to promote expression of virtually all genes. One pathway that we found to be especially sensitive to BET protein inhibition post-PHx was the Wnt/β-catenin signaling pathway, which is an important pathway in both liver development and multiple models of liver regeneration. One of these models involves liver regeneration when hepatocyte proliferation is impaired, a model in which BECs are theorized to differentiate into hepatocytes to mediate liver regeneration. We demonstrated that mice which lack liver-specific Wnt/β-catenin signaling (KO mice) exposed to choline-deficient, ethionine-supplemented (CDE) diet-induced liver injury have impaired hepatocyte proliferation.

Furthermore, we utilized genetic lineage tracing of both hepatocytes and BECs to prove that BECs differentiate into hepatocytes in KO mice but not their wild-type counterparts following CDE diet-induced liver injury and recovery. Overall, our work has elucidated important signaling pathways driving liver regeneration in multiple models of liver injury and sets the stage for future work to identify clinically-relevant treatments which can enhance hepatic repair.

Table of Contents

List of Tables

List of Figures

Preface

The road to completing graduate school has been long and bumpy, but I've enjoyed every second of it, and the journey has only reaffirmed my passion for science. I would have never made it this far without the steadfast support of my family and friends. I would like to thank my parents, whose constant support and lifelong encouragement of my curiosity are undoubtedly why I have felt empowered to pursue my dreams. I would like to thank both of my sisters, who have provided me with friendship and emotional support when I needed it most, and who I will now require to address me as "Dr." in all casual conversation as a form of thanks. I also would like to thank all of the friends I have made here at the University of Pittsburgh, who provided me with a life outside of the lab and memories of exploring the city that I will cherish for the rest of my life.

I would especially like to thank all of the members of the Monga lab, who created such a fun and supportive work environment. It's thanks to their help and advice that I have grown as both a person and a scientist. I was always happy to come to work and see my "lab family". I will miss all of you dearly when I leave, but the memories and friendships we've formed will last a lifetime. Thanks to all of the members of the Pathology 4th floor; your humor and company always made coming to work enjoyable. Special thanks to Dr. Monga's office staff; without their help I would have no doubt drowned in paperwork or obliviously missed a crucial deadline. I would like to thank all of the members of my thesis committee for their support in all of my scientific endeavors, as well as thanks to all of the members of the CATER training grant.

Finally, I would like to thank my mentor Dr. Monga. It is thanks to his support and guidance that I have become the scientist I am today. Dr. Monga always fostered my independence and critical thinking and always was enthusiastic and supportive of my ideas. He has facilitated

the growth of my career through traveling to conferences, applying for grants, and writing papers, and I can say conclusively that my success as a graduate student is a direct result of his excellent mentorship. Although my time in his lab has drawn to a close, I know I will continue to look to Dr. Monga for advice and mentorship throughout my career. Thank you for everything.

1.0 Introduction

As an organ that performs a multitude of functions critical to homeostasis, liver health is pertinent and indispensable to survival. Thus, the cellular and molecular machinery driving the hepatic functions is of utmost relevance to human health. Hepatic epithelial cells are composed of hepatocytes, which are the functional units of the liver and perform synthetic, metabolic, detoxification and secretory functions; and biliary epithelial cells (BECs), which line bile ducts and regulate bile composition and secretion. After injury, both hepatocytes and BECs are capable of proliferation to mediate liver regeneration. Many signaling pathways are known to regulate these proliferative responses, and in this dissertation we will demonstrate a key role for bromodomain and extraterminal (BET) proteins as well as Wnt/β-catenin signaling in hepatocyte-driven liver regeneration. We will also discuss secondary mechanisms of liver regeneration that are activated when hepatocyte proliferation fails, namely BEC-to-hepatocyte transdifferentiation. Thus, this dissertation identifies mechanisms of diverse forms of liver regeneration, which may eventually be utilized to develop therapies for CLD patients. Some of the information in this background was published as a review article in Annual Review of Pathology: Mechanisms of Disease, PMID 29125798 (1). A second first-author review article was submitted to Annual Review of Pathology: Mechanisms of Disease and is currently under review. As first author, the publisher Annual Reviews has granted full permission to reuse the manuscripts in this dissertation.

1.1 Bromodomain and Extraterminal Protein Signaling

The bromodomain and extraterminal (BET) protein family is a family of chromatin readers which play major roles in regulating gene transcription. The family consists of four members: Brd2, Brd3, Brd4, and Brdt. The hallmark of the BET protein family are the N-terminal bromodomains, which recognize acetylated lysine residues on the tails of histones and allow BET proteins to interact directly with chromatin (2). BET proteins function to regulate gene transcription by interacting with Mediator, the multi-protein complex which facilitates RNA polymerase II-mediated gene transcription (3). A well-studied BET protein is Brd4, which is a well-known component of the Mediator complex and is thought to act as an interface between transcription factors (TFs) and the RNA polymerase II activation (4, 5). Due to its chromatin interaction modules, Brd4 recruits Mediator to the promoter of the target gene (3) (Fig. 1A). Brd4 also directly interacts with P-TEFb, a heterodimer of cyclin-dependent kinase 9 (6). When RNA polymerase II is recruited to a transcription start site, after initiation it becomes arrested within approximately 60 nucleotides. This is in part due to the inhibitory function of proteins DSIF and NELF, which keep RNA polymerase II in a reversible paused state (7). P-TEFb binds to Brd4 and then can phosphorylate and deactivate DSIF and NELF, leading to productive transcript elongation (6) (Fig. 1B). Thus, BET proteins such as Brd4 are important for both recruitment of the basic transcriptional machinery but also rapid transcriptional induction. In fact, Brd4 has been found to be associated with nearly all active promoters and a large portion of enhancers in the genomes of multiple cell types (3, 8-10).

Several inhibitors have been developed to block the interaction of BET proteins with chromatin. One of these is JQ1, which has a high affinity for the bromodomains of the BET protein family, resulting in displacement of the BET proteins from chromatin and impairing downstream

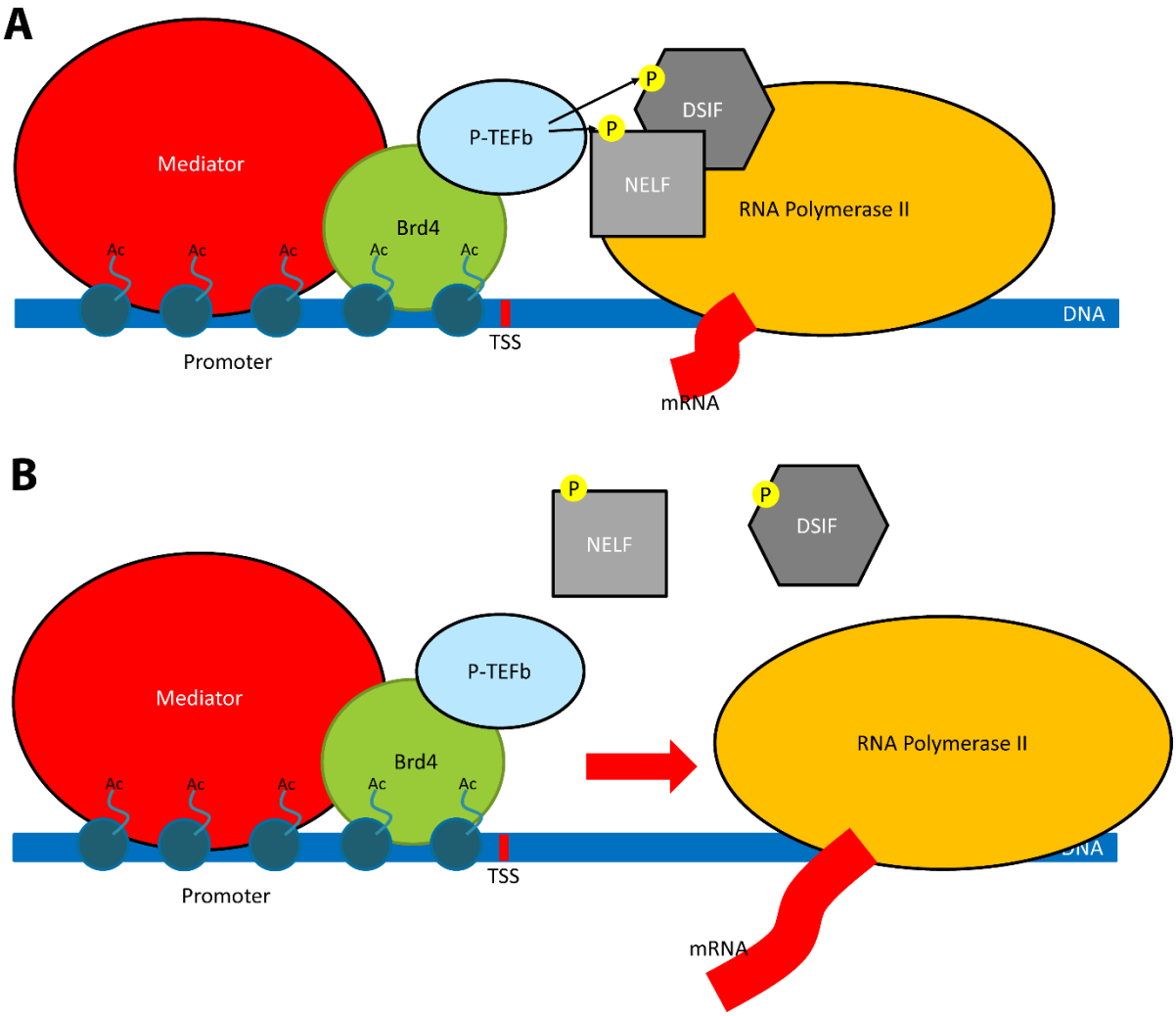

Figure 1: BET protein signaling

(*a*) BET protein Brd4 binds to the acetylated lysine resides (Ac) of histone proteins and recruits both Mediator and P-TEFb to the promoter. RNA polymerase II is arrested within a short distance of the transcription start site (TSS). P-TEFb phosphorylates and deactivates the regulatory proteins NELF and DSIF. (*b*) The inactivation of NELF and DSIF releases RNA Polymerase II, allowing rapid transcript elongation.

transcription (3). This drug was identified as a potential treatment for cancer, as it was found to extend the survival of mice with patient-derived midline carcinoma xenografts as a dose which had little toxicity on non-cancerous tissue (11). It was subsequently found that BET inhibitors had a therapeutic effect in other cancers including multiple myeloma, lymphoma, and acute myeloid leukemia, and this effect was found to be mediated by suppression of proto-oncogenes such as *MYC* and *BCL2* (12-14). It was further described that these genes which were particularly sensitive to BET inhibition had particularly high Brd4 occupancy in their nearby enhancers (3, 12). These enhancers have been termed "super-enhancers", which can extend for tens of kilobases with high Brd4 occupancy throughout (3, 8). In addition to the role of BET proteins in cancer cell survival, there have been some reports on the role of BET proteins in liver pathophysiology. Expression of a shRNA against BRD4 in a hepatocellular carcinoma cell line resulted in reduced proliferation, migration, and invasion (15). Another group found that co-treatment of JQ1 in mice with carbon tetrachloride-induced liver fibrosis reduced hepatic stellate cell activation and overall fibrosis levels (16). We have previously reported that treatment of JQ1 impairs BEC-driven liver regeneration in both zebrafish and mouse models (17). In this dissertation we will further describe the role of BET proteins in hepatocyte-driven liver regeneration.

1.2 The Wnt/β-catenin Signaling Pathway

1.2.1 Canonical Wnt/β-catenin Signaling

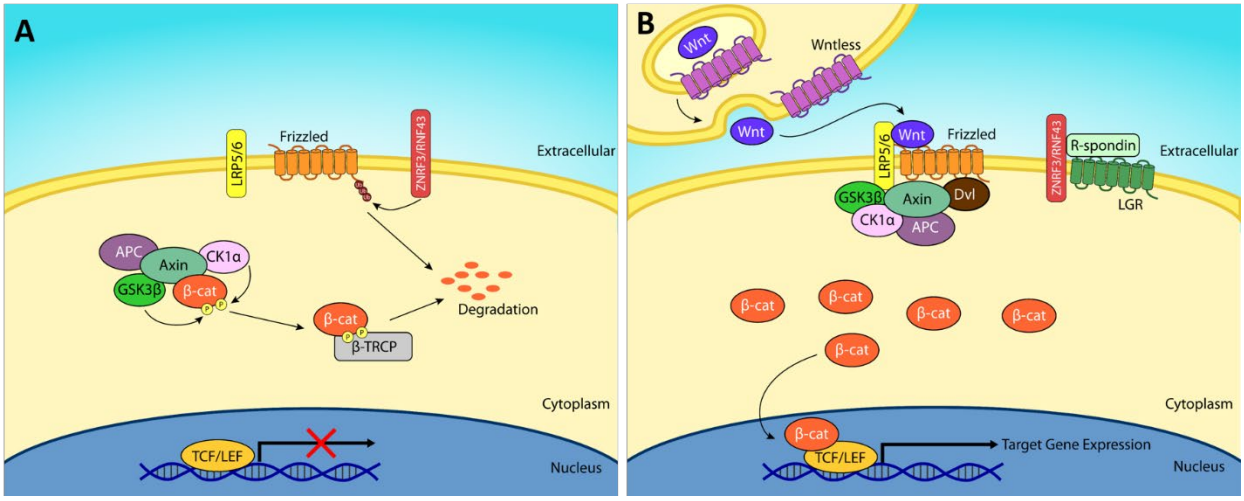

Figure 2: Canonical Wnt/β-catenin Signaling

(*a*) In the absence of Wnt binding to its receptor and co-receptor, β-catenin is phosphorylated by its destruction complex and targeted for proteasomal degradation by β-TRCP. The Frizzled receptor is targeted for proteasomal degradation via the activity of ZNRF3/RNF43. (*b*) Upon release of biologically-active Wnt from a neighboring cell by cargo receptor Wntless, the Wnt protein bind its receptor and co-receptor, which triggers recruitment of the β-catenin destruction complex to the plasma membrane through scaffolding protein Dishevelled. This interaction is further stabilized by R-spondin binding to an LGR receptor. β-catenin cannot be phosphorylated, accumulates in the cytoplasm, and translocates to the nucleus to bind the TCF/LEF family of transcription factor to induce target gene transcription.

When canonical Wnt/β-catenin signaling is inactive, the levels of the major transducer of Wnt signaling, β-catenin, are kept low via its degradation by the destruction complex (Fig. 2A). This complex consists of the proteins Axin, adenomatous polyposis coli (APC), glycogen synthase kinase 3β (GSK3β), and casein kinase 1α (CK1α) (18, 19). The scaffold protein Axin brings together the components of the destruction complex, mediating the phosphorylation of β-catenin first by CK1α at serine 45 and subsequently phosphorylation of serines 33 and 37 and threonine

41 by GSK3β (20, 21). Phosphorylated β-catenin is recognized by β-transducin repeat-containing protein (βTRCP), a component of the E3 ubiquitin ligase complex, which triggers the ubiquitination and subsequent proteasomal degradation of β-catenin (22, 23).

Activation of the Wnt/β-catenin signaling pathway is mediated through Wnt ligands, a family of secreted glycoproteins (Fig. 2B). In order to be bioactive, Wnt ligands must be glycosylated and palmitoylated by the enzyme porcupine (24). This modification occurs in the endoplasmic reticulum, and palmitoylation, the hydrophobic lipid modification, renders Wnts relatively insoluble (25). Secretion of hydrophobic Wnts from the cell requires the cargo receptor Wntless, a multi-pass transmembrane protein which mediates protein trafficking between the Golgi apparatus and cell membrane (26, 27). Once secreted, the Wnt ligand binds to a Frizzled receptor and the co-receptor low-density lipoprotein receptor-related protein (LRP) 5 or 6 to mediate activation of the Wnt/β-catenin signaling pathway (28-31). Wnt binding to Frizzled and LRP5/6 triggers recruitment of the scaffolding protein Dishevelled (Dvl), phosphorylation of LRP5/6, and phosphorylated LRP5/6-mediated recruitment of Axin to the plasma membrane (32, 33). Interestingly, the family of R-spondin secreted proteins enhance Wnt signaling through binding to the leucine-rich repeat-containing G-protein coupled receptor-4 (LGR4) and LGR5 receptors, which in turn increase Wnt-dependent phosphorylation of LRP6 (34, 35). R-spondin ligands also enhance Wnt signaling through the clearance of transmembrane E3 ubiquitin ligases zinc and ring finger 3 (ZNRF3) and its homologue ring finger 43 (RNF43), which ubiquitinate Frizzled and LRP6 and target them for proteasomal degradation (36, 37) (Fig. 2A-B). The recruitment of Axin to the plasma membrane leads to disruption of the destruction complex, promoting stabilization and cytoplasmic accumulation of β-catenin. Non-phosphorylated β-catenin

is translocated to the nucleus where it forms a complex with T cell factor/lymphoid enhancer factor (TCF/LEF) transcription factors to mediate expression of target genes (38).

1.2.2 Non-canonical Wnt Signaling

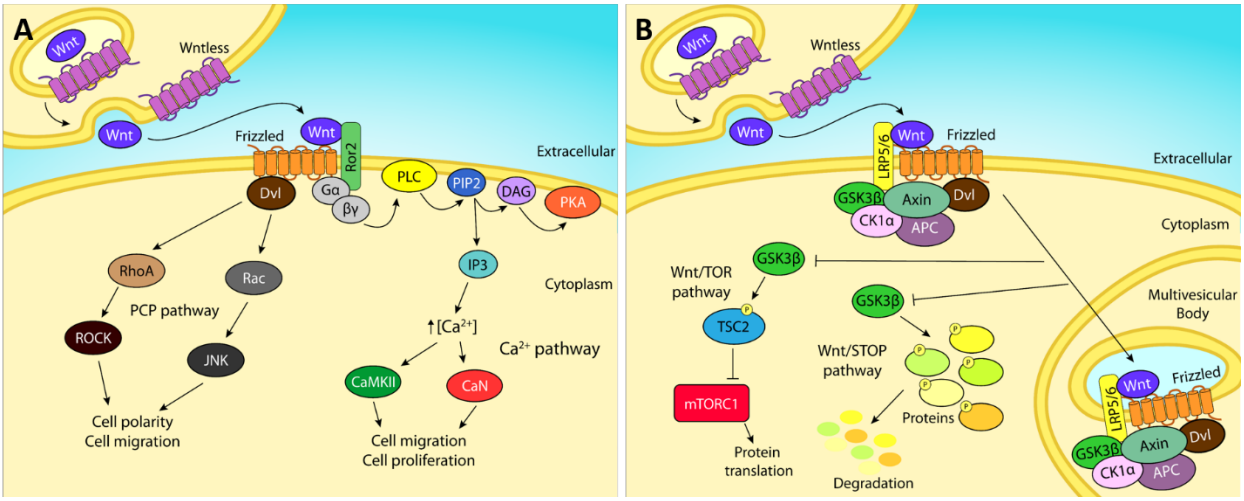

Figure 3: Non-canonical Wnt Signaling

(*a*) In the Planar Cell Polarity (PCP) pathway (left), Wnt ligands bind to a complex consisting of certain Frizzled receptors, Ror2, and Dishevelled, which triggers activation of RhoA and ROCK, or alternatively activation of Rac and JNK signaling, to regulate cell polarity and migration. In the Wnt/calcium pathway (right), Wnt ligands bind to a complex consisting of Frizzled receptors, Dishevelled, and G proteins, leading to the activation of PLC, generation of DAG and IP3. DAG activates PKC while IP3 promotes increased intracellular calcium levels, leading to activation of CaMKII and CaN, which in turn regulate cell migration and proliferation. (*b*) In the Wnt/TOR pathway (left), in the absence of Wnt ligands GSK3β phosphorylates and activates TSC2, which in turn inhibits mTORC1 activity. Binding of the Wnt protein to its receptor and co-receptor leads to sequestration of the destruction complex, including GSK3β, into multivesicular bodies. This prevents activation of TSC2, leading to activation of mTORC1 and promotion of protein translation. In the Wnt/STOP pathway (right), the activity of GSK3β promotes phosphorylation and proteasomal degradation of a multitude of target proteins. Upon Wnt ligand binding and sequestration of GSK3β into multivesicular bodies, these GSK3β-target proteins are no longer targeted for degradation and accumulate in the cytoplasm.

There are 19 Wnts and 10 Frizzled receptors in the mammalian genome (39), and not all of them utilize the same downstream signaling components. Certain Wnt ligands can signal

independently of β-catenin, and this form of signaling is referred to as non-canonical Wnt signaling. Two classic non-canonical Wnt signaling pathways have been described: the Wnt/calcium pathway and the planar cell polarity (PCP) pathway (Fig. 3A).

In the Wnt/calcium pathway, non-canonical Wnt ligands such as Wnt5a bind to Frizzled receptors (Frizzled-2 or Frizzled-7) or with receptor tyrosine kinase-like orphan receptor 2 (Ror2) (40) (Fig. 3A). After Wnt binding, a complex forms between Frizzled, Dishevelled and G proteins, promoting the activation of Phospho Lipase C (PLC), which cleaves phosphatidylinositol 4,5 biphosphate (PIP2) into diacylglycerol (DAG) and inositol 1,4,5-triphosphate (IP3). DAG in turn activates Protein Kinase C (PKC) and IP3 promotes increased intracellular calcium levels. This increase in calcium activates calcium-calmodulin dependent kinase II (CaMKII) and calcineurin (CaN), which in turn regulate cell migration and proliferation (41, 42).

In the PCP pathway, Wnt ligands bind to the Ror2/Frizzled/Dishevelled complex and trigger the activation of Rho-family small GTPases including RhoA and Rac (Fig. 3A). These subsequently activate Rho-associated protein kinase (ROCK) and c-Jun N-terminal kinase (JNK), which regulate cell polarity and migration (41-43). To add further complexity to Wnt signaling pathways, non-canonical Wnt5a can inhibit canonical Wnt/β-catenin signaling by promoting the degradation of β-catenin (44).

More recently, other β-catenin-independent Wnt signaling pathways have been described (Fig. 3B). One of these is the Wnt-dependent stabilization of proteins, known as the Wnt/STOP pathway (45). The central mediator of this pathway is GSK3β, which was found to phosphorylate many additional proteins besides β-catenin and target them for proteasomal degradation (46-49). Wnt binding to its co-receptors can trigger the sequestration of GSK3β in multivesicular bodies, allowing the cytoplasmic accumulation of GSK3β-target proteins (50-52) (Fig. 3B). It was recently

described that Wnt/STOP signaling during mitosis slows protein degradation, stabilizes cell cycle effectors such as c-MYC, and promotes increase in cell size as cells prepare to divide (45). Wnt/STOP signaling is thought to play a role in many cellular processes including cell division, regulation of the cytoskeleton, and DNA remodeling (53).

Another Wnt signaling pathway independent of β-catenin is Wnt-dependent regulation of mechanistic target of rapamycin (mTOR) signaling (Wnt/TOR signaling) (Fig. 3B). In this pathway GSK3β phosphorylates and activates tuberous sclerosis complex 2 (TSC2), which in turns inhibits the function of mTOR complex 1 (mTORC1). The presence of Wnt ligands prevents GSK3β-mediated phosphorylation of TSC2, leading to the activation of the mTORC1 signaling pathway and stimulation of protein translation (54). These studies collectively demonstrate that Wnt ligands are pleiotropic signaling molecules.

1.2.3 β-catenin at Adherens Junctions

In addition to its role in Wnt signaling, β-catenin plays a role in cell-cell adhesion as a component of adherens junctions. Adherens junctions are subapical junctions which promote homotypic cell-cell adhesion in epithelial tissues (55). A class of transmembrane proteins called cadherins perform the extracellular interactions during cell-cell adhesion, and E-cadherin is the prototypical cadherin of adherens junctions. The extracellular domain of E-cadherin forms calcium-dependent complexes with E-cadherin molecules of neighboring cells to mediate homotypic cell-cell adhesion. β-catenin functions in adherens junctions by linking E-cadherin to the actin cytoskeleton through binding to α-catenin, which in turn binds directly to actin and to actin-binding proteins such as vinculin (56). In addition, β-catenin facilitates the assembly of adherens junctions. β-catenin was shown to bind to newly synthesized E-cadherin (57) and

promote delivery of E-cadherin from the endoplasmic reticulum to the basal-lateral plasma membrane (58). Later, it was shown that binding of β-catenin to E-cadherin blocks a peptide sequence which, if exposed, would target E-cadherin for proteasomal degradation (59). However, β-catenin is not permanently incorporated into adherens junctions. Tyrosine phosphorylation of β-catenin at residues Y142, Y654, and Y670 by the activity of hepatocyte growth factor (HGF)/c-met, Y489 by Abl, and Y654 by the epidermal growth factor receptor (EGFR) and Src may induce dissociation of β-catenin from adherens junctions and may activate β-catenin signaling (60-62). β-catenin may also play a role in the development of tight junctions, which serve to prevent bile from the bile canaliculi from mixing with blood in hepatic sinusoids (63). Catenins may participate in the trafficking of tight junctional protein zonula occludens-1 (ZO-1) from the cytosol to the plasma membrane early in tight junction development (64). Additionally, tight junctional protein claudin-2 is a transcriptional target of β-catenin (65), and depletion of claudin-2 in a polarized hepatic cell line resulted in defects in bile canalicular formation (66).

1.2.4 Wnt/β-catenin Signaling in Liver Homeostasis

As hepatocytes are the main parenchymal cell type of the liver, consisting of approximately 80% of liver mass (67), a great deal is known about the role of Wnt/β-catenin signaling in hepatocytes during both homeostasis and liver regeneration. In a baseline liver, hepatocytes display molecular heterogeneity depending on their location within the hepatic lobule (68). A liver lobule is divided into three zones; hepatocytes near a portal triad (which consists of the portal vein, bile ducts, and hepatic artery) are labeled zone 1, hepatocytes surrounding central veins constitute zone 3, and hepatocytes in between constitute zone 2 (69). The process of hepatic zonation begins in the first few weeks after birth (70). This process serves to compartmentalize opposing metabolic

processes, as periportal hepatocytes perform gluconeogenesis, cholesterol biosynthesis, and urea metabolism, while pericentral hepatocytes perform glycolysis, bile acid biosynthesis, and glutamine synthesis (71). Wnt/β-catenin signaling has proven to be a master regulator of liver zonation. Pericentral hepatocytes show active Wnt/β-catenin signaling as demonstrated by pericentral-specific expression of Wnt/β-catenin targets Axin2 (72), glutamine synthetase (GS), and cytochrome P450 enzymes CYP2E1 and CYP1A2 (73, 74). Importantly, mice with liver-specific deletion of both LRP5 and LRP6 (68), as well as mice with hepatocyte-specific deletion of LGR4 and LGR5 (75), lack liver zonation and fail to express the pericentral metabolic genes. Mice with inducible loss of β-catenin in hepatocytes display a periportal phenotype throughout the whole liver (76). In contrast, overactivation of β-catenin specifically in hepatocytes due to conditional APC deletion led to a pericentral phenotype throughout the entire hepatic lobule (77). These results are explained by the finding that HNF4α and β-catenin compete for binding to TCF; HNF4α/TCF dictates periportal gene expression while β-catenin/TCF dictates pericentral gene expression (76). This hypothesis is supported by the finding that HNF4α-deficient livers show a pericentral phenotype (78). Hepatocyte differentiation is also key for metabolic zonation. In mice with liver-specific Yes-associated protein (YAP) deletion, there was an expansion of GS-positive cells in the pericentral domain. Alternatively, mice with liver-specific deletion of macrophage stimulating 1 (Mst1)/Mst2, the kinases responsible for phosphorylation and inactivation of YAP, led to disruption of metabolic zonation, with loss of expression of pericentral genes such as GS. YAP overexpression led to dedifferentiation of hepatocytes, with downregulation of HNF4α target genes and promotion of a stem cell-like phenotype (79). Yap was found to be normally expressed in the periportal domain, suggesting an opposing function to Wnt/β-catenin signaling.

1.2.5 Wnt/β-catenin Signaling in Liver Regeneration and Metabolic Diseases

A notable feature of the liver is that normal cell turnover and liver regeneration following most models of acute liver injury is mediated by proliferation of existing differentiated hepatocytes (80). A well-studied model of liver regeneration is the two-thirds partial hepatectomy (PHx) model, where two-thirds of a rat or mouse liver are removed and within days the remaining lobes enlarge to replace lost liver mass via mostly cellular hyperplasia and some through cellular hypertrophy (81). Wnt/β-catenin signaling is an important driver of liver regeneration in this model; within minutes of PHx in the rat there is a transient 2.5-fold increase in β-catenin protein and rapid translocation to the nucleus (82). This increase in nuclear β-catenin helps to promote hepatocyte proliferation through the expression of target genes such as cell-cycle regulator cyclin D1, which shows increased expressed as early as six hours post-PHx (83) (Fig. 4). Mice with hepatocyte-specific loss of β-catenin display a delay in regeneration following PHx, as there was a two-fold reduction in proliferating hepatocytes at the 40 hour post-PHx time point, which is the peak of hepatocyte proliferation in the wild-type mice. However, there was a subsequent increase in hepatocyte proliferation three days post-PHx, indicating activation of a compensatory signaling pathway (74). Mice lacking both Wnt co-receptors LRP5 and LRP6 in hepatocytes show a similar delay in liver regeneration after PHx (68), as do mice lacking both LGR4 and LGR5 in hepatocytes (75). Interestingly, non-canonical Wnt signaling was shown to be involved in the conclusion of liver regeneration post-PHx. Wnt5a was found to inhibit canonical Wnt/β-catenin signaling in cultured primary hepatocytes, and mice with liver-specific deletion of Wntless displayed continued hepatocyte proliferation for up to 4 days longer than control littermates due to reduced expression of inhibitory Wnt5a between 24-48 hours post-PHx (84) (Fig. 4). This suggests an autocrine

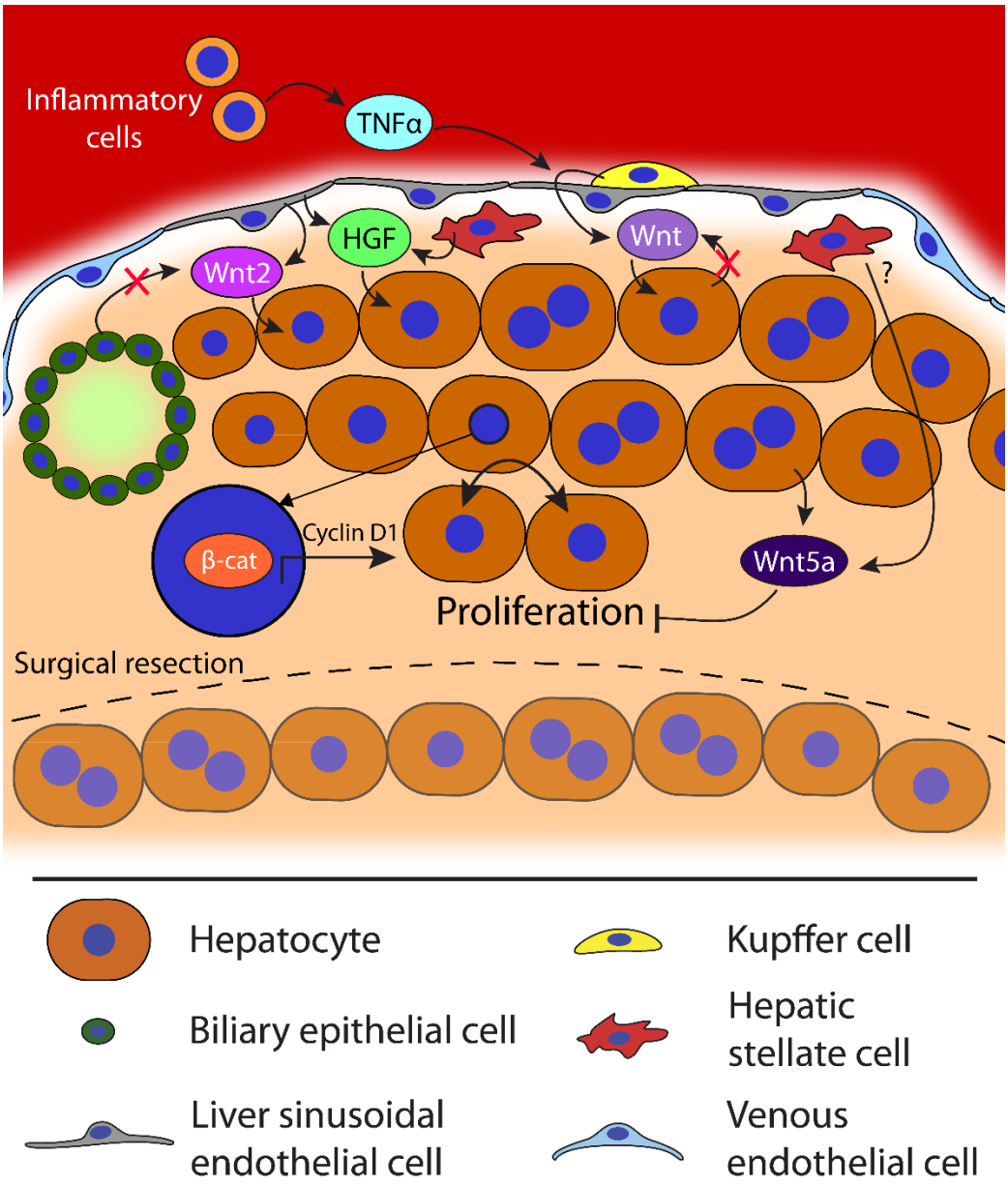

Figure 4: Role of Wnt/β-catenin signaling in liver regeneration following surgical resection

Following surgical resection of liver mass, Wnt/β-catenin signaling is activated to promote liver regeneration. Infiltrating inflammatory cells secrete TNFα and IL-6, which in turn promote Wnt secretion from macrophages. Additionally, liver sinusoidal endothelial cells secrete Wnt2 and HGF, which is also secreted by hepatic stellate cells. Neither biliary epithelial cells nor hepatocytes secrete mitogenic Wnts following surgical resection. The secreted Wnt ligands act on hepatocytes to promote β-catenin translocation to the nucleus, where it promotes expression of target genes such as cyclin D1 to promote hepatocyte proliferation. Following restoration of sufficient liver mass, hepatocytes secrete Wnt5a to inhibit canonical Wnt/β-catenin signaling and promote termination of liver regeneration.

mechanism of proliferation termination following acquisition of required hepatocyte mass during regeneration.

A common cause of acute liver injury in patients is overdose of acetaminophen (APAP) leading to hepatotoxicity (85). In the liver, APAP is metabolized by the enzymes CYP2E1 and CYP1A2 into a reactive metabolite, N-acetyl-p-benzoquinone imine (NAPQI), which covalently binds to cellular macromolecules and induces hepatic necrosis (86). Both CYP2E1 and CYP1A2 are β-catenin target genes, so mice with hepatocyte-specific β-catenin loss are resistant to APAP-induced hepatotoxicity (73). However, β-catenin may also promote liver regeneration following APAP overdose, as liver-specific β-catenin knockout mice given APAP following induction of CYP1A2 and CYP2E1 showed significant defects in hepatocyte proliferation following APAP-induced hepatic necrosis (87).

A role for Wnt/β-catenin signaling has also been implicated in ischemia/reperfusion injury. Under conditions of hypoxia, hypoxia inducible factor-1α (HIF1α) directly competes with TCF4 for binding to β-catenin, leading to enhancement of HIF1α-mediated transcription and the promotion of cell survival (88). Mice with β-catenin-deficient hepatocytes displayed reduced HIF1α signaling and were more susceptible to ischemia/reperfusion injury, while mice with hepatocyte-specific Wnt1-overexpression had enhanced HIF1α signaling and were protected (89).

Deficient Wnt/β-catenin signaling may also exacerbate the development of hepatic steatosis. Loss-of-function point mutations in LRP6 have been identified in humans with early-onset cardiovascular disease, hyperlipidemia, and metabolic syndrome traits (90). Mice with mutant LRP6 develop fatty liver due to increased AKT/mTOR signaling causing elevated hepatocyte lipogenesis, which can be normalized through exogenous Wnt3a treatment (91). Additionally, β-catenin has been found to regulate hepatic mitochondrial homeostasis, as mice

with β-catenin-deficient hepatocytes subjected to acute ethanol intoxication displayed reduced mitochondrial function in addition to impaired Sirtuin 1 (Sirt1)/peroxisome proliferator-activated receptor α (PPARα)-signaling, leading to increased steatosis and oxidative damage (92). The role of Wnt/β-catenin signaling in hepatic metabolism was further expanded by the discovery of the interaction of β-catenin and forkhead box protein O (FOXO) transcription factors. Under conditions of oxidative stress, β-catenin binds directly to FOXO and enhances transcription of FOXO target genes (93). It was also found that β-catenin modulated hepatic insulin signaling, and the association of β-catenin and FOXO1 was promoted in mice under starved conditions. Interestingly, β-catenin and FOXO1 promoted the expression of rate-limiting enzymes in hepatic gluconeogenesis, and the liver-specific deletion of β-catenin in mice fed a high-fat diet displayed increased glucose tolerance due to decreased gluconeogenesis (94). Collectively, these results demonstrate the importance of Wnt/β-catenin signaling in hepatic metabolism and could implicate a role of this pathway in the pathogenesis of conditions such as non-alcoholic fatty liver disease.

Wnt/β-catenin may also play a role in bile acid secretion and homeostasis. Hepatocytes are responsible for the conversion of cholesterol into bile acids, which are secreted into bile canaliculi for eventual transport to the lumen of the small intestine for aid in the digestion of dietary lipids and cholesterol (95). Two of the key enzymes in bile acid biosynthesis, CYP7A1 and CYP27, are expressed in pericentral hepatocytes, suggesting they are regulated by Wnt/β-catenin signaling (96). Mice with liver-specific deletion of β-catenin fed a methionine-choline-deficient diet to induce liver injury displayed significant steatohepatitis, accumulation of hepatic cholesterol and bile acids, and elevated serum bilirubin, suggesting a defect in bile acid export (97). Furthermore, mice with liver-specific deletion of β-catenin displayed dilated and tortuous bile canaliculi and reduced bile flow rates, and feeding these mice a diet supplemented with cholic acid to induce bile

acid-mediated liver toxicity led to the development of intrahepatic cholestasis and fibrosis (65). These results suggest aberrant Wnt/β-catenin signaling may play a role in the development of cholestatic liver disease.

1.3 The Ductular Reaction and BEC-to-Hepatocyte Differentiation

Adult mammals possess very limited organ repair capabilities, unlike lower vertebrates including fish or amphibians (98, 99). During post-natal development, they lose most of their competence for regeneration, except for minimal levels of maintenance during tissue homeostasis (98, 100, 101). In general, mammalian organs produce non-functional connective tissues after injury instead of functional restoration of lost parenchyma (102, 103). While acute and chronic deposition of scar tissue is a protective response to reduce organ damage caused by additional insults, it results in a progressive loss of function that underlies a majority of chronic diseases, particularly in aging populations (99, 103). However, the mammalian liver is a unique organ which maintains the ability to regenerate tissue into adulthood at comparable levels to the regenerative capacity of fetal liver and the livers of lower vertebrates. The liver can restore lost functional parenchyma after various hepatic injuries, including restoration of hepatic mass after surgical removal (104, 105). This extraordinary regenerative capacity is mainly based on the self-replication ability of the two main epithelial cell types: hepatocytes and biliary epithelial cell (BECs, also known as cholangiocytes) (104, 105). These two cell populations exit quiescence and replicate to compensate for lost functional parenchyma in response to acute/chronic injuries.

However, regenerative mechanisms following acute liver injury (such as surgical removal of liver tissue or damage from hepatotoxic drug overdoses) exhibit distinct phenotypic differences

from liver regeneration in the setting of chronic liver disease (CLD). Within a healthy liver, BECs are usually confined to the interlobular bile ducts which form the biliary tree, a complex network of tubules which function to collect hepatocyte-derived bile and eventually transport it to the common bile duct, which drains into the duodenum (106). Hepatocytes secrete bile into the bile canaliculi, which connect with the smallest proximal ductules at the ductular-hepatocellular junctions known as the canals of Hering (106, 107). The bile ducts are located anatomically near the portal vein and hepatic artery in a structure known as the "portal triad", which is separated by linear chords of hepatocytes from the central vein (106) (Fig. 5A, B). However, during many types of liver injury there is expansion of cells which express BEC markers, known as reactive BECs, from the periportal region into the surrounding parenchyma. This phenomena is termed the ductular reaction (DR), defined as "a reaction of ductular phenotype, possibly but not necessarily of ductular origin" (107). This definition affords flexibility to the cell-of-origin of the DR, as there is evidence that cells besides BECs can give rise to cells of the DR, which will be discussed further later in this review. The DR is considered by some to be activation and expansion of liver progenitor cells (LPCs), also known as oval cells in rodents, which are bipotent cells capable of giving rise to hepatocytes or BECs (105). Another theory is there is no progenitor cell population in the liver, but in the context of liver injury hepatocytes and BECs can function as facultative stem cells, and the DR is evidence of this cellular plasticity (104). The DR is a complex process which has different phenotypes in different injury conditions, but in general is associated with infiltration of inflammatory cells, activation of myofibroblasts, and matrix deposition (108). Despite the prevalence of DR after liver injury, the origin, fate and exact roles of LPCs in the diseased liver are heavily debated and remain largely elusive.

Currently, liver transplantation is the only reliable treatment to prolong the lives of patients with advanced liver diseases. However, the number of donor livers is not sufficient to match increasing demand (109). Therefore, alternative therapeutic options are desperately needed. Given the prevalence of DR in human diseased liver and recent findings which suggest LPCs could be a reliable source for new hepatocytes in diseased liver, promoting the differentiation of activated LPCs into parenchymal liver cells has recently garnered attention as a powerful potential therapeutic option for patients with advanced liver diseases. However, the pathophysiologic and molecular mechanisms underlying DR and subsequent LPC differentiation still remain largely unknown. In this dissertation, we utilize the choline-deficient, ethionine-supplemented (CDE) diet as a model of chronic liver injury, and we demonstrated that lack of Wnt/β-catenin signaling in hepatocytes impairs hepatocyte proliferation after CDE diet-induced liver injury and promotes BECs to differentiate into hepatocytes.

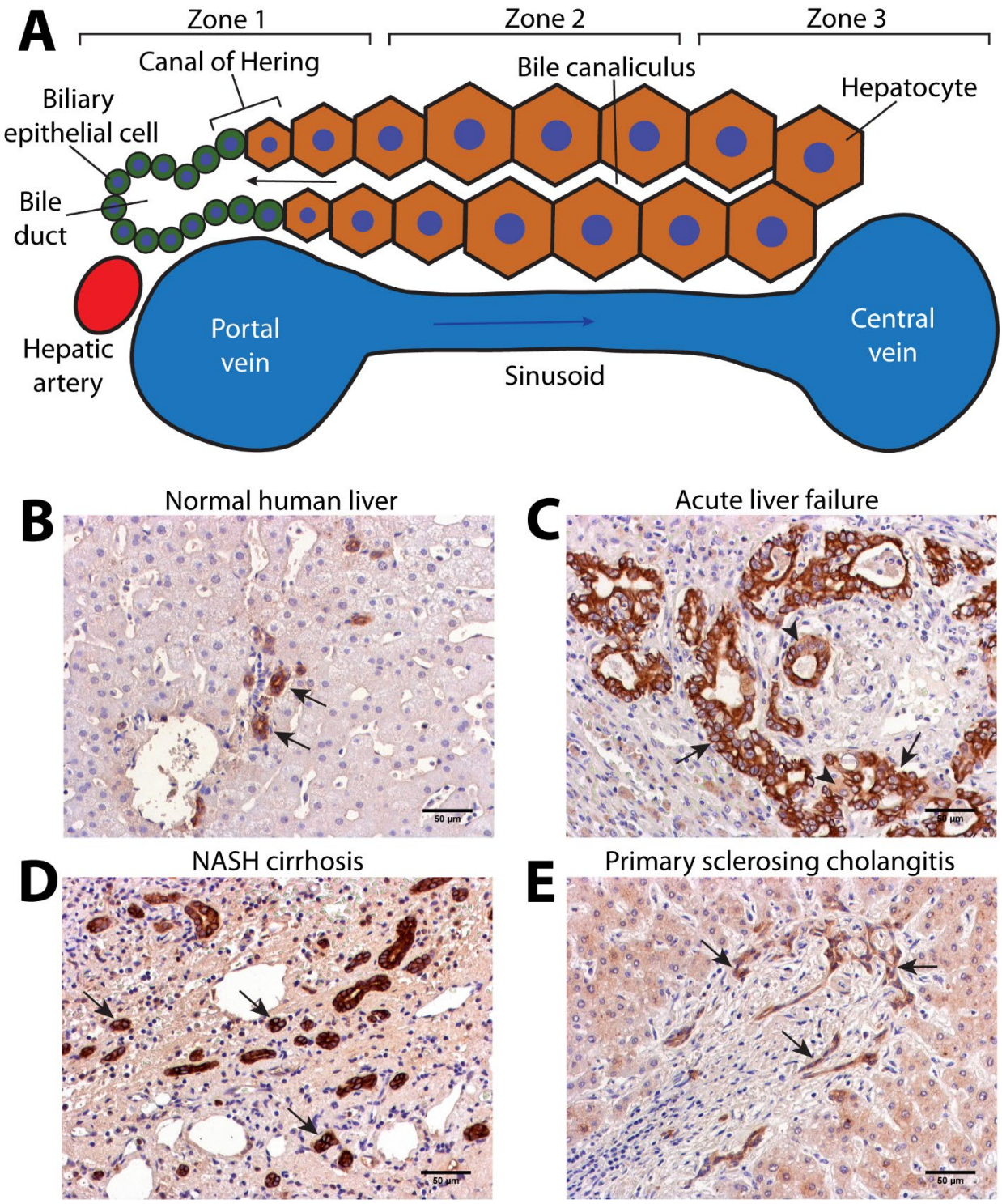

Figure 5: Normal and diseased liver architecture.

(*a*) The structure of a liver lobule, which consists of three zones. Zone 1 consists of the portal vein, bile ducts, and hepatic artery, which together form the "portal triad". Oxygenated blood from the hepatic artery mixes with blood from the portal vein and flows through the hepatic sinusoids towards the central vein, which constitutes zone 3. Chords of hepatocytes form the bile canaliculi,

which transport hepatocyte-derived bile in the opposite direction of blood flow to the bile ducts. The interface between the end of the bile canaliculus and the start of the bile duct is known as the Canal of Hering. (*b*) Normal human liver stained with a pan-cytokeratin (panCK) antibody. The arrows denote bile ducts, structures with obvious lumina lined by panCK-positive cells. Scale bar: 50 μm. (*c*) Liver from an acute liver failure patient stained with a panCK antibody. A ductular reaction (DR) is evidenced by a large increase in the number of panCK-positive cells (arrows). Intermediate hepatocytes, or cells which are panCK-positive but exhibit hepatocyte morphology (arrowheads), can be observed adjacent to cells of the DR. Scale bar: 50 μm. (*d*) Liver from a patient with nonalcoholic steatohepatitis (NASH)-induced cirrhosis stained with a panCK antibody. A DR is evident in the increase in the number of panCK-positive cells, which form bile duct-like structures without obvious lumina (arrows). Scale bar: 50 μm. (*e*) Liver from a patient with primary sclerosing cholangitis stained with a panCK antibody. A DR is evident by the increase in the number of panCK-positive cells (arrows), which have a distinctly different morphology from normal bile ducts. Scale bar: 50 μm.

1.4 Overview of the Ductular Reaction

1.4.1 Ductular Reaction in Human Liver Disease

The activation of the DR is thought to be triggered by impairment of the regenerative capacity of the differentiated epithelial cells of the liver during liver injury. In support of this theory, analysis of patients diagnosed with acute liver failure or severe liver impairment which exhibited severe loss (>50%) of hepatocytes in combination with impaired proliferation of remaining hepatocytes developed a robust ductular reaction (Fig. 5C). This study also tracked the appearance of intermediate hepatocytes (those which express BEC markers CK7 or CK19) and concluded that LPCs appear early but need approximately one week's time to differentiate to hepatocytes (110). In line with this theory, spontaneous recovery of patients with massive hepatic necrosis, a condition where nearly all parenchymal cells are acutely lost, is theorized to be due to LPC-mediated liver regeneration (reviewed in (111)). There is also evidence of LPC-derived hepatocytes in human cirrhosis patients with parenchyma extinction (112). However, even in the

setting of acute liver failure, the degree of the DR is positively correlated with liver stiffness and hepatic stellate cell (HSC) activation (111, 113), demonstrating the intricate relationship between the cells of the DR and the non-parenchymal cells of the liver (reviewed in (114)).

In chronic liver injury, the degree of the DR positively correlates with disease severity in a wide range of pathological settings (111, 115-118). Indeed, in chronic hepatitis C virus (HCV) infection, advanced fibrosis stage was associated with higher numbers of activated HSCs and LPCs in both adult (119) and pediatric patients (120). In patients with nonalcoholic steatohepatitis (NASH), the degree of the DR was strongly correlated with the degree of portal inflammation, hepatocyte replicative arrest, and fibrosis stage (Fig. 5D) (121). There were similar findings in non-alcoholic fatty liver disease (NAFLD), where the portal inflammatory infiltrate was dominated by CD68+ macrophages and CD8+ lymphocytes (122). Furthermore, in patients with NASH, expansion of the DR reaction into the centrilobular region was correlated with fibrosis stage and fibrosis progression (123). In a study of pediatric NASH patients, the degree of pro-inflammatory macrophage polarization was correlated with disease severity, DR, and portal fibrosis (124).

Although DR is observed in almost all forms of severe and chronic liver injury, there are thought to be disease-specific phenotypic differences. The cells of the DR can differ in morphology, ranging from organized ductules with clear lumina to more disorganized strings of cells with no visible lumina, and the morphology varies depending on the etiology of the liver injury (reviewed in (116)). A recent study characterized the DR in the cholangiopathies primary sclerosing cholangitis (PSC) and primary biliary cholangitis (PBC) and found that while the DR was a prognostic marker in both conditions (Fig. 5E), DR phenotype and activation of signaling pathways differed between PSC and PBC (125). Another study used laser capture microdissection

to isolate cells of the DR from HCV or PSC patients, and high throughput RNA sequencing revealed numerous differences, including a neo-angiogenesis signature in HCV in contrast to a profile of oxidative stress-related and pro-inflammatory gene expression in PSC (126).

There is evidence that LPCs themselves can secrete proinflammatory and profibrogenic cytokines (127). In alcoholic hepatitis, the expansion of the DR correlates with disease progression, and cells of the DR were found to express chemokines and inflammatory mediators promoting neutrophil infiltration in the periportal area (128). A recent study found that activation of non-canonical NF-κB signaling via RELB in BECs was important for BEC proliferation during the DR in a variety of pathologies including PSC, PBC, NASH, autoimmune hepatitis, viral hepatitis, and alcoholic liver disease. In early-stage PBC and PSC, the expression of the cytokine lymphotoxin beta increased in BECs and induced RELB activation, and a corresponding mouse model found that deletion of RELB reduced inflammatory cell infiltration and expression of inflammatory cytokines (129), providing further evidence that cells of the DR can promote inflammation.

A subset of patients with chronic liver disease will go on to develop liver cancer, such as hepatocellular carcinoma (HCC), and chronic inflammation is known to be a driver of hepatic carcinogenesis (130). There's a long-standing debate on the role of LPCs in hepatic tumorigenesis (131). LPCs are thought to be a potential source of HCC, due to the strong association of the DR and progression of chronic liver disease and the fact that up to 50% of human HCC express markers of BECs. Additionally, in humans approximately 55% of small cell dysplastic foci are composed of LPCs and intermediate hepatocytes (132). Furthermore, a proliferating peritumoral DR was found to be a strongly correlated with inflammation and fibrosis, and was an independent prognostic factor for disease-free survival after surgical resection of HCC (133, 134). A

proliferating peritumoral DR was also found to be correlated with overall survival and disease-free survival post-hepatectomy in patients with combined hepatocellular-cholangiocarcinoma (135). These data underscore the clear clinical significance of the DR in liver disease, providing the impetus to study the role of the DR in liver disease and tumorigenesis in a variety of animal models.

1.4.2 Evidence for Hepatic Stem Cells in Fetal and Adult Liver

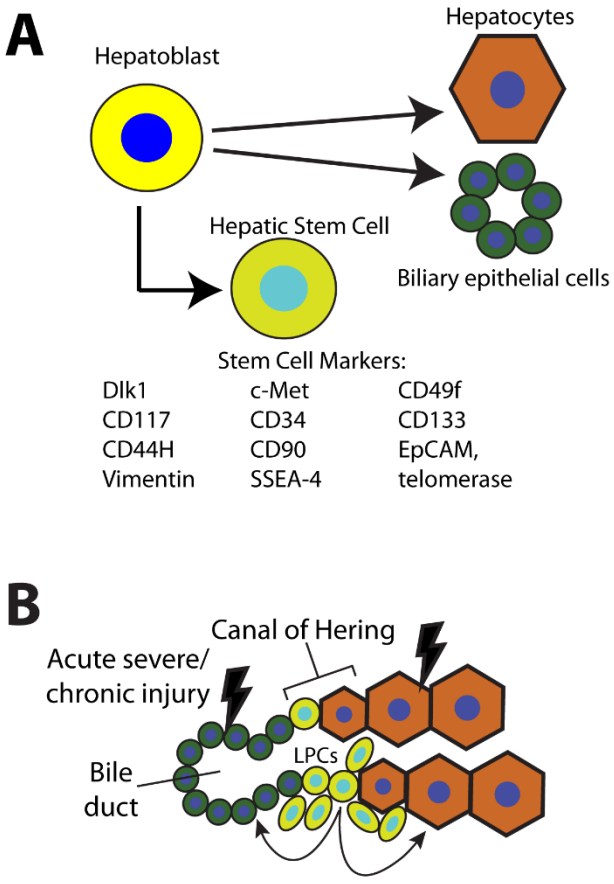

Figure 6: The liver progenitor cell theory.

(*a*) During fetal liver development, hepatoblasts give rise to the two primary epithelial cell types of the mature liver: hepatocytes and biliary epithelial cells. Studies have identified potential markers of hepatoblasts with pluripotent stem cell characteristics, listed above. (*b*) It is theorized that quiescent liver progenitor cells (LPCs), potentially residing the Canal of Hering, are activated in the context of severe acute injury or chronic liver injury. These LPCs proliferate and are capable of giving rise to both hepatocytes and cholangiocytes, thus contributing to liver repair.

While the idea of a LPC population in the liver remains an intensely controversial topic, the concept of LPCs has roots in liver development. The liver originates from the foregut endoderm, and during hepatic specification there is formation of the liver bud which is composed of hepatoblasts, embryonic cells which give rise to both hepatocytes and BECs (for a full review of liver development see references (67, 136)). Within the hepatoblasts, several groups have reported the existence of a subset of cells with stem cell-like properties, termed hepatic stem cells (HpSCs) (Fig. 6A) (67). Cells expressing c-Met and CD49f and negative for c-Kit, CD45, and TER119 isolated from E13.5 fetal mouse liver were found to self-renew in culture and give rise to hepatocytes and BECs, and found to be multipotent by their capability to differentiate into pancreatic ductal and acinar cells or intestinal epithelial cells during *in vivo* transplantation experiments (137). Another group identified that the Dlk-positive cell fraction isolated from E14.5 fetal mouse liver contained cells that were highly proliferative, could differentiate into BECs and hepatocytes *in vitro*, and gave rise to hepatocytes when transplanted intrasplenically *in vivo* (138). In human fetal liver samples, CD117+/CD34+/CD90- cells were found to express both hepatic and biliary markers *in vitro* (139). Other groups identified cells that express markers such as CD133, cytokeratins 8, 18, and 19, CD44H, telomerase, claudin 3, with weak expression of albumin (140); additional markers include CD34, CD90, c-kit, EpCAM, c-met, vimentin, and SSEA-4, and these cells have displayed over 100 population doublings in culture and the ability to differentiate into fat, bone, cartilage, and endothelial cells (141). When AFP+/CK19+/albumin+ HpSCs were isolated from E14 rat livers and transplanted into rats subjected to two-thirds 70% partial hepatectomy, they transdifferentiated into both hepatocytes and BECs and represented 23.5% of total liver mass after 6 months, suggesting continuous proliferation of the donor cells over the

duration of the experiment (142). However, the question remains whether HpSCs are confined to fetal liver development or persist into adulthood.

A potential location for HpSCs in the adult liver is in the canals of Hering (Fig. 6B). Examination of human postnatal liver samples have revealed that "hybrid" cells in the canal of Hering which express HpSC markers (140, 143, 144), such as BECs which weakly express Hnf4α and hepatocytes which weakly express Hnf1β (145). In normal adult mice, a small fraction of cells expressing markers such as EpCAM, CD133, CD13, and SOX9 have been isolated and reported as adult LPCs (146-148), although the efficiency of these cells to form colonies and differentiate into hepatocytes *in vitro* was reduced with age (149). In line with these results, single-cell isolated SOX9-positive ductal progenitors formed self-renewing organoids in culture (150). More recently, ST14 was identified as a marker of clonogenic cholangiocytes which could give rise to organoids that could be serially passaged, although it was not determined if these ST14-positive BECs were localized to the canals of Hering (151). Studies using sub-lethal acetaminophen overdose have demonstrated through BrdU administration that the cells in the canals of Hering are label-retaining cells, a property characteristic of stem cell niches (152, 153). Additionally, cells in the canals of Hering have been shown to be regulated by Hedgehog signaling, similar to the progenitor compartments of other organs such as skin, bone marrow, and intestine (154). A laminin-containing basement membrane is present in the canals of Hering (153, 155), and laminin has been shown to be important for the proliferation and maintenance of LPCs in culture (156), and laminin surrounds LPCs during liver injury *in vivo* (157, 158). Additionally, morphological studies after severe liver injury in mice indicated that LPCs were derived from the canals of Hering (159). Taken together, these data suggest there may be a population of LPCs in the adult liver, although

their function in liver regeneration has been more clearly elucidated in models of liver injury as opposed to studies of homeostatic adult liver.

1.4.3 Evidence for Liver Progenitor Cells and BEC-to-Hepatocyte Differentiation in Rodent Models

1.4.3.1 Original Description of Oval Cells in Rats

The first description of what came to be known as putative adult LPCs after hepatic injury was a study of liver injury in rats published in the 1950s. In a study cataloguing the histological changes following administration of chemical carcinogens in rats, Dr. Emmanuel Farber noted that a very early change was the proliferation of "oval cells", which first appeared in the periportal area and over time expanded throughout the entire liver lobule, a phenomenon also described as a ductular reaction. These cells were presumed to be of BEC origin (160). It was noted that expansion of these cells preceded liver regeneration and it was speculated that oval cells were giving rise to a subset of hepatocytes in hyperplastic liver nodules. It was further found that oval cells expressed fetal liver markers such as α-fetoprotein (AFP) (161). Studies of azo dye carcinogenesis similarly reported transitioning of oval cells into hepatocytes (162, 163), and it was suggested that oval cells may function to provide new hepatocytes during prolonged severe liver injury. However, the origin and fate of oval cells was intensely controversial (105). Other groups performed cell labeling experiments with tritiated thymidine in multiple models of liver injury including chemical carcinogenesis, bile duct ligation, and partial hepatectomy in combination with carbon tetrachloride administration and argued that oval cells did not give rise to hepatocytes and instead underwent removal by cell death (164-166).

The study of oval cells was furthered by the development of new rodent models, including the Solt-Farber model of hepatocarcinogenesis, in which rats were injected with 2-acetylaminofluorene (2-AAF) to block hepatocyte proliferation and then subjected to partial hepatectomy (PHx), which led to a massive expansion of oval cells (167). Administration of the biliary toxin methylene dianiline (DAPM) prior to the 2-AAF/PHx protocol blocked the expansion of oval cells and prevented the expression of AFP, providing further evidence that oval cells were derived from cholangiocytes (168). Pulse-chase labeling of specifically oval cells with tritiated thymidine (169, 170) and careful immunohistochemical analysis (171) in the 2-AAF/PHx model demonstrated the conversion of oval cells into hepatocytes, leading to the hypothesis that oval cells only give rise to hepatocytes when hepatocyte proliferation is impaired in the context of liver injury, which is remains a popular hypothesis for the condition of LPC-to-hepatocyte differentiation to this day.

1.4.3.2 The Choline-Deficient, Ethionine-Supplemented Diet Model

Another model used to study oval cells in rats involved the combination of the hepatocarcinogen ethionine with choline deficiency. Prolonged choline deficiency was known to induce liver tumors in rats (172, 173). Ethionine is an analog of methionine and is extremely toxic to cells, causing incorporation of ethionine into proteins, reduced protein translation, inhibition of DNA replication (174), and prolonged administration of ethionine promotes development of liver tumors in rats (160). Administration of a choline-deficient, ethionine-supplemented (CDE) diet in rats acutely led to immune infiltration, cell necrosis, fat accumulation, and massive oval cell proliferation (175). The CDE diet model has since been adapted for use in mice, where it also gives rise to steatohepatitis and oval cell expansion (176). The efficiency and speed of the CDE diet in promoting expansion of putative LPCs has made it a widely used model in this field. Sophisticated

quantitative liver intravital microscopy revealed compromised blood-bile barrier in mice fed CDE diet for four days, which was accompanied by disruption of tight junctions and increase in liver injury (177). Deposition of matrix around the portal tract occurs as early as after three days of CDE diet and increases over the course of injury, but expansion of the DR begins around day seven of CDE diet-induced liver injury and continues to increase over time (158, 178).

It has been theorized that hepatic injury-mediated inflammatory signaling is required for the initiation of the DR. Previously it was shown that a Th1-mediated cellular immune response is necessary for DR by demonstrating impaired LPC activation in CDE diet-fed immunocompromised mice by genetic deletion of key genes for T-cell-mediated immune response, such as CD3, Rag2 and IFNr (179, 180). More recently, it was reported that bone marrow cell transplantation or recombinant TWEAK (TNF-like weak inducer of apoptosis) injection is sufficient to induce DR in healthy mice without additional hepatic injury (181). This result may suggest that hepatic damage-induced macrophage infiltration and secretion of TWEAK is critical for triggering DR. However, it must be noted that there is no DR following 2/3 PHx, which also induces TWEAK/Fn14 (receptor for Tweak)-mediated innate immune responses (182). Therefore, it would be interesting to investigate the immunologic profiles at early stage of the livers with or without DR.

Although it has long been speculated that oval cells give rise to hepatocytes in the CDE diet injury model, the advent of lineage tracing technology in mice has allowed researchers to directly test this hypothesis. First it was shown that the cells of the DR observed after CDE diet feeding are of BEC origin; one group labeled ductal plate cells (an embryonic structure consisting of a single-layered sleeve of Sox9-positive cells around the periportal mesenchyme which gives rise to cholangiocytes and periportal hepatocytes) with yellow fluorescent protein (YFP) via *Sox9-*

Cre^{ERT} and found that after CDE diet administration the CK19-positive oval cells also expressed YFP, indicating ductal plate origin (183). Other lineage tracing systems to label BEC-derived oval cells in CDE diet-fed mice include *Osteopontin* (*OPN*)-*Cre*^{ERT} (155), *Foxl1-Cre* (184), *Hnf1β-Cre*^{ERT} (185), and *Krt19-Cre*^{ERT} (186-188). While these BECs do not contribute to hepatocytes during homeostasis or during toxic or surgical loss of liver mass (150, 155, 186), several groups have demonstrated that LPCs give rise to hepatocytes after CDE diet-induced liver injury followed by a recovery period on normal chow, with numbers of LPC-derived hepatocytes ranging from 1.86% (185), 2.45% (155), to 29% in one study where analysis was limited to mice that lost more than 14% of their initial body weight upon exposure to CDE diet (184). However, other groups performing lineage tracing in the CDE diet model have found that BECs do not significantly contribute to hepatocytes. One studying utilizing *Sox9-Cre*^{ERT} to label BECs found no BEC-derived hepatocytes after CDE diet and recovery (150). Another group utilized *Krt19-Cre*^{ERT} to label BECs and failed to detect BEC-derived hepatocytes after CDE diet and recovery (186). Several groups have utilized adeno-associated virus serotype 8 (AAV8), a virus which preferentially infects hepatocytes (189), to deliver Cre recombinase driven by a hepatocyte-specific promoter. With this technique, greater than 99% of hepatocytes can be genetically labeled (186, 188-190). In these hepatocyte lineage tracing studies, several groups found no contribution of BECs to hepatocytes during CDE diet and recovery (186, 190).

However, a potential explanation for the very few to no BEC-derived hepatocytes after CDE diet-induced liver injury in mice is due to the fact that hepatocyte proliferation is not impaired during CDE diet (150, 188, 190). One group utilized the *AhCre* system to conditionally delete the E3 ubiquitin ligase *Mdm2* in up to 98% of hepatocytes, leading to overexpression of p21, hepatocyte senescence, hepatocyte injury, and widespread DR. LPCs isolated from CDE diet-fed

mice were transfected with a GFP plasmid and transplanted into *Mdm2* hepatocyte-null mice, and after three months GFP-positive hepatocytes and BECs represented approximately 15% of liver tissue, suggesting LPC-to-hepatocyte differentiation (191). In a follow-up study, *Krt19-Cre*^{ERT} was utilized to label BECs, and animals were injected with AAV8-p21 to overexpress p21 in hepatocytes followed by CDE diet and recovery, which resulted in approximately 15.3% of hepatocytes being derived from BECs. In the same study, the authors used AAV8-thyroid binding globulin (TBG)-Cre in order to delete β1 integrin specifically in hepatocytes, which were simultaneously labeled with the marker tdTomato. These animals were given methionine, choline-deficient (MCD) diet to induce liver injury followed by a recovery normal diet, where 20-30% of hepatocytes were found to be tdTomato-negative, indicating they did not originate from a pre-existing hepatocyte. These results were confirmed in *Krt19-Cre*^{ERT} mice with tdTomato-labeled BECs given RNAi against *Itgb1* (β1 integrin) and subjected to MCD diet followed by recovery, where tdTomato-positive hepatocytes were observed (187). In a recent study from our group, mice with hepatocyte-specific EYFP-labeling and simultaneous deletion of β-catenin via AAV8-TBG-Cre subjected to CDE diet displayed a profound impairment of hepatocyte proliferation. Following recovery on normal diet for two weeks, there was expansion of β-catenin-positive, EYFP-negative hepatocytes, accounting for approximately 20% of periportal hepatocytes. Interestingly, between three and seven days of recovery on normal diet after CDE diet, very small β-catenin-positive hepatocytes were observed, along with β-catenin+/CK19+/Hnf4α+ cells, suggesting BECs in the process of differentiating into hepatocytes (Fig. 7B). Positive lineage tracing via *Krt19-Cre*^{ERT} mice with tdTomato-labeled BECs injected with *Ctnnb1* RNAi and placed on CDE diet followed by recovery resulted in tdTomato-positive hepatocytes, confirming that BECs were giving rise to

hepatocytes in this model (188). All together, these results suggest that when hepatocyte proliferation is impaired in the CDE diet model, BECs/LPCs give rise to hepatocytes.

1.4.3.3 The DDC Diet Model

Another model that has been used to study potential BEC-to-hepatocyte differentiation is the 3,5-diethoxycarbonyl-1,4-dihydrocollidine (DDC) diet model, which causes porphyrin pigment plugs in the biliary tract, leading to bile duct obstruction, DR, cholangitis, and periportal fibrosis (192). A notable feature of the DDC diet in addition to the robust proliferation of hepatocytes and BECs is the appearance of biphenotypic hepatocytes which express Hnf4α and biliary marker A6 (193). However, much like work in the CDE diet, different groups have reported conflicting conclusions regarding LPC-to-hepatocyte differentiation. Groups utilizing *Krt19-Cre^{ERT}* mice (186) or *Sox9-Cre^{ERT}* mice (150) with labeled BECs found no BEC-derived hepatocytes after four weeks of DDC diet-induced liver injury (150) or 2-3 weeks of DDC diet followed by recovery on normal diet (186). However, when hepatocyte proliferation was impaired through hepatocyte-specific β1 integrin deletion or p21 overexpression and animals were subjected to DDC diet and recovery, significant numbers of BEC-derived hepatocytes were observed (187). One group lineage traced Lgr5+ cells, and found that while Lgr5 was not readily detectable in normal liver, treatment with DDC diet led to labeling of both BECs and hepatocytes. When single Lgr5+ cells were isolated, they could be cultured into self-renewing organoids expressing markers of both BECs and hepatocytes. These organoids could differentiate to hepatocytes when transplanted *in vivo*, suggesting these Lgr5+ cells marked damage-induced LPCs (194). Excitingly, a recent study theorized prolonged exposure to severe liver injury, as is the case for human patients, would lead to BEC-derived hepatocytes in wild-type animals. To this end, they subjected *Krt19-Cre^{ERT}* mice with labeled BECs to DDC diet for 24 weeks, and observed approximately 9.1% of

hepatocytes were BEC-derived (195). This work has important implications because of the appearance of BEC-derived hepatocytes in the absence of genetic manipulation.

It has also been reported that epigenetic chromatin remodeling plays important roles in LPC activation in models such as the DDC diet. Polycomb repressive complexes (PRCs) have been reported as crucial regulators of proliferation of hepatoblasts (196, 197) and LPCs (198) via repressing Bim1 expression (196). Jalan-Sankrikar et al. suggested hedgehog signaling as an upstream regulator of EZH2/PRC during proliferation of LPCs in DDC-fed mice (198). Recently, it was reported that chromatin readers, bromodomain and extraterminal (BET) proteins, regulate LPC activation in a Myca-dependent manner using both zebrafish and mouse systems (17). Altogether, these results may suggest that chromatin modification is necessary for transition of a quiescent LPC into active status for further expansion. However, distinct roles for chromatin remodeling in reprogramming/dedifferentiation of parenchymal cell and LPCs during regeneration remains to be further investigated.

1.4.3.4 The Thioacetamide Liver Injury Model

Another model that has been used to study BEC-to-hepatocyte differentiation is the thioacetamide (TAA)-induced liver injury model. TAA is metabolized into a toxic metabolite in hepatocytes and induces centrilobular hepatic necrosis (199). Chronic administration of TAA in drinking water leads to the development of cirrhosis (200). A recent study utilized AAV8-*TBG-Cre* to label hepatocytes with tdTomato and simultaneously delete β1 integrin specifically in hepatocytes, and when these mice were exposed to TAA for three weeks followed by a recovery period on normal diet, 20-30% of hepatocytes were tdTomato negative (187). A more recent study subjected *Krt19-Cre*^{ERT} mice with labeled BECs to TAA treatment for 24 weeks, and found around 10% of hepatocytes were BEC-derived. Excitingly, the authors of this study identified bi-

phenotypic cells with BEC-morphology that expressed CK19 and Hnf4α, which accounted for approximately 3.87% of ductular cells. These cells had reduced expression of mature BEC markers such as PKCζ and primary cilia, and did not express Lgr5 or AFP, which led the authors to argue these cells were BECs directly converting into hepatocytes, as opposed to differentiation through a LPC intermediate stage (195). However, expression of more widely accepted LPC markers were not assessed in this study, and the renewal capacity of these cells was not tested through *in vitro* culture, so the question remains if these bi-phenotypic cells represent differentiation of mature BECs or activation of LPCs.

1.4.4 Transdifferentiation of Hepatocytes into BECs: Evidence for the Facultative Stem Cell Hypothesis

An alternative theory to that of LPCs is that there is no "stem cell" population in the liver and instead hepatocytes and cholangiocytes serve as facultative stem cells (104, 201), meaning the normal cell population dedifferentiates in response to injury. By this theory, cholangiocytes directly transdifferentiate into hepatocytes, and vice versa, to mediate liver regeneration when the normal proliferation of one of these populations is impaired (Fig. 7A, C). In the case of hepatocyte-to-cholangiocyte transdifferentiation, this theory is supported by *in vitro* organoid cultures. Rats which do not express the enzyme Dipeptidyl Peptidase IV (DPPIV) were given retrorsine, an agent which blocks hepatocyte proliferation, and transplanted with DPPIV-positive hepatocytes, which resulted in livers with colonies of donor-derived DPPIV-positive hepatocytes. When organoid cultures were derived from these hybrid livers, cells resembling BECs on the surface of the organoid culture were found to be DPPIV-positive, indicating hepatocyte origin (202). This finding was further confirmed when DPPIV-negative rats were given retrorsine and subjected to

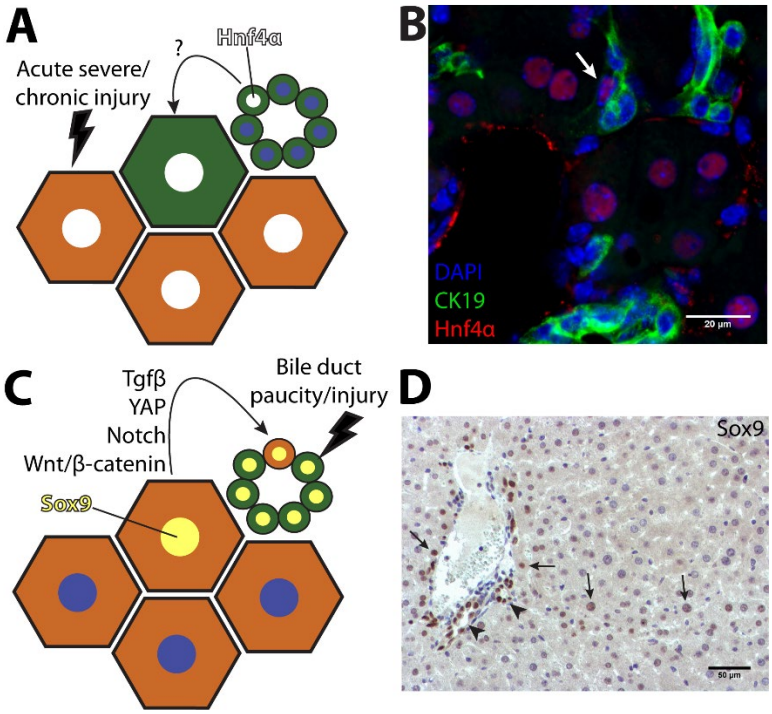

Figure 7: The transdifferentiation theory.

(*a*) During acute severe or chronic liver injury where hepatocyte function is significantly impaired, BECs can directly transdifferentiate into hepatocytes to mediate liver repair. During this process, BECs express hepatocyte markers such as Hnf4α. (*b*) The liver from a mouse fed CDE diet for two weeks followed by three days of recovery on normal diet stained for CK19 (green) and Hnf4α (red). A transdifferentiating cell which expressed both CK19 and Hnf4α is evident (white arrow). Scale bar: 20 μm. (*c*) Following bile duct paucity or severe injury to BECs, hepatocytes can transdifferentiate into BECs, and during this process hepatocytes will express BEC markers such as Sox9. Signaling pathways including Tgfβ, YAP, and Notch, and Wnt/β-catenin have been identified as playing a role in promoting this process. (*d*) Liver from a mouse two days post-bile duct ligation stained for Sox9 reveals the appearance of hepatocytes which express Sox9 (arrows) in comparison to the presence of Sox9 in the BECs lining the bile ducts (arrowheads).

PHx followed by transplantation with DPPIV-positive hepatocytes. When these chimeric livers were pretreated with DAPM and subjected to bile duct ligation (BDL) (a surgical procedure where the common bile duct is ligated, leading to obstructive cholestasis, proliferation of BECs, and periportal fibrosis (203)) appearance of DPPIV-positive ductules was observed (204). A similar study found that GFP-labeled hepatocytes transplanted into rats after BDL adopted a cholangiocyte phenotype, indicating hepatocyte-to-BEC transdifferentiation (205).

The DDC diet has also been used to study hepatocyte-to-cholangiocyte differentiation. When mice were given AAV8-TBG-Cre to label hepatocytes with YFP and subjected to DDC diet or BDL, YFP-positive cells with biliary morphology which expressed BEC markers were detected (193). A different group found that SOX9+; EpCAM- negative cells isolated from DDC diet-fed mice could be differentiated into hepatocytes or BECs *in vitro* (206). One study utilized β-galactosidase-labeled hepatocytes transplanted into mice subjected to retrosine treatment in conjunction with PHx to promote engraftment of donor cells, and subsequently induced liver injury with CCL_4 or DDC diet and observed β-galactosidase-positive BECs (207). Interestingly, a recent study where telomerase reverse transcriptase-expressing hepatocytes were labeled with the lineage marker tdTomato described the appearance of tdTomato-positive BECs following DDC diet-induced liver injury (208).

In terms of signaling pathways that drive hepatocyte-to-BEC transdifferentiation, the crucial role of Notch signaling has been confirmed by numerous groups (Fig. 7C). Hepatocyte-specific overexpression of Notch intracellular domain (NICD) in the absence of injury was sufficient to induce hepatocyte-to-BEC conversion, and hepatocyte-specific deletion of *Rbpj* (the principal effector of Notch signaling) in mice fed DDC diet significantly reduced the number of hepatocyte-derived BECs, suggesting that Notch signaling is required for hepatocyte reprogramming (193). Another group found that the majority of cholangiocytes were derived from hepatocytes in chronic DDC diet-induced liver injury, and the ductular reaction in these mice was significantly increased with NICD overexpression and significantly reduced via *Hes1* deletion (209). Notch signaling was also shown to be required for *in vitro* differentiation of LPCs into BECs, and *in vivo* blockage of Notch receptor cleavage during DDC diet administration reduced the extent of the DR, which was attributed to impaired hepatocyte dedifferentiation (210).

Importantly, overexpression of Yes-Associated Protein (YAP) in hepatocytes was sufficient to dedifferentiate hepatocytes into ductal-like cells, and Notch signaling was found to be a downstream target of YAP signaling during the dedifferentiation process (211). Similarly, another group described periportal hepatocytes which express SOX9 and differentiate to ductal cells after DDC diet-induced liver injury (212). Another signaling pathway putatively involved in hepatocyte-to-BEC transdifferentiation is the Wnt/β-catenin signaling pathway. Mice overexpressing a stabilized form of β-catenin showed increased hepatocyte expression of BEC markers after DDC diet-induced liver injury, and blocking Wnt secretion from BECs via deletion of *Wntless* reduced the number of hepatocytes expressing BEC markers following DDC diet-induced liver injury (213).

However, the findings of hepatocyte-to-BEC transdifferentiation during liver regeneration are disputed. Some lineage tracing studies performed on mice fed DDC diet or subjected BDL detected no evidence of hepatocyte-derived BECs (189). Other groups have found that the hepatocytes which adopt a biliary phenotype during injury revert back to the hepatocyte fate upon the cessation of injury, arguing that it is hepatocyte metaplasia as opposed to true transdifferentiation (214). Interestingly, a recent paper demonstrated the transdifferentiation of hepatocytes into BECs in a mouse model of human Alagille syndrome. Mice with *Albumin*-Cre mediated deletion of *Rbpj* and *Hnf6* in both hepatocytes and cholangiocytes are born lacking peripheral bile ducts but spontaneously form bile ducts by approximately four months of age. Hepatocytes in these mice were labeled with GFP via injection of AAV8 encoding flippase under a hepatocyte-specific promoter. The newly-derived BECs were GFP-positive, indicating their hepatocyte origin. The authors further proved that this transdifferentiation of hepatocytes into BECs required TGFβ signaling, as *Albumin-cre*$^{+/-}$;*Rbpj*$^{f/f}$; *Hnf6*$^{f/f}$; *Tgfbr2*$^{f/f}$ mice failed to form *de*

novo peripheral bile ducts. These hepatocyte-derived bile ducts were stable throughout life, indicating true transdifferentiation as opposed to metaplasia (215).

2.0 Bromodomain and Extraterminal Proteins (BET) Proteins Regulate Hepatocyte Proliferation in Hepatocyte-Driven Liver Regeneration

In this section we investigate the role of BET proteins after PHx, a hepatocyte-proliferation driven liver regeneration model, by treating C57BL6 mice with BET-inhibitor JQ1 or a vehicle control two hours post-PHx and assessing hepatocyte proliferation at 40-45 hours post-PHx, which corresponds to the peak of hepatocyte proliferation in mice. We predict that JQ1 will block hepatocyte proliferation, and we discuss our results, interpretations, and future directions in detail. This study was published in The American Journal of Pathology PMID: 29545201 (216). As first author, the publisher Elsevier has granted full permission to reuse the manuscript in this dissertation.

2.1 Paper Summary

Bromodomain and extraterminal (BET) proteins recruit key components of basic transcriptional machinery to promote gene expression. Aberrant expression and mutations in BET genes have been identified in many malignancies. Small molecule inhibitors of BET proteins like JQ1 have shown efficacy in preclinical cancer models including affecting growth of hepatocellular carcinoma. BET proteins also regulate cell proliferation in non-tumor settings. We recently showed BET proteins regulate cholangiocyte-driven liver regeneration. Here, we sought to study the role of BET proteins in hepatocyte-driven liver regeneration in partial hepatectomy (PHx) and acetaminophen (APAP)-induced liver injury models in mice and zebrafish. JQ1 was injected 2 or

16 hours post-PHx in mice to determine effect on hepatic injury, regeneration and signaling. Mice treated with JQ1 after PHx display increased liver injury and a near-complete inhibition of hepatocyte proliferation. Levels of *Ccnd1* mRNA and Cyclin D1 protein were reduced in 16 hour post-PHx JQ1 injected animals, and even further reduced in 2 hours post-PHx JQ1-injected mice. JQ1-treated zebrafish larvae after APAP-induced injury also displayed notably impaired hepatocyte proliferation. In both models, Wnt signaling was prominently suppressed by JQ1. Our results show BET proteins regulate hepatocyte proliferation-driven liver regeneration and Wnt signaling is particularly sensitive to BET protein inhibition.

2.2 Background

The liver is a highly regenerative organ which is able to recover from repeated bouts of injury through proliferation of the main epithelial cell type of the liver, the hepatocytes (80). Alternatively, in conditions of extreme liver injury where proliferation of hepatocytes is impaired, biliary epithelial cells (BECs) can give rise to liver progenitor cells (LPCs) which can subsequently differentiate into hepatocytes to restore lost cell mass (217, 218). Despite this innate capacity for regeneration, chronic liver disease and cirrhosis is the 12th leading cause of death in the United States (219). Patients with chronic liver disease and cirrhosis are at a major risk for developing hepatocellular carcinoma (HCC), the fifth most common cancer in men worldwide and the second leading cause of cancer-related death (220). The prognosis for HCC is exceedingly poor, with an overall 5-year survival rate of 5.1% in the United States, as there are currently no curative therapies for advanced HCC (221). Clearly, there is a great need to develop new therapies for HCC and underlying chronic liver disease. As failure of endogenous liver regeneration is thought to drive

progression in chronic liver disease (222, 223), understanding the mechanisms of liver regeneration may lead to the development of new therapies.

Recently, a class of drugs has been developed which inhibits bromodomain and extraterminal (BET) proteins and shows promise in the treatment of cancer and inflammation (3). The BET protein family consists of Brd2, Brd3, Brd4, and Brdt which share conserved bromodomains, chromatin interaction modules that bind to acetylated lysine residues on histone tails (2). Brd4 in particular has been identified as a component of Mediator, a multiprotein complex that promotes transcription by interacting with transcription factors (TFs) to recruit and activate RNA polymerase II (3, 4). Moreover, Brd4 has been found to occupy the promoters or enhancers of virtually all actively transcribed genes in a variety of cells types (8-10). The recently developed drug JQ1 displays potent and specific inhibition of Brd4 through competitively binding its bromodomains (11). Interestingly, JQ1 has shown potent anti-cancer effects by selectively inhibiting oncogenic gene expression in various cancer cells lines and murine models (8, 12, 224). The dosage of JQ1 required to inhibit tumors is well-tolerated in mice, despite widespread expression of Brd4 in mouse tissues (8, 11, 12).

Recent reports have additionally implicated a role of Brd4 in liver pathology. Brd4 was found to be overexpressed in HCC cell lines compared to normal liver, and knockdown of Brd4 expression impaired proliferation, migration, and invasion of HCC cells (15, 225, 226). Furthermore, treatment with JQ1 reduced cell growth in both HCC cell lines and a xenograft tumor model (226). JQ1 treatment was also shown to be protective in a mouse model of carbon tetrachloride-induced liver fibrosis through abrogation of cytokine-induced activation of hepatic stellate cells (16). These reports would suggest Brd4 inhibitors as a viable treatment option for certain liver diseases. However, Brd4 has also been implicated in the promotion of liver

regeneration. In a previous study, we showed that JQ1 inhibited BEC-driven liver regeneration in both zebrafish and mice (227). However, the role of Brd4 in the more common hepatocyte-driven liver regeneration has not been assessed. In the current study, we determine the effect of JQ1 treatment in two independent models of hepatocyte-driven liver regeneration: partial hepatectomy in mice and acetaminophen-overdose in zebrafish. We show that JQ1 is a potent inhibitor of hepatocyte proliferation after liver injury. Therefore, the potential use of JQ1 in treatment of liver disease must be carefully considered in order to avoid negatively impacting normal liver regeneration.

2.3 Methods

2.3.1 Animals and Surgery

All animal experiments and procedures were performed under the guidelines of the National Institutes of Health and after approval by the Institutional Animal Use and Care Committee at the University of Pittsburgh, School of Medicine. Male C57BL6/J mice (The Jackson Laboratory, Bar Harbor, ME) underwent partial hepatectomy as previously described (228). Either 2 hours or 16 hours after surgery animals were injected intraperitoneally with 50 mg/kg JQ1 (ApexBio, Taiwan, Cat# A1910). A stock solution of 50 mg/ml JQ1 was prepared in DMSO and subsequently diluted to a working concentration of 5 mg/ml in a solution of 10% hydroxypropyl β-cyclodextrin in sterile water (vehicle solution). As a control, mice were injected with the vehicle solution alone at the indicated time point after surgery. Animals were also injected with either JQ1 or vehicle solution after sham surgeries (where surgery was performed but no liver

was removed). At the time of harvest, either 40 – 45 hours or 72 hours after surgery, animals were anesthetized with isoflurane and blood was drawn from the inferior vena cava. Subsequently, anesthetized mice were euthanized by cervical dislocation. Livers were washed in phosphate buffered saline (PBS), flash frozen in liquid nitrogen, and stored at -80℃ until subsequent protein and RNA analysis, or alternatively were drop fixed in 10% buffered formalin for 48 hours prior to paraffin embedding. Serum aspartate aminotransferase (AST) levels were determined by automated methods at the University of Pittsburgh Medical Center clinical chemistry laboratory.

2.3.2 Immunohistochemistry

Tissue samples embedded in paraffin were cut into 4 μm sections. Tissue sections were deparaffinized in in xylene and hydrated through changes of 100% ethanol followed by 95% ethanol, washed in distilled water, and finally washed in PBS. Antigen retrieval was performed by microwaving slides in pH 6 sodium citrate buffer (Cyclin D1) or zinc sulfate buffer (PCNA). After cooling, endogenous peroxidase activity was blocked through incubation in 3% H_2O_2 in distilled water for 10 minutes. Slides were then washed in PBS and blocking was performed using Super Block (ScyTek Laboratories, Logan, UT, AAA500) for 10 minutes (Cyclin D1) or 20 minutes (PCNA). Primary antibodies were diluted in 1% bovine serum albumin (BSA) (Fisher BioReagents, Pittsburgh, PA, BP1605100) with 0.1% Tween™ 20 (Fisher BioReagents, BP337-500) in PBS as follows: Cyclin D1 (Abcam, Cambridge, United Kingdom, ab134175, 1:200) and PCNA (Santa Cruz, sc-56, 1:5000) and incubated on the slides for 1 hour at room temperature. Sections were washed 3 times in PBS and the correct biotinylated anti-rabbit (Vector Laboratories, Burlingame, CA, BA-1000, 1:500) or biotinylated anti-mouse (Millipore, Burlington, MA, AP181B, 1:700) secondary antibodies were incubated on the tissue sections for 30 minutes. After

washing with PBS 3 times, slides were sensitized with the Vectastain® ABC kit (Vector Laboratories, PK-6101) for 30 minutes. Sections were washed 3 times with PBS and color was developed with the DAB Peroxidase Substrate Kit (Vector Laboratories, SK-4100) followed by quenching in distilled water for 5 minutes. Sections were counterstained in hematoxylin (Thermo Scientific, Pittsburgh, PA, 7211) for approximately 8 – 20 seconds and washed under running tap water for 5 minutes. Slides were then dehydrated in changes of alcohol (70%, 95%, 100%) followed by xylene and coverslips were applied with Cytoseal™ XYL (Thermo Scientific, 8312-4). Images were taken on Axioskop 40 (Zeiss, Oberkochen, Germany) inverted brightfield microscope.

2.3.3 Protein Extraction and Western Blots

Whole-cell lysates of liver tissue were prepared using RIPA buffer containing fresh protease and phosphatase inhibitors (Thermo Scientific, Prod# 1861282) as described previously (229). Gel electrophoresis was performed with 30 µg of protein run on precast 7.5% polyacrylamide gels (BioRad, Hercules, CA, Cat# 456-1025) and transferred onto nitrocellulose membranes using the Trans-Blot® Turbo™ Transfer kit (BioRad, Cat# 170-4270). Membranes were blocked in 5% milk (LabScientific, Highlands, NJ, Cat# M0841) in Blotto blocking buffer (0.15 M NaCl, 0.02 M Tris pH 7.5, 0.1% Tween in dH2O) for 30 minutes at room temperature. Primary antibodies were diluted in 5% milk/Blotto as follows: Cyclin D1 (Thermo Scientific, RB-9041-P; 1:200), β-catenin (BD Biosciences, San Jose, CA, 610154; 1:1000), and GAPDH (Santa Cruz Biotechnology, Dallas, TX, sc-25778, 1:1000) and incubated on membranes at 4°C overnight. Membranes were washed in Blotto for 15 minutes prior to incubation with the correct HRP-conjugated mouse (Millipore, AP308P; 1:10,000) or rabbit (Thermo Scientific, Cat# 31460,

1:20,000) secondary antibodies diluted in 5% milk/Blotto for 1 hour at room temperature. Membranes were then washed for 15 minutes in Blotto prior to exposure with SuperSignal® West Pico Chemiluminescent Substrate (Thermo Scientific, Prod# 34080) for 3 minutes at room temperature. The resulting bands were viewed by autoradiography.

2.3.4 RNA Isolation and Real-Time PCR

Cellular RNA was isolated by homogenizing liver tissue in TRIzol™ Reagent (Thermo Scientific, Cat# 15596026), followed by a cholorform extraction, precipitating nucleic acid with isopropanol at -20°C, and dissolving the resulting dried nucleic acid pellet in nuclease-free water (QIAGEN, Hilden, Germany, Cat# 129117). DNase treatment was performed with the DNA-free™ Kit (Ambion, Pittsburgh, PA, AM1906) according to manufacturer instructions. Approximately 1 µg of RNA was reverse-transcribed using SuperScript® III (Invitrogen, Carlsbad, CA, 18080-044). Real-time PCR was performed on a StepOnePlus™ Real-Time PCR System (Applied Biosystems, Foster City, CA, Cat# 4376600) using the Power SYBR® Green PCR Master Mix (Applied Biosystems, 4367660) with the mouse-specific primers listed Table 1. Fold changes in gene expression were calculated after normalizing target gene expression to the average of two housekeeping genes (*Gapdh* and *Rn18s*) using the ΔΔ-Ct method.

Table 1: Sequence of Real Time PCR primers used in the study in mice.

Gene	Forward Primer	Reverse Primer
Ccnd1	5'-TTTCTTTCCAGAGTCATCAAGTGT-3'	5'-TGACTCCAGAAGGGCTTCAA-3'
Ctnnb1	5'-GGGTCCTCTGTGAACTTGCTC-3'	5'-TTCTTGTAATCCTGTGGCTTGTCC-3'
Axin2	5'-GAGAGTGAGCGGCAGAGC-3'	5'-CGGCTGACTCGTTCTCCT-3'
Regucalcin	5'-CGATTCAATGATGGGAAGGT-3'	5'-CGTTTCCTCAGCCATGGTA-3'
Lect2	5'-CCCACAACAATCCTCATTTCA-3'	5'-GTTAGCCCATGGTCCTGCTA-3'
Brd4	5'-TTCAGCACCTCACTTCGACC-3'	5'-CTGGTGTTTTTGGCTCCTGC-3'
Gapdh	5'-AACTTTGGCATTGTGGAAGG-3'	5'-ACACATTGGGGGTAGGAACA-3'
Rn18s	5'-GTAACCCGTTGAACCCCATT-3'	5'-CCATCCAATCGGTAGTAGCG-3'

2.3.5 Cell Culture

HepG2 liver tumor cells were grown to approximately 30 – 40% confluency in Eagle's Minimum Essential Medium (ATCC®, Manassas, VA, Cat# 30-2003) supplemented with 10% fetal bovine serum (Gemini Bio-Products, West Sacramento, CA, Cat# 100-106) and penicillin-streptomycin (ATCC®, 30-2300) and then serum starved overnight. Cells were transfected with 800 ng TopFlash (Millipore, 21-170) or the p65 reporter (gift from Dr. David Geller (230)) and 200 ng Renilla in Opti-MEM media (Gibco, Gaithersburg, MD, Cat# 31985-070) using the Lipofectamine® 3000 Transfection Kit (Invitrogen, L3000-008) according to manufacturer instructions. After 5 hours incubation with transfection reagents, 0.25 μm, 0.5 μm, or 1 μm JQ1, or DMSO alone as a control, in EMEM media supplemented with 4% FBS and penicillin-streptomycin was added to the cells. Treated cells were harvested 24 hours later and luciferase activity was measured using the Dual-Luciferase® Reporter Assay System (Promega, Madison, WI, Cat# E1960) and normalized to Renilla levels.

For siRNA experiments, HepG2 or Hep3B hepatocellular carcinoma cells were seeded at a density of 200,000 cells/well in 6-well plates. After 48 hours of culture, cells were transfected with Silencer® Select BRD4 siRNA S23901 (Ambion, 4390824) or Silencer® Select Negative Control #2 siRNA (Ambion, 4390847) in Opti-MEM media (Gibco, 31985-070) using the Lipofectamine® RNAiMAX kit (Invitrogen, 13778-150) and incubated for 24 hours at 37°C. Next, TopFlash transfections were performed as described earlier, and luciferase activity was measured 24 hours post-TopFlash transfection.

2.3.6 Zebrafish Studies

Experiments were performed with approval of the Institutional Animal Care and Use Committee (IACUC) at the University of Pittsburgh. Embryos and adult fish were raised and maintained under standard laboratory conditions (231). We used the following transgenic lines: *Tg(fabp10a:CFP-nfsB)*^{s931} (232), *Tg(EPV.Tp1-Mmu.Hbb:hist2h2l-mCherry)*^{s939} (233), and *Tg(fabp10a:mAGFP-gmnn,cryaa:ECFP)*^{pt608} (227) [referred to here as *Tg(fabp10a:CFP)*, *Tg(Tp1:H2B-mCherry)*, and *Tg(fabp10a:mAGFP-gmnn)*, respectively] and *Tg(OTM:d2EGFP)*^{kyu2} (234). Liver injury was induced by treating *Tg(fabp10a:CFP)* larvae with 10 mM acetaminophen (APAP) from 3.5 to 5 dpf for 36 hours. The 10 mM APAP working solution was freshly made by dissolving APAP powder in egg water supplemented with 0.2% dimethyl sulfoxide (DMSO) and 0.2 mM 1-phenyl 2-thiourea (PTU). Hepatocyte ablation was performed by treating *Tg(fabp10a:CFP)* larvae with 10 mM metronidazole (Mtz) in egg water supplemented with 0.2% dimethyl sulfoxide (DMSO) and 0.2 mM PTU. For BET inhibition, larvae were treated with 3 μM JQ1 or 50 μM iBET151 from R0h to R48h, and *fabp10a:*CFP expression was imaged using the Leica M205 FA epifluorescence microscope (227). To quantify liver size and Wnt/β-catenin

activity, corrected total cell fluorescence (CTCF) of *fabp10a:*CFP and *OTM:*d2EGFP, respectively, was measured using the ImageJ software as previously described (235).

2.3.7 Zebrafish Whole-Mount Confocal Microscopy

Whole-mount immunostaining was performed as previously described (236), using the following antibodies: mouse anti-Alcam (1:20; ZIRC, Eugene, OR) and Alexa Fluor 647-conjugated secondary antibodies (1:500; Life Technologies, Grand Island, NY). Zeiss LSM700 confocal microscope was used to obtain image data and confocal stacks were analyzed using the Zen 2009 software. All figures, labels, arrows, scale bars, and outlines were assembled or drawn using the Adobe Illustrator (version CS5) software.

2.3.8 Zebrafish qPCR

Total RNA was extracted from 50 dissected livers using the RNeasy Mini Kit (Qiagen, Valencia, CA); cDNA was synthesized from the RNA using the SuperScript® III First-Strand Synthesis SuperMix (Life Technologies, Grand Island, NY) according to the kit protocols. qPCR was performed as previously described (237), using the Bio-Rad iQ5 qPCR machine with the iQ™ SYBR Green Supermix (Bio-Rad, Hercules, CA). Fold changes were calculated after normalizing target gene expression to *eef1a1l1* using the ΔΔ-Ct method. At least three independent experiments were performed. The zebrafish-specific primers used for qPCR are listed in Table 2.

Table 2: Sequence of Real Time PCR primers used in the study in zebrafish.

Gene	Forward Primer	Reverse Primer
brd4	5'-GGCCCCTTCTTCCTTCAACC-3'	5'-TGTAGAATGCGCTCTCTAGGC-3'
ccnd1	5'-GGAACTGCTGGCGCTTAAATA-3'	5'-GACTTGCGAGAGGAAGTTGG-3'
pcna	5'-ATCTGGATGTGGAGCAGCTT-3'	5'-TGTGACCGTCTTGGACAGAG-3'
myca	5'-TATTGTTAACCCGCCCCCAC-3'	5'-ATGCATTCACCAGCAGTCCA-3'
axin2	5'-GGCTACAGGTCCTACAGAC-3'	5'-GCTTGTAAGGAGGAATGGC-3'
eef1α1l1	5'-CTGGAGGCCAGCTCAAACAT-3'	5'-ATCAAGAAGAGTAGTACCGCTAGCATTAC-3'

2.3.9 Statistical Analyses

Statistical analysis was performed with GraphPad Prism software (version 7). For analyses concerning only two groups, a two-tailed Student's t-test was performed, with $p < 0.05$ considered significant. For analyses concerning more than two groups, a one-way ANOVA test was performed, with $p < 0.05$ considered significant. For survival curves, a Gehan-Breslow-Wilcoxon test was performed, with $p < 0.05$ considered significant.

2.4 Results

2.4.1 JQ1 Administration 16 Hours Post-Partial Hepatectomy Impairs Cyclin D1 Expression and Hepatocyte Proliferation at 40 Hours.

To determine if JQ1 would have an impact on hepatocyte proliferation-driven liver regeneration, we utilized the mouse partial hepatectomy (PHx) model, a common model of liver regeneration where two-thirds of the liver is surgically removed and remaining hepatocytes proliferate to restore lost liver mass (81). In order to allow time for mice to recovery from the

surgery prior to injection, we administered a single injection of JQ1 at 16 hours post-PHx. We harvested mice within the 40 – 45 hours post-PHx window, which is the peak of DNA synthesis in mouse hepatocytes after PHx (238, 239) (Fig. 8A). JQ1-injected mice at 40 hours post-PHx displayed significantly elevated levels of serum liver injury marker aspartate aminotransferase (AST) compared to control mice injected with the vehicle solution (10% hydroxypropyl β-cyclodextrin in distilled water) (Fig. 8B). When hepatocyte proliferation was assessed by immunohistochemistry (IHC) for proliferating cell nuclear antigen (PCNA) (240), there were many PCNA-positive hepatocytes in vehicle-injected animals, whereas JQ1-injected animals had very few PCNA-positive hepatocytes (Fig. 8C). Cyclin D1, which is involved in promoting the G1/S phase transition in the cell cycle, is known to be highly upregulated in order to drive hepatocyte proliferation after PHx in mice (241, 242). We detected robust hepatocyte expression of Cyclin D1 in vehicle-injected mice post-PHx, while JQ1-injected mice displayed a marked reduction in Cyclin D1 staining (Fig. 8C). Cyclin D1 was also dramatically reduced at both the gene expression (Fig. 8D) and protein levels (Fig. 8E) in JQ1-injected animals.

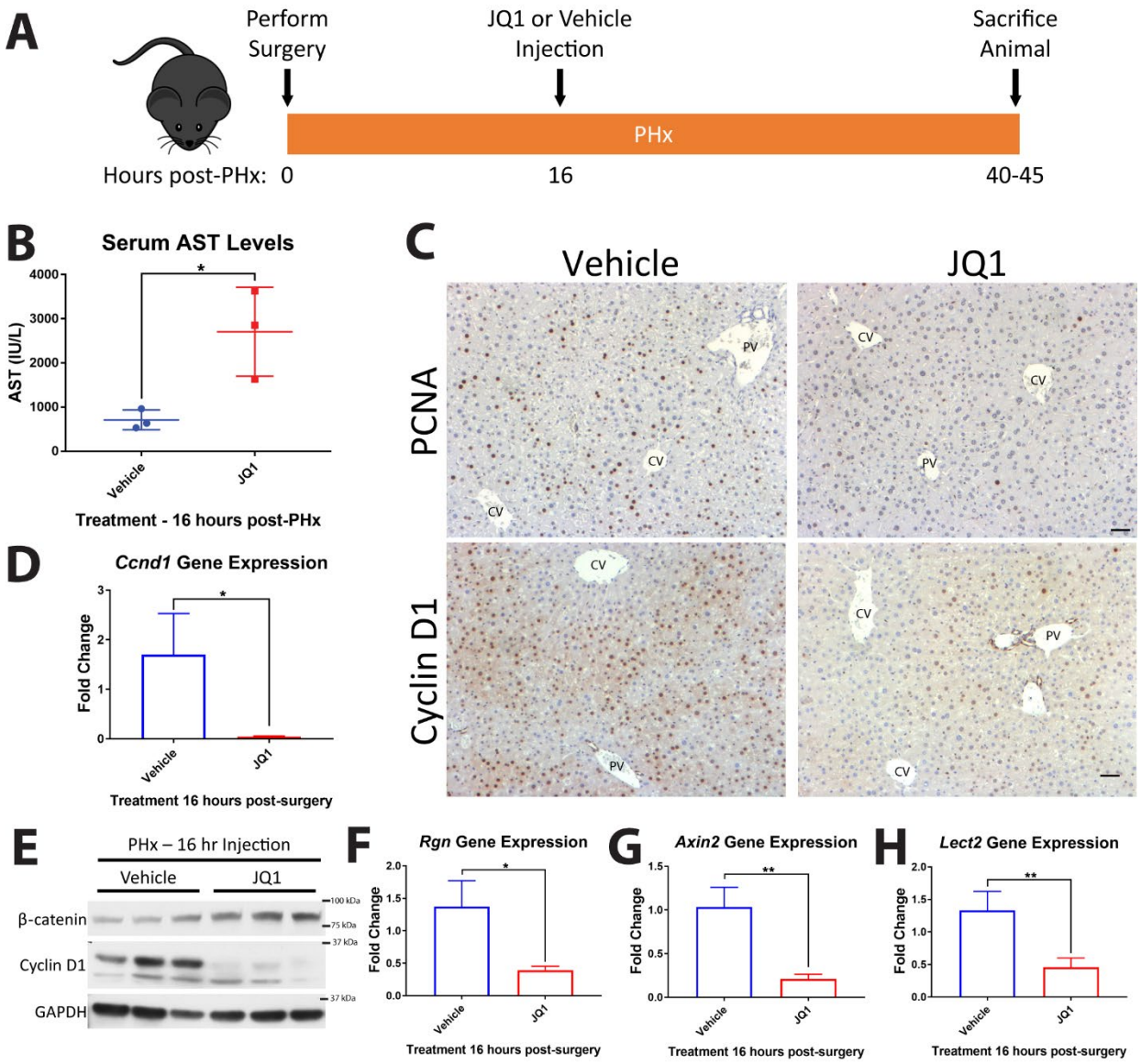

Figure 8: Injection of JQ1 16 hours post-PHx impairs liver regeneration.

(*a*) Schematic for experimental plan for injection of JQ1 (50 mg/kg) or vehicle solution 16 hours post-PHx, followed by harvest at 40-45 hours post-PHx. (*b*) Serum AST levels are significantly elevated in JQ1-injected mice compared to vehicle-injected controls 40 hours post-PHx (t-test, * = $p < 0.05$). (*c*) IHC for PCNA and Cyclin D1 reveals significantly reduced hepatocyte proliferation and Cyclin D1 expression in JQ1-injected mice (scale bar 50 μm, PV = portal vein, CV = central vein). (*d*) Significantly reduced *Ccnd1* gene expression in JQ1-injected mice (t-test, * = $p < 0.05$). (*e*) No reduction in total β-catenin levels but a significant reduction in Cyclin D1 protein levels are evident in JQ1-injected mice. (*f*) Significant reduction in *Rgn* gene expression in JQ1-injected mice (t-test, * = $p < 0.05$). (*g*) Significant reduction in *Axin2* gene expression in JQ1-injected mice (t-test, ** = $p < 0.01$). (*h*) Significant reduction in *Lect2* gene expression in JQ1-injected mice (t-test, ** = $p < 0.01$). Error bars are mean $\pm$ SD.

2.4.2 JQ1 Administration 16 hours Post-Partial Hepatectomy Impairs Expression of Additional Wnt Target Genes in Addition to Cyclin D1.

Cyclin D1 is a known target of the Wnt/β-catenin signaling pathway (243, 244), and mice with liver-specific deletion of β-catenin display dramatically reduced Cyclin D1 levels and a delay in liver regeneration post-PHx (229). Therefore, we hypothesized JQ1 may be inhibiting Wnt/β-catenin signaling in post-PHx mice. Indeed, in JQ1-injected mice there were significant decreases in gene expression of β-catenin targets regucalcin (*Rgn*) (245) (Fig. 8F), *Axin2* (72) (Fig. 8G), and leukocyte cell-derived chemotaxin 2 (*Lect2*) (246) (Fig. 8H) compared to vehicle-injected controls at 40 hours post-PHx. However, there was no reduction in total protein levels of β-catenin in JQ1-injected mice (Fig. 8E), suggesting JQ1 is inhibiting transcription of β-catenin target genes rather than directly inhibiting expression of β-catenin.

2.4.3 An Earlier Administration of JQ1 at 2 Hours After Partial Hepatectomy Completely Prevents Cyclin D1 Expression and Hepatocyte Proliferation Leading to Enhanced Injury and Mortality at 40 Hours.

Previous reports have shown that Cyclin D1 can be induced as early as 12 hours post-PHx in mice (247, 248), so we decided to administer JQ1 at 2 hours post-PHx (Fig. 9A) rather than 16 hours post-PHx to investigate if this would completely abrogate any increases in Cyclin D1. We again chose to harvest tissue at the peak of hepatocyte proliferation (40-45 hours post-PHx). As a control, we injected mice with either JQ1 or the vehicle solution 2 hours after a sham surgery and harvested at 40 hours post-surgery to assess the effects on JQ1 on a non-injured liver. Injection of JQ1 had no effect on the gross appearance of sham animal livers (Fig. 9B). However, JQ1

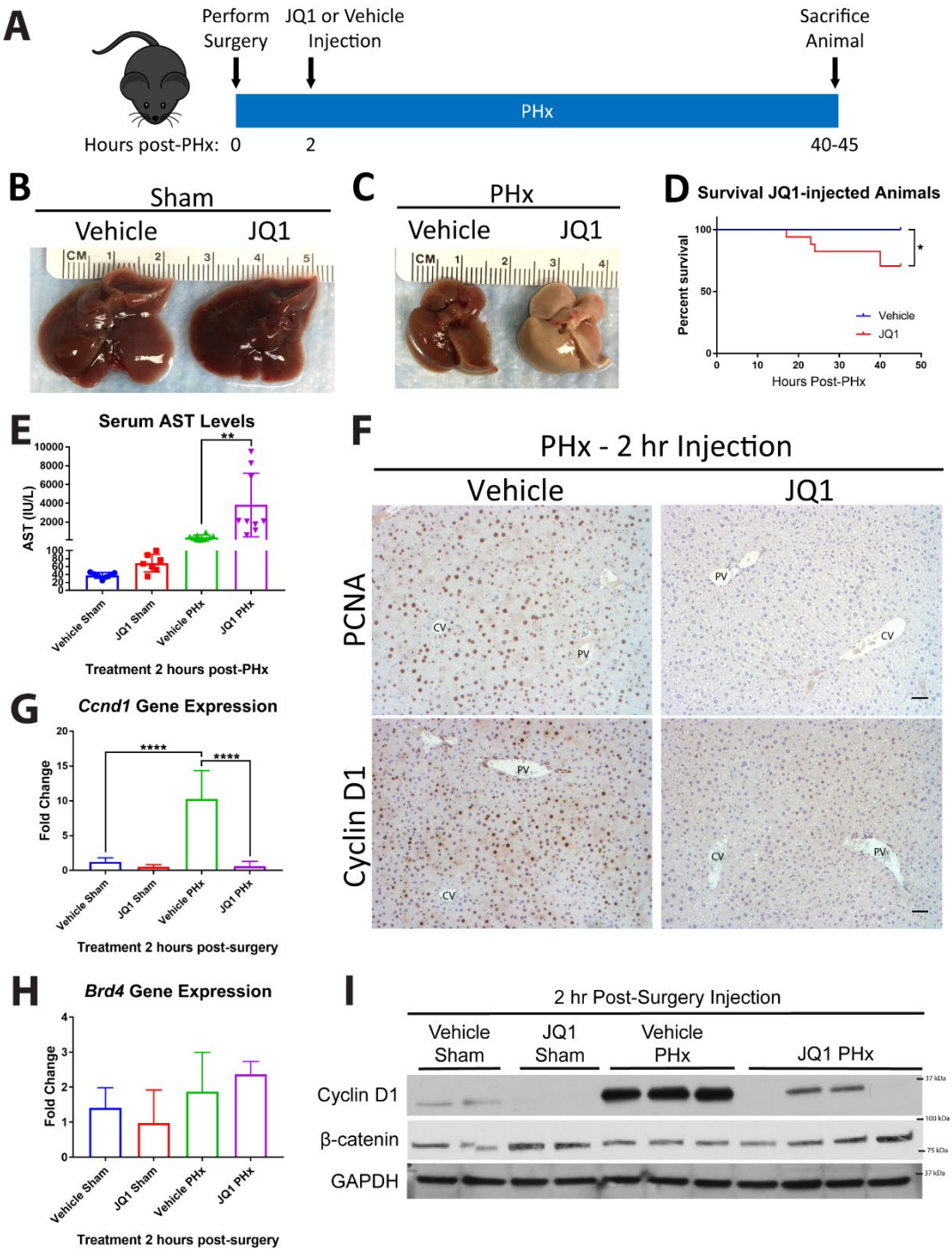

Figure 9: Injection of JQ1 2 hour post-PHx impairs liver regeneration.

(*a*) Schematic for experimental design of injecting JQ1 (50mg/kg) or vehicle solution 2 hour post-PHx and harvesting at 40-45 hours post-PHx. (*b*) No effect on the gross morphology of livers from JQ1-injected sham surgery animals. (*c*) Striking discoloration of the livers of JQ1-injected animals 40 hours post-PHx. (*d*) Reduced survival of animals injected with JQ1 2 hours post-PHx (Gehan-Breslow-Wilcoxon test, * = $p < 0.05$, Vehicle n = 12, JQ1 n = 17). (*e*) No increase in serum AST

in JQ1-injected sham animals, but a significant increase in serum AST in JQ1-injected PHx animals compared to vehicle-injected PHx mice (one-way ANOVA, ** = $p < 0.01$). (*f*) IHC staining for PCNA and Cyclin D1 reveals robust staining in vehicle-injected controls, but virtually no staining in JQ1-injected mice 40 hours post-PHx (scale bar 50 μm, PV = portal vein, CV = central vein). (*g*) Dramatic upregulation of *Ccnd1* gene expression in vehicle-injected animals post-PHx, but no upregulation in JQ1-injected animals (one-way ANOVA, **** = $p < 0.0001$). (*h*) No change in *Brd4* expression after either PHx or JQ1 injection. (*i*) Reduced Cyclin D1 protein in JQ1 injected animals compared to vehicle-injected controls, but no reduction in total β-catenin protein levels. Error bars are mean ± SD.

injection 2 hours post-PHx resulted in severe liver injury, with the livers from JQ1-injected animals 40 hours post-PHx exhibiting striking discoloration (Fig. 9C). Animals injected with JQ1 2 hours post-PHx had significantly reduced survival compared to vehicle-injected controls, with 30% of mice exhibiting notable morbidity requiring euthanasia at or before 45 hours post-PHx (Fig. 9D). Although there was no increase in serum AST in JQ1-injected animals that underwent sham surgery, JQ1-injected PHx mice displayed significantly elevated serum AST levels compared to vehicle-injected PHx animals (Fig. 9E). While in vehicle-injected animals there was robust hepatocyte expression of PCNA and Cyclin D1, in mice injected with JQ1 2 hours post-PHx there were almost no PCNA-positive hepatocytes in addition to extremely little Cyclin D1 staining (Fig. 9F). In accordance with these results, *Ccnd1* gene expression was significantly upregulated in vehicle-injected PHx mice compared to sham controls, but this upregulation was completely absent in mice injected with JQ1 2 hours post-PHx (Fig. 9G). Additionally, levels of Cyclin D1 protein were dramatically lower in JQ1-injected mice compared to vehicle-injected controls after PHx, while levels of β-catenin were not reduced (Fig. 9I). Expression of *Brd4* was not significantly altered in JQ1-injected mice (Fig. 9H), demonstrating that JQ1 does not induce compensatory upregulation of *Brd4*.

Another factor known to play a critical role in promoting cell cycle progression is the E2f2 transcription factor, which has been shown to be required for hepatocyte proliferation after PHx

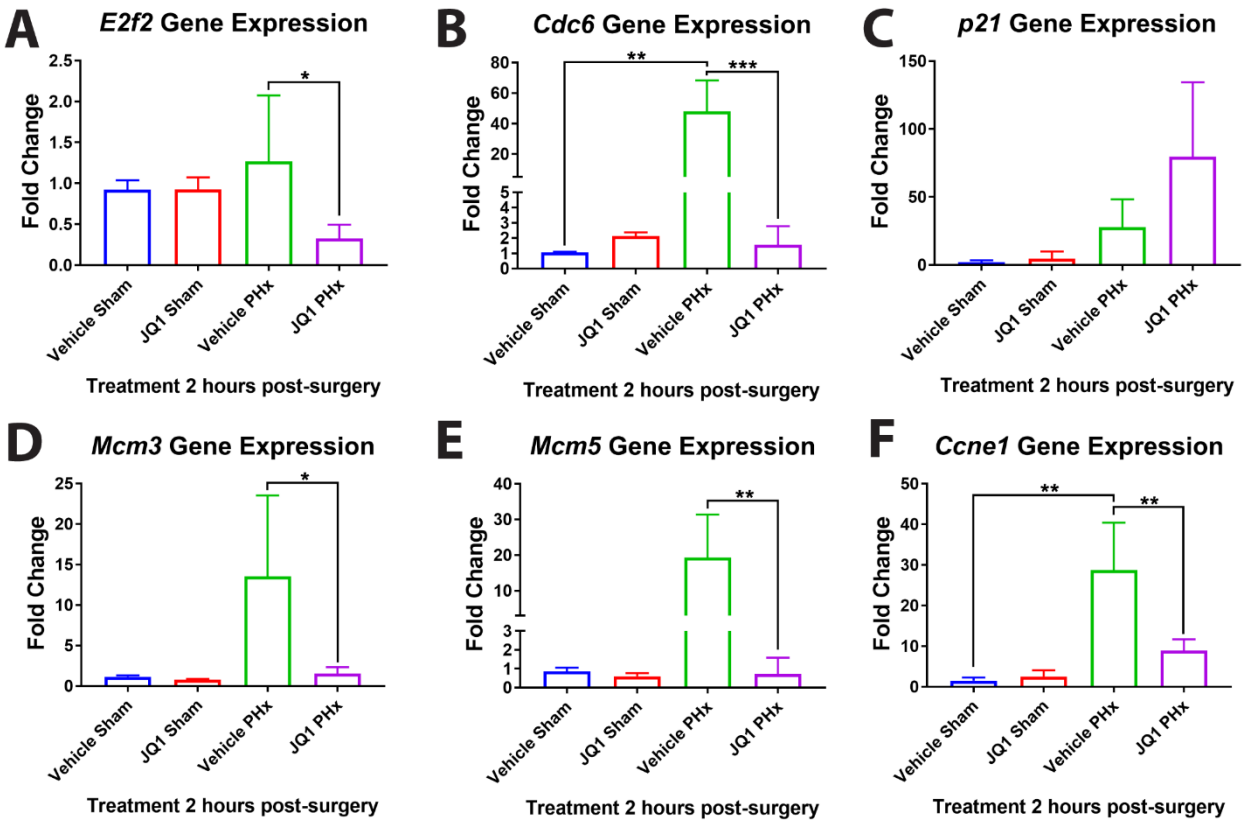

Figure 10: E2f2-driven transcription is inhibited in JQ1-injected animals after PHx.

(*a*) Expression of *E2f2* is significantly reduced in JQ1-injected mice after PHx (one-way ANOVA, * = $p < 0.05$). (*b*) Expression of *Cdc6* is induced in vehicle-injected but not JQ1-injected mice after PHx (one-way ANOVA, ** = $p < 0.01$, *** = $p < 0.001$). (*c*) Expression of *p21* is further increased in JQ1-injected mice after PHx. (*d*) Expression of *Mcm3* is induced in vehicle-injected but not JQ1-injected mice after PHx (one-way ANOVA, * = $p < 0.05$). (*e*) Expression of *Mcm5* is induced in vehicle-injected but not JQ1-injected mice after PHx (one-way ANOVA, ** = $p < 0.01$). (*f*) Expression of *Ccne1* is induced in vehicle-injected but not JQ1-injected mice after PHx (one-way ANOVA, ** = $p < 0.01$). Error bars are mean $\pm$ SD.

(249). Additionally, E2F2 has been shown to be a direct target of JQ1-mediated BRD4 inhibition in human liver cancer cells (250). Therefore, we investigated if E2f2 signaling was inhibited in our JQ1-injected mice after PHx. Although there was no increase in *E2f2* expression in vehicle-injected mice after PHx compared to sham controls, we observed a decrease in *E2f2* expression in JQ1-injected animals after PHx (Fig. 10A). We next assessed expression of E2f2 target genes known to be involved in cell cycle progression. Expression of E2f2 targets *Cdc6* and *Mcm3*, which

are induced in late G1 phase (251), were dramatically induced in vehicle-injected mice after PHx, and this increase was blocked in JQ1-injected animals (Fig. 10B and D). Disruption of E2f2 signaling can lead to the induction of *p21* (251), and indeed there was an increase in *p21* expression in JQ1-injected mice after PHx compared to vehicle-injected controls (Fig. 10C). Additional E2f2 targets *mcm5* and *ccne1* (249, 251) were induced in vehicle-injected animals after PHx, but this induction was blocked in JQ1-injected animals (Fig. 10E and F). Interestingly, expression of E2f2 targets genes was largely unaffected in JQ1-injected mice which underwent sham surgery (Fig. 10). Thus our data indicates that JQ1, in addition to inhibiting β-catenin target gene expression, is inhibiting expression of E2f2-driven target genes after PHx, resulting in cell cycle arrest. Collectively, these results show that injection of JQ1 2 hours post-PHx nearly completely abrogates hepatocyte proliferation and liver regeneration, but JQ1 injection is well tolerated in animals in the absence of liver injury.

2.4.4 Earlier JQ1 Administration after Hepatectomy Impairs Expression of Additional Wnt Target Genes, Which was Validated *In Vitro*.

We wanted to confirm that the hepatic expression of β-catenin target genes that were downregulated in animals injected with JQ1 16 hours post-PHx were also downregulated in the mice injected with JQ1 2 hours post-PHx. Expression of *Rgn* was significantly reduced in JQ1-injected PHx animals compared to both JQ1-injected sham and vehicle-injected PHx mice (Fig. 11A). Similarly, gene expression of *Lect2* was significantly reduced in JQ1-injected PHx mice reduced compared to both JQ1-injected sham and vehicle-injected PHx animals (Fig. 11B). Expression of *Axin2* tended to be lower in JQ1-injected PHx mice compared to vehicle-injected PHx animals (Fig. 11C). There was no significant change in *Ctnnb1* gene expression in mice

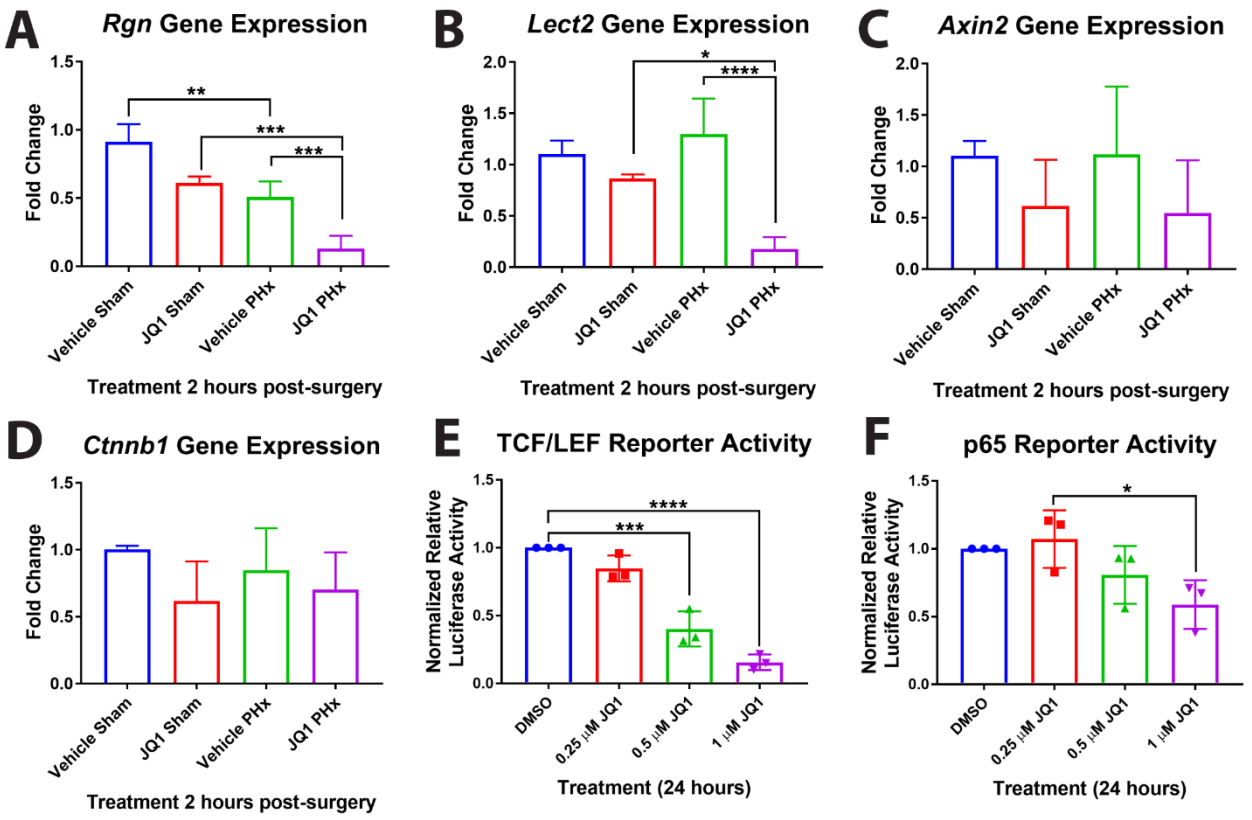

Figure 11: β-catenin-driven transcription is sensitive to JQ1 inhibition.

(*a*) *Rgn* gene expression in significantly reduced in JQ1-injected mice compared to vehicle-injected controls post-PHx (one-way ANOVA, ** = $p < 0.01$, *** = $p < 0.001$). (*b*) *Lect2* gene expression is significantly reduced in JQ1-injected mice post-PHx (one-way ANOVA, * = $p < 0.05$, **** = $p < 0.0001$). (*c*) Expression of *Axin2* tended to be lower in JQ1-injected mice post-PHx. (*d*) No change in the gene expression of *Ctnnb1* was observed in JQ1-injected mice. (*e*) HepG2 cells transfected with a TCF/LEF luciferase reporter and treated with JQ1 for 24 hours showed a dose-dependent decrease in reporter activity after JQ1 treatment. Data is the pooled results of three independent experiments (one-way ANOVA, *** = $p < 0.001$, **** = $p < 0.0001$). (*f*) HepG2 cells transfected with a p65 luciferase reporter and treated with JQ1 for 24 hours showed a reduction of reporter activity after 1 μm JQ1 treatment. Data is pooled results of three independent experiments (one-way ANOVA, * = $p < 0.05$). Error bars are mean ± SD.

injected with JQ1 2 hours post-PHx compared to mice injected with the vehicle solution (Fig. 11D).

To determine if JQ1 could directly inhibit β-catenin-driven transcriptional activity, we transfected HepG2 cells, which has constitutively active β-catenin owing to a deletion affecting

exon-3 of the *CTNNB1* gene, with a TopFlash luciferase reporter. JQ1 was able to, in a dose-dependent manner, significantly inhibit β-catenin-TCF/LEF reporter activity (Fig. 11E). To determine if β-catenin-driven transcriptional activity is especially sensitive to inhibition by JQ1 treatment, we tested the effect of JQ1 on the NFκB signaling pathway, another pathway implicated in liver regeneration after PHx due to the observed activation of the NFκB subunit p65/RelA within 30 minutes of PHx in mice and rats (252, 253). When HepG2 cells transfected with a p65 luciferase reporter were treated with JQ1, at the highest concentration of JQ1 there was only a 50% reduction in reporter activity (Fig. 11F), compared to up to a 90% reduction in β-catenin-TCF/LEF reporter activity. These results suggest β-catenin-driven transcriptional activity is particularly sensitive to inhibition by JQ1.

To determine if the JQ1-mediated reduction in β-catenin-TCF/LEF reporter activity was specifically due to inhibition of BRD4 activity, we treated two liver tumor cell lines, HepG2 and Hep3B, with *BRD4* siRNA and subsequently measured TCF/LEF reporter activity. We first validated that we achieved robust knockdown of *BRD4* expression in our siRNA-treated cells (Fig. 12A). Interestingly, HepG2 cells treated with *BRD4* siRNA showed no reduction in TCF/LEF reporter activity (Fig. 12B). As HepG2 cells have constitutively-active mutant β-catenin, we speculated that reduction in *BRD4* expression levels may not be sufficient to reduce signaling driven by mutant β-catenin protein. Therefore, we treated Hep3B cells, a hepatocellular carcinoma cell line with wild-type β-catenin, with *BRD4* siRNA. In Hep3B cells we saw a modest but significant reduction in TCF/LEF reporter activity (Fig. 12C), which was roughly on-par with the reduction of TCF/LEF reporter activity seen in HepG2 cells with low-dose JQ1 treatment (Fig. 11E). As JQ1 is known to inhibit the bromodomains of BET proteins (11), and the BET family proteins share conserved bromodomains (2), we assessed the expression levels of *BRD2* and

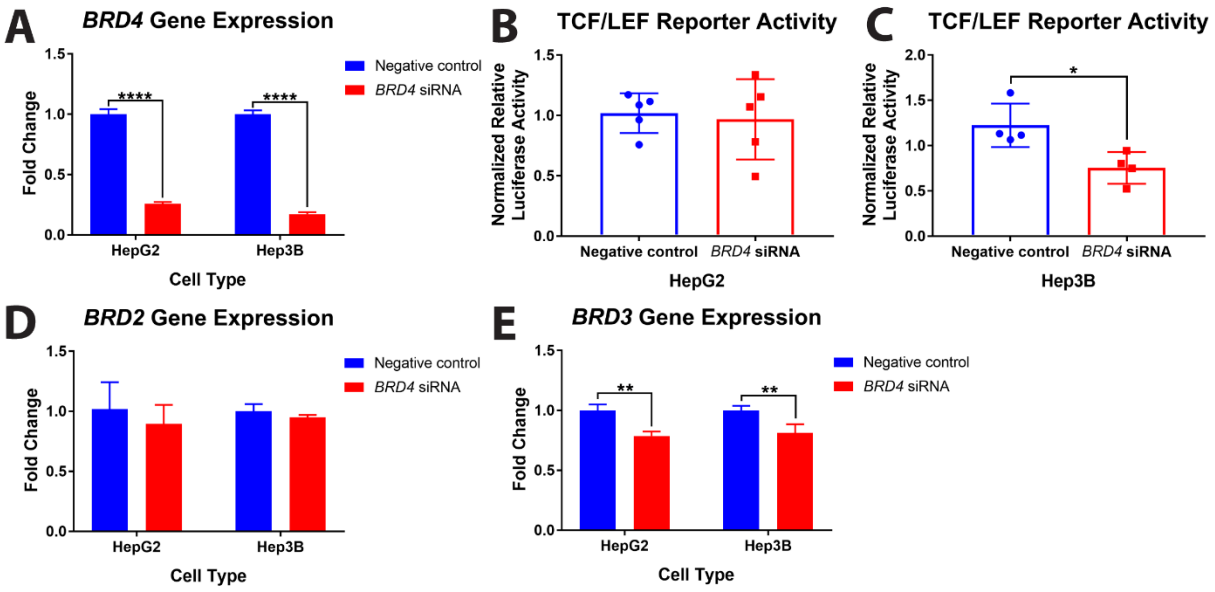

Figure 12: BRD4 siRNA reduces TCF/LEF transcriptional activity in Hep3B cells.

(*a*) *BRD4* siRNA treatment dramatically reduces *BRD4* expression in both HepG2 and Hep3B cells (two-way ANOVA, **** = $p < 0.0001$). (*b*) No reduction in TCF/LEF reporter activity in HepG2 cells treated with *BRD4* siRNA. Data is pooled results of five independent experiments. (*c*) Significant reduction in TCF/LEF reporter activity in Hep3B cells treated with *BRD4* siRNA. Data is pooled from four independent experiments (t-test, * = $p < 0.05$). (*d*) No change in expression of *BRD2* in cells treated with *BRD4* siRNA. (*e*) Slight reduction in the expression of *BRD3* in cells treated with *BRD4* siRNA (two-way ANOVA, ** = $p < 0.01$).

BRD3 in our liver cancer cells to determine if there was compensatory upregulation of other members of the BET protein family upon *BRD4* knockdown. The expression of *BRD2* was unchanged by *BRD4* siRNA treatment (Fig. 12D), while the expression level of *BRD3* was slightly reduced in both HeG2 and Hep3B cells (Fig. 12E). It is possible that BRD2 and BRD3 would able to partially compensate for BRD4 transcriptional activity, while all BET proteins would be inhibited by high-dose JQ1 treatment, offering a potential explanation for the relatively minor effects of *BRD4* siRNA on TCF/LEF reporter activity. Overall, our data suggest that JQ1-inhibition of BRD4 is at least partially responsible for the reduction in β-catenin-driven transcriptional activity in a wild-type β-catenin setting.

2.4.5 A Single Early Dose of JQ1 2 Hours Post-Hepatectomy is Insufficient to Have an Impact on Cyclin D1 Expression and Hepatocyte Proliferation at 72 Hours Post-Hepatectomy.

To determine the extent to which a single dose of JQ1 can block liver regeneration, we injected mice with JQ1 or the vehicle solution 2 hours post-PHx and assessed the level of liver regeneration at 72 hours post-PHx (Fig. 13A). The 70% of JQ1-injected animals that survived to 72 hours post-PHx showed serum liver injury marker AST levels that were comparable with vehicle-injected animals (Fig. 13B). Robust proliferation of hepatocytes was evident via PCNA IHC in both vehicle and JQ1-injected mice (Fig. 13C). There was also appearance of Cyclin D1 staining in the hepatocytes of JQ1-injected mice at this time point (Fig. 13C), which was accompanied by an upregulation of *Ccnd1* gene expression in the JQ1-injected mice (Fig. 13D). Most likely this induction of liver regeneration coincides with the clearance of JQ1 from the mice, as our previous work demonstrated that liver regeneration in zebrafish resumed after washout of JQ1 (227).

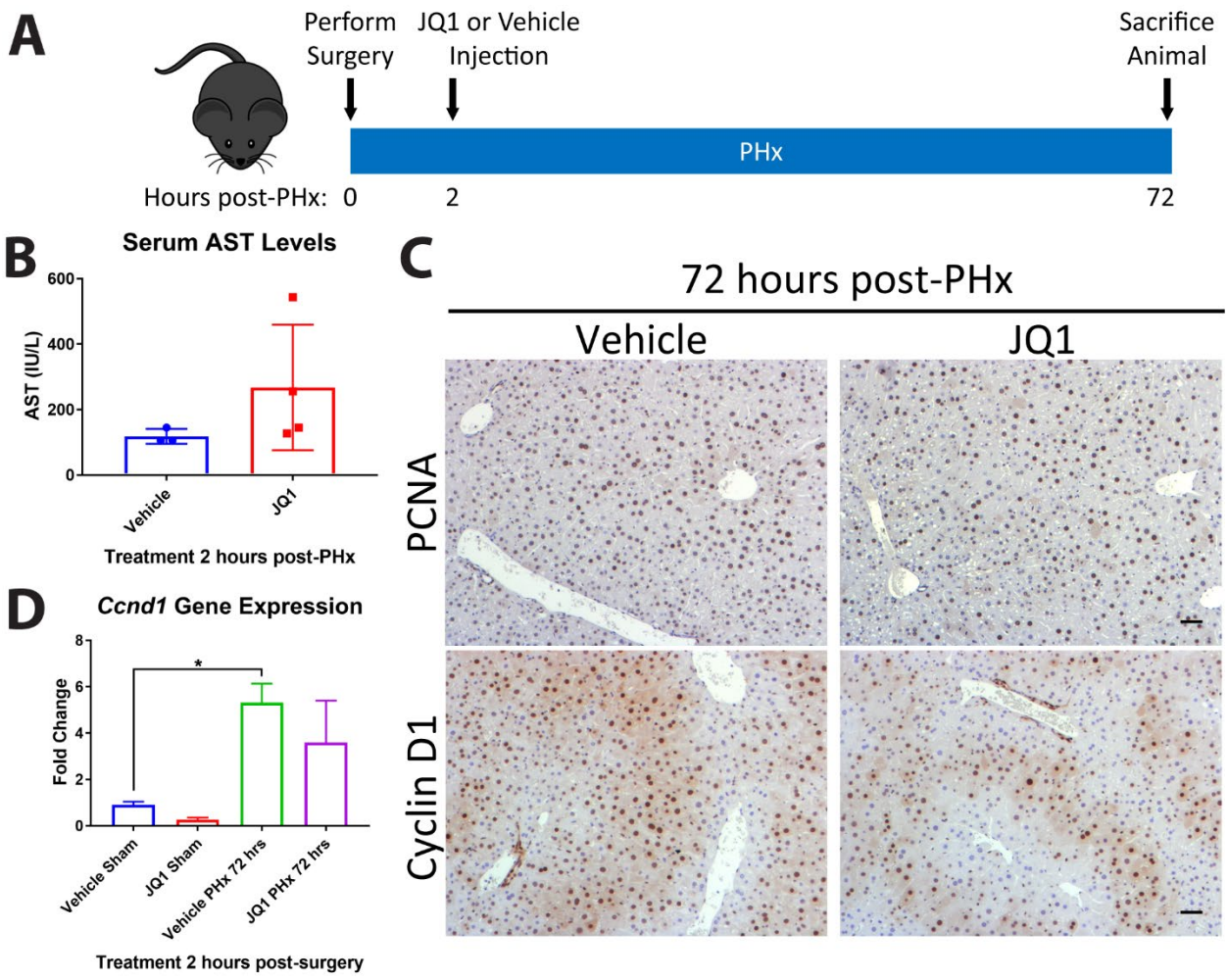

Figure 13: Induction of liver regeneration in JQ1-injected animals 72 hours post-PHx.

(*a*) Schematic of experimental design, with a 50 mg/kg JQ1 injection (or vehicle injection) 2 hours post-PHx and harvest at 72 hours post-PHx. (*b*) Serum AST levels are normalizing in both JQ1 and vehicle-injected mice 72 hours post-PHx. (*c*) PCNA staining reveals robust hepatocyte proliferation in both vehicle and JQ1-injected mice 72 hours post-PHx, and Cyclin D1 staining is present in hepatocytes in both vehicle and JQ1-injected animals 72 hours post-PHx (scale bar 50 μm). (*d*) Upregulation of *Ccnd1* gene expression is present in both vehicle and JQ1-injected animals 72 hours post-PHx (one-way ANOVA, * = $p < 0.05$). Error bars are mean $\pm$ SD.

2.4.6 BET Protein Inhibition also Impairs Hepatocyte Proliferation and Liver Size in a Zebrafish Model of Hepatic Injury and Hepatocyte-Mediated Regeneration.

To further validate the effect of BET protein inhibition on hepatocyte-driven liver regeneration, we next used a zebrafish model in which N-acetyl-p-aminophenol (APAP) overdose induces liver damage and subsequent regeneration (254, 255). The APAP overdose model has been widely used in rodents (256) and zebrafish (254, 255, 257), because it mimics human APAP-induced acute liver failure (ALF), the most common cause of ALF in the United States (256, 258). As previously reported (254, 255), treating zebrafish larvae with APAP greatly reduced liver size and following APAP washout liver size gradually recovered (Fig. 14A and B). We first determined whether hepatocytes solely or together with BECs contribute to regenerating hepatocytes in the APAP-induced injury model. As a positive control for BEC contribution to regenerating hepatocytes, we used our previous model of BEC-driven liver regeneration (232), in which *Tg(fabp10a:CFP-NTR)* zebrafish, which express nitroreductase (NTR) fused with cyan fluorescent protein (CFP) specifically in hepatocytes via the hepatocyte-specific *fabp10a* promotor (Fig. 14C). NTR metabolizes the prodrug metronidazole (Mtz) into a cytotoxic compound, resulting in the ablation of NTR-expressing cells. Thus treating *Tg(fabp10a:CFP-NTR)* larvae with Mtz induces hepatocyte-specific cell death. In this model, near-complete ablation of hepatocytes induces the dedifferentiation of BECs into LPCs, which subsequently differentiate into either hepatocytes or BECs (232). Given the BEC-restricted Notch activity in the zebrafish liver (259), in order to mark BECs, we used a Notch reporter line, *Tg(Tp1:H2B-mCherry)*, which expresses H2B-mCherry fusion proteins under the promoter containing the Notch-responsive element (233). Due to the prolonged stability of H2B-mCherry proteins, this line also reveals BEC-derived cells even after Notch signaling is turned off. In Mtz-treated larvae after 24 hours of recovery (R24h),

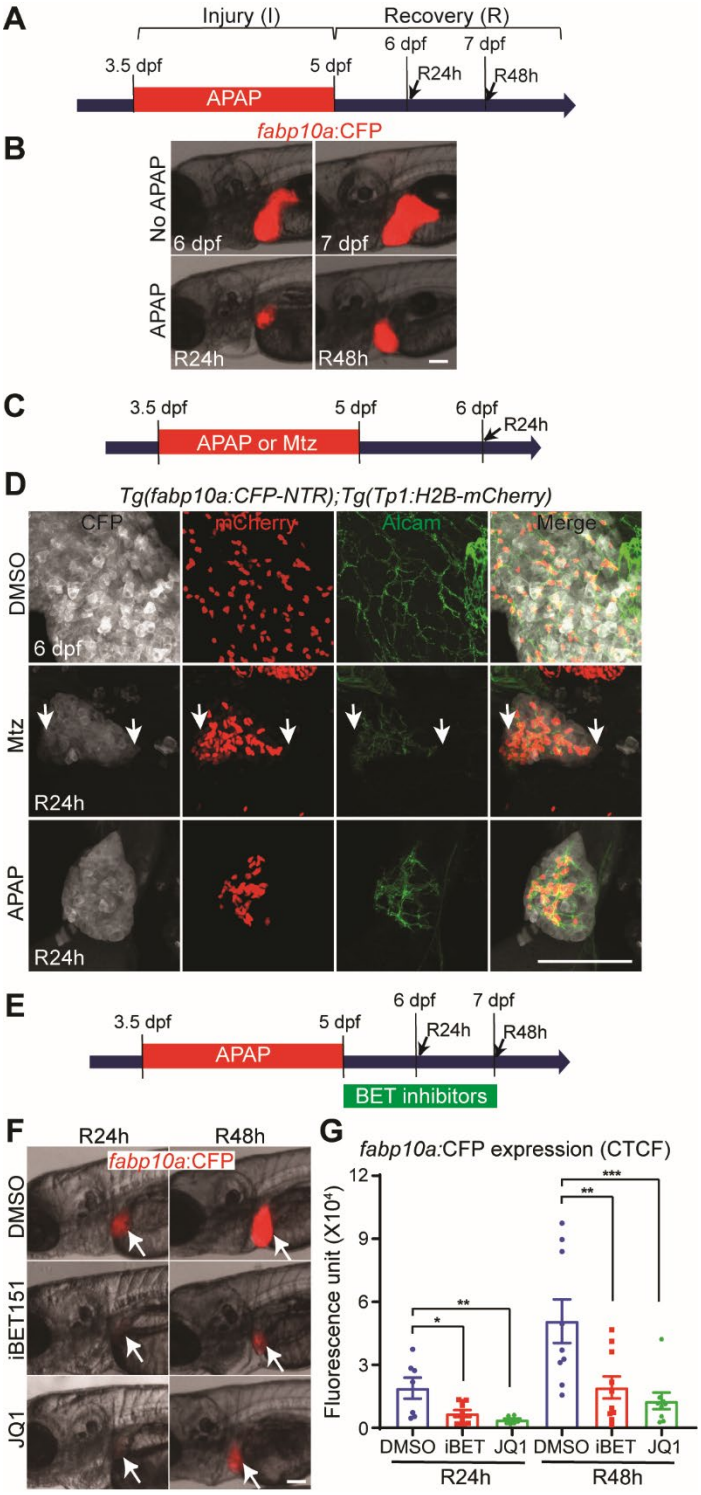

Figure 14: BET inhibition impairs hepatocyte-driven liver regeneration in zebrafish.

(*a*) Scheme illustrating the periods of APAP treatment (I, injury) and liver regeneration (R). An arrow indicates analysis stage. (*b*) Epifluorescence images showing *fabp10a:*CFP expression in the untreated larvae or larvae treated with APAP. (*c*) Scheme illustrating the periods of APAP or

Mtz treatment and liver regeneration. (*d*) Confocal images showing the expression of Alcam (*green*), *Tp1:*H2B-mCherry (red), and *fabp10a:CFP-NTR* (grey) in regenerating livers at R24h. Arrows point to BEC-derived hepatocytes, which weakly express *Tp1:*H2B-mCherry. (*e*) Scheme illustrating the periods of APAP and BET inhibitor treatments. Arrows indicate analysis stages. (*f*) Epifluorescence images showing *fabp10a:*CFP expression in the regenerating larvae treated with two different BET inhibitors, iBET151 and JQ1. Arrows point to the liver. (*g*) Quantification of *fabp10a:*CFP expression in the regenerating larvae treated with DMSO or BET inhibitors, as shown in (*d*) (one-way ANOVA, * = $p < 0.05$, ** = $p < 0.01$, *** = $p < 0.001$). Error bars: ± SEM; scale bars: 100 μm.

all hepatocytes weakly expressed *Tp1:*H2B-mCherry (Fig. 14D, arrows) but not mature BEC marker Alcam as previously reported (232), indicating hepatocytes with BEC origin. However, in APAP-treated larvae at R24h no hepatocytes expressed *Tp1:*H2B-mCherry (Fig. 14D), revealing that liver regeneration in the zebrafish APAP-induced injury model is hepatocyte- but not BEC-driven. To inhibit BET proteins, we used two different BET inhibitors, JQ1 (11) and iBET151 (13), which both block BET proteins by specifically binding to acetyl-recognizing BET pockets. Treatment with JQ1 or iBET151 immediately following 36-hour APAP treatment (R0h) significantly reduced liver size after 24 or 48 hours of recovery (R24h and R48h, respectively), as assessed by hepatocyte-specific *fabp10a:*CFP expression (Fig. 14E-G), supporting the positive role of BET proteins in hepatocyte-driven liver regeneration.

Given the reduced liver size in BET-inhibited larvae (Fig. 14G) and the role of BET proteins in proliferation (227), we examined hepatocyte proliferation using the *Tg(fabp10a:mAGFP-gmnn)* line that expresses geminin fused with monomeric Azami green fluorescent proteins in hepatocytes (227). As geminin is degraded in G0 and G1 phases (260), this line reveals proliferating hepatocyte in S/G2/M phases (227). Hepatocyte proliferation was greatly increased in APAP-treated larvae compared with control larvae at 5 days post-fertilization (dpf) (Fig. 15B and C). JQ1 treatment significantly reduced the hepatocyte proliferation induced by APAP overdose (Fig. 15B and C), suggesting the crucial role of BET proteins in hepatocyte

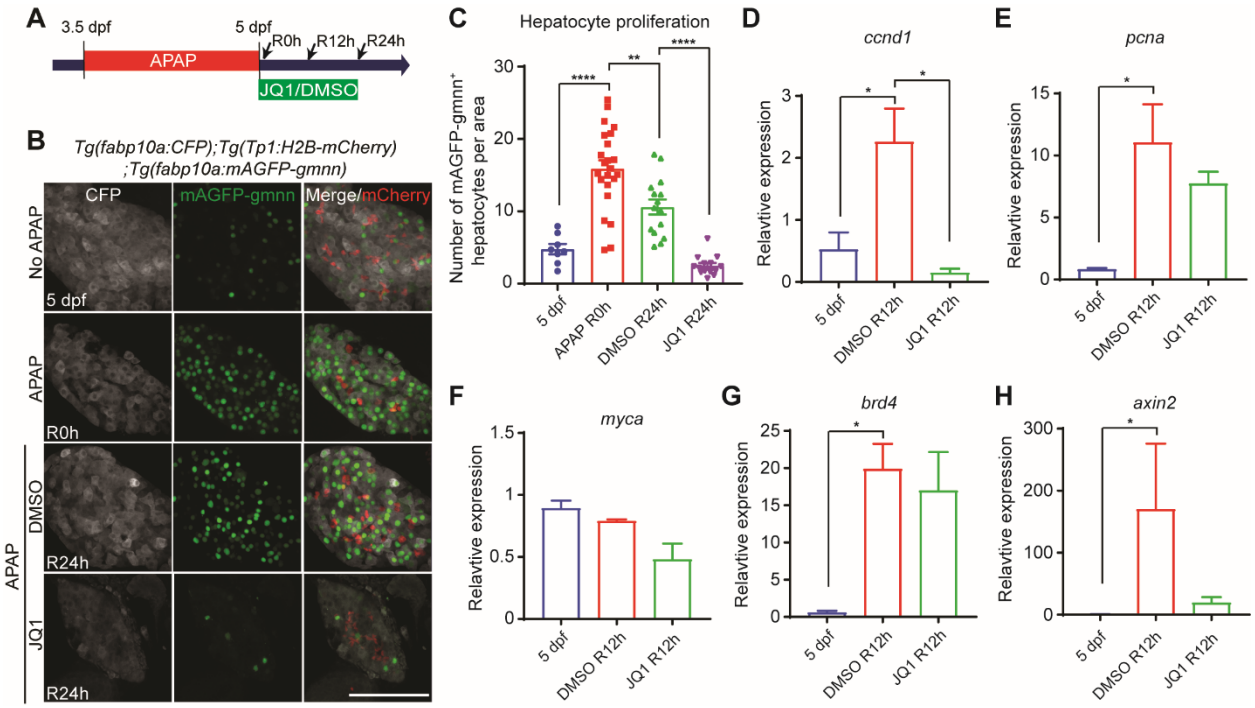

Figure 15: BET inhibition reduces hepatocyte proliferation in the zebrafish APAP-induced injury model.

(*a*) Scheme illustrating the periods of APAP and JQ1 treatments and analysis stages (arrows). (*b*) Confocal images showing the hepatic expression of *fabp10a:*CFP (grey, hepatocytes), *Tp1:*H2B-mCherry (red, BECs) and *fabp10a:*mAGFP-gmnn (green, proliferating hepatocytes). (*c*) Quantification of the number of mAGFP-gmnn$^+$ cells, as shown in (B) (one-way ANOVA, ** = $p < 0.01$, **** = $p < 0.0001$). (*d-h*) qPCR data showing the relative expression levels of *ccnd1*, *pcna*, *myca*, *brd4* and *axin2* among uninjured control livers at 5 dpf and DMSO- and JQ1-treated regenerating livers at R12h (one-way ANOVA, * = $p<0.05$). Error bars, ± SEM; scale bar, 100 µm.

proliferation during regeneration. This proliferation phenotype was further supported by the reduced expression of *ccnd1* (Fig. 15D), consistent with our mouse data (Fig. 8D). However, other proliferation-related genes, such as *pcna* and *myca*, were not significantly reduced in JQ1-treated livers (Fig. 15E and F). *brd4* expression was significantly upregulated in APAP-treated livers compared with untreated control livers (Fig. 15G), as observed in a zebrafish BEC-driven liver regeneration model (227). Additionally, similar to the mouse PHx model (Fig. 8G), expression of Wnt/β-catenin signaling target *axin2* tended to be lower in JQ1-treated larvae after APAP overdose

(Fig. 15H). Altogether, these zebrafish data together with our mouse data strongly support the observation that BET proteins regulate hepatocyte-driven liver regeneration.

2.4.7 BET Inhibition Represses Wnt/β-catenin Signaling in APAP-Treated Zebrafish Livers.

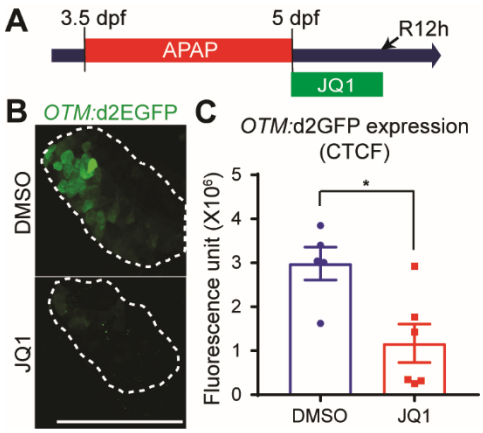

Figure 16: BET inhibition reduces Wnt/β-catenin signaling in the zebrafish APAP-induced injury model.

(*a*) Scheme illustrating the periods of APAP and JQ1 treatments and analysis stage (arrow). (*b*) Confocal images showing the hepatic expression of *OTM:*d2EGFP (green, Tcf/Lef reporter activity) in regenerating larvae at R12h. Dotted white line outlines the liver. (*c*) Quantification of *OTM:*d2EGFP expression in the regenerating larvae treated with DMSO or JQ1, as shown in (*b*) (t-test, * = $p < 0.05$). Error bars, ± SEM; scale bar, 100 μm.

Given the crucial role of Wnt/β-catenin signaling in liver regeneration induced by APAP overdose (87, 254) and the reduced expression of Wnt target genes *ccnd1* and *axin2* in JQ1-treated regenerating zebrafish livers (Fig. 15D and H), we hypothesized that BET inhibition could suppress Wnt/β-catenin signaling in livers injured by APAP treatment. To test this hypothesis, we used a Wnt reporter zebrafish line, *Tg(OTM:d2EGFP)*, which expresses destabilized GFP under a promoter containing six copies of Tcf/Lef binding site (234), meaning that the level of GFP expression is driven by β-catenin signaling. GFP expression was significantly reduced in JQ1-

treated regenerating livers compared with DMSO-treated control livers (Fig. 16A-C). These zebrafish data together with the *in vitro* data (Fig. 11 and 12) suggest that BET proteins regulate hepatocyte-driven liver regeneration by regulating Wnt/β-catenin signaling in addition to other signaling pathways.

2.5 Discussion

BET protein inhibitors, such as JQ1, have been proposed for use in the treatment of a variety of conditions due to their ability to inhibit oncogenic gene expression (8, 12, 224), reduce inflammation (261, 262), and protect against liver fibrosis (16). Adding to their therapeutic potential, effective anti-neoplastic doses of JQ1 are well tolerated in animals despite the widespread activity of Brd4 in nearly every tissue type (8, 11, 12). JQ1 has also been shown to be effective in reducing cell growth in a tumor xenograft HCC model (226), which may suggest BET protein inhibitors to be a potential treatment for liver cancer. However, BET proteins also play a role in biliary-driven liver regeneration (227). In the current study, we show that JQ1-mediated inhibition of BET proteins significantly blocks hepatocyte proliferation in two independent models of hepatocyte-driven liver regeneration. Since the majority of HCC cases occur in the patients with chronic liver diseases which in turn are characterized by ongoing regeneration, inadvertent suppression of regeneration during HCC treatment may adversely affect hepatic function. Hence, our findings suggest the use of BET proteins in the treatment of liver pathologies must be carefully considered, as BET protein inhibitors are liable to inhibit the regeneration of normal liver tissue.

Two-thirds partial hepatectomy in rodents is widely used to study the mechanisms of hepatocyte proliferation during liver regeneration (81) and is a useful model for the study of

temporal changes in gene expression during liver regeneration. In our study, we used either early (2 hours post-PHx) or late (16 hours post-PHx) injections of JQ1 to study the effects of BET protein inhibition on hepatocyte proliferation. In both instances, injection of JQ1 resulted in a near total block of hepatocyte proliferation with significant reduction in expression of cell cycle-regulator Cyclin D1, suggesting that transcriptional activation of pro-regeneration genes occurs even many hours after the initial injury. We additionally observed impaired induction of E2f2 downstream targets involved in cell cycle progression, further demonstrating the complete block of hepatocyte proliferation in JQ1-injected mice after PHx.

Our second model to study the role of BET proteins in hepatocyte proliferation was APAP overdose, as APAP-induced ALF is the most common cause of ALF in the United States (256, 258). We performed APAP overdose experiments in zebrafish, as their large clutch sizes, growth in water, optical transparency, and fully developed livers by 5 dpf (263) make them ideal for drug treatment studies. Consistent with our results from our mouse PHx study, we found that JQ1-treated zebrafish larvae displayed significant reductions in hepatocyte proliferation and Cyclin D1 expression during recovery from APAP overdose. Interestingly, in comparison to our mouse PHx model, we detected a large increase in *brd4* expression in zebrafish larvae during recovery from APAP overdose. This finding suggests BET proteins are important regulators of liver regeneration in this model, although there are presently very few studies on the role of BET proteins in liver regeneration after acetaminophen injury. Thus, our work presents an opportunity to study signaling pathways under the control of BET proteins during liver regeneration.

A signaling pathway well-known to be active in promoting liver regeneration (68, 87, 229) in addition to being an oncogenic driver in subsets of liver cancer (264-267) is the Wnt/β-catenin signaling pathway. Our results demonstrate that Wnt/β-catenin signaling targets, such as Cyclin

D1, are significantly reduced in JQ1-treated animals after liver injury. In this respect, mice injected with JQ1 post-PHx are reminiscent of liver-specific β-catenin knockout animals subjected to partial hepatectomy, which show an early lag in hepatocyte proliferation in conjunction with reduced Cyclin D1 levels (229). Furthermore, activation of Wnt/β-catenin signaling is thought to promote liver regeneration after APAP-induced liver injury (87, 254), and our zebrafish results demonstrate that JQ1 is a potent inhibitor of hepatocyte proliferation and Wnt/β-catenin signaling after APAP overdose. Additionally, our *in vitro* experiments revealed that Wnt/β-catenin signaling was sensitive to inhibition by JQ1. Our *in vitro* data showed that knockdown of *BRD4* in Hep3B cells with wild-type β-catenin leads to a reduction in TCF/LEF reporter activity, suggesting the ability of JQ1 to impair β-catenin signaling is mediated at least partially through inhibition of BRD4. However, treatment of HepG2 cells with high doses of JQ1 led to a robust decrease in TCF/LEF reporter activity, suggesting that other BET proteins such as BRD2 and BRD3 may also play a role in regulating β-catenin signaling, although this hypothesis remains to be tested. Together, these data suggest JQ1 as a potent inhibitor of Wnt/β-catenin signaling. However, these results must be considered in a cell type-specific context, as JQ1 had minimal effect on β-catenin/TCF-mediated transcription in colorectal cancer cells (268). This raises the interesting question of whether JQ1 would be especially effective in treating liver cancer with activating β-catenin mutations, as these cancers have been shown to be sensitive to inhibition of β-catenin (267). Although we have demonstrated that JQ1 is capable of inhibiting normal liver regeneration, with careful dose titration BET inhibitors may be capable of inhibiting oncogenic Wnt signaling without impinging signaling pathways required for normal hepatic function. As tumors tend to be addicted to several oncogenic signaling pathways, such as Met and Wnt/β-catenin signaling, while normal liver regeneration occurs through many redundant signaling mechanisms, low doses of

BET inhibitors may be able to selectively inhibit oncogenic Wnt/β-catenin signaling while sparing compensatory regeneration mechanisms in normal liver.

The sensitivity of Wnt/β-catenin signaling to JQ1 may be due in part to proficiency of BET inhibitors to reduce BRD4 enhancer occupancy at super enhancers (8), or large enhancers with multiple TF binding sites, high levels of Mediator occupancy, and high levels of associated gene expression (269-271). Interestingly, super enhancers in colorectal cancer were found to be occupied by TCF4 and thus were sensitive to perturbation of oncogenic Wnt signaling (272), and TF targets of Wnt signaling were found to be enriched for super enhancers in embryonic stem cells (271). Additionally, Cyclin D1 was found to be regulated by a super enhancer in a model of Ewing sarcoma (273). These data suggest that super enhancers under the control of the Wnt/β-catenin signaling pathway may regulate the expression of genes activated during hepatocyte-driven liver regeneration, such as Cyclin D1, although this hypothesis remains to be tested. Very little is known about the role of super enhancer-driven gene expression during liver regeneration, and our model of JQ1 treatment post-PHx may provide a useful platform for the identification of these important signaling mechanisms.

In conclusion, our work has identified the key role of BET proteins in multiple models of hepatocyte-driven liver regeneration. Additionally, we have identified the Wnt/β-catenin signaling pathway, a known important driver of liver regeneration (68, 229), to be sensitive to JQ1-mediated BET protein inhibition resulting in an abrogation of hepatocyte proliferation. Although more work remains to be done to identify the mechanism behind JQ1-mediated inhibition of Wnt/β-catenin signaling, our work has important implications for the clinical use of BET inhibitors. As these drugs are herein demonstrated to be potent inhibitors of normal liver regeneration, their potential

use to treat liver pathologies must be carefully considered, as patients may become more susceptible to liver failure under a regimen of BET protein inhibitors.

3.0 Hepatocyte-Specific β-Catenin Deletion during Severe Liver Injury Provokes Cholangiocytes to Differentiate into Hepatocytes

In this section, we describe how mice with hepatocyte-specific deletion of β-catenin exposed to choline deficient, ethionine-supplemented diet-induced liver injury develop severe liver injury with an impairment of hepatocyte proliferation. We further describe how in the β-catenin knockout mice BECs transdifferentiate into hepatocytes to mediate liver regeneration using both negative and positive lineage tracing models. The work in this section was published in Hepatology, PMID 30215850 (188). As first author, the publisher John Wiley & Sons has granted full permission to reuse the manuscript in this dissertation.

3.1 Paper Summary

Liver regeneration after injury is normally mediated by proliferation of hepatocytes, although recent studies have suggested biliary epithelial cells (BECs) can differentiate into hepatocytes during severe liver injury when hepatocyte proliferation is impaired. We investigated the effect of hepatocyte-specific β-catenin deletion in recovery from severe liver injury and BEC-to-hepatocyte differentiation. To induce liver injury, we administered choline-deficient, ethionine-supplemented (CDE) diet to three different mouse models, the first being mice with deletion of β-catenin in both BECs and hepatocytes (*Albumin-Cre; Ctnnb1*$^{flox/flox}$ mice). In our second model, we performed hepatocyte lineage tracing by injecting *Ctnnb1*$^{flox/flox}$; *Rosa-stop*$^{flox/flox}$*-EYFP* mice with the adeno-associated virus serotype 8 encoding Cre recombinase under the control of the

thyroid binding globulin promoter (AAV8-TBG-Cre), a virus which infects only hepatocytes. Finally, we performed BEC lineage tracing via *Krt19-Cre*^{ERT}; *Rosa-stop*$^{flox/flox}$*-tdTomato* mice. To observe BEC-to-hepatocyte differentiation, mice were allowed to recover on normal diet following CDE diet-induced liver injury. Livers were collected from all mice and analyzed by quantitative real-time polymerase chain reaction, western blotting, immunohistochemistry, and immunofluorescence. We show that mice with lack of β-catenin in hepatocytes placed on the CDE diet develop severe liver injury with impaired hepatocyte proliferation, creating a stimulus for BECs to differentiate into hepatocytes. In particular, we use both hepatocyte and BEC lineage tracing to show that BECs differentiate into hepatocytes, which go on to repopulate the liver during long-term recovery. Conclusion: β-catenin is important for liver regeneration after CDE diet-induced liver injury, and BEC-derived hepatocytes can permanently incorporate into the liver parenchyma to mediate liver regeneration.

3.2 Background

Despite the liver's capacity for regeneration, chronic liver disease and cirrhosis is the 12th leading cause of death in the United States (219). This significant morbidity is attributable to lack of treatments for advanced liver disease besides liver transplantation, for which there is a severe shortage of donor organs (274). Often, hepatocytes and biliary epithelial cells (BECs) can replicate to replenish their respective cell types and eventually restore hepatic mass following injury. However, livers of patients with chronic liver disease exhibit ductular reaction (116, 275, 276), with the degree of BEC expansion correlating with disease severity (115, 277). The role of ductular reaction in liver regeneration (LR) remains controversial, although studies are beginning to show

BECs may be giving rise to hepatocytes. Indeed, experimentally, when endogenous hepatocyte proliferation is impaired, reactive BECs (183, 194) can differentiate into hepatocytes to mediate repair (80, 218). Alternatively, hepatocytes can differentiate into BECs, which can then be incorporated into biliary ductules (208, 215) and may revert back to hepatocytes when injury is withdrawn (214). There is evidence of BEC-to-hepatocyte differentiation in both humans (104, 112) and animal models of liver injury where hepatocyte proliferation is blocked (171, 187, 191) or after near total loss of hepatocytes (232).

The choline-deficient, ethionine-supplemented (CDE) diet is a well-known liver injury diet which induces proliferation of reactive BECs (175, 176). Recent lineage tracing studies have demonstrated limited contribution of BECs to hepatocytes in CDE diet fed mice (150, 190, 278), leading to the conclusion that BECs do not contribute significantly to the restoration of hepatocyte mass after chronic liver injury. However, the CDE diet does not block hepatocyte proliferation (190), and thus is unable to provide the correct milieu for BEC-to-hepatocyte transdifferentiation. Since the Wnt/β-catenin signaling pathway is a major driver of hepatocyte proliferation during LR (68, 279), we investigated if CDE diet-induced injury to conditional β-catenin knockout mice will necessitate BEC-mediated liver repair. We utilized multiple mouse models to perform hepatocyte and BEC lineage tracing in mice that underwent modulation of β-catenin expression and were administered CDE diet. Our results demonstrate that loss of β-catenin in hepatocytes during CDE diet-induced liver injury indeed impairs hepatocyte proliferation, triggering the expansion of BECs which subsequently differentiate into hepatocytes. We have successfully established a model which will lend itself well to the study of the mechanisms of BEC expansion and differentiation.

3.3 Methods

3.3.1 Mouse strains, Viral Infections, Tamoxifen Administration, In Vivo RNAi, and Diet

All animals are housed in temperature and light-controlled facilities and are maintained in accordance with the Guide for Care and Use of Laboratory Animals and the Animal Welfare Act. *Albumin-Cre;Ctnnb1*$^{flox/flox}$ mice or KO1 and wild-type littermate controls (WT1) (74) were maintained on a C57BL/6 background. *Ctnnb1*$^{flox/flox}$;*Rosa-stop*$^{flox/flox}$*-EYFP* reporter mice were generated through breeding *Ctnnb1*$^{flox/flox}$ mice with *Rosa-stop*$^{flox/flox}$*-EYFP* mice (Jackson Laboratories). *Krt19-Cre*^{ERT};*Rosa-stop*$^{flox/flox}$*-tdTomato* reporter mice were described previously (191). To label hepatocytes and generate KO2 mice, 23–25 day-old *Ctnnb1*$^{flox/flox}$;*Rosa-stop*$^{flox/flox}$*-EYFP* mice were injected intraperitoneally with $1x10^{12}$ genome copies (GCs) of adeno-associated virus serotype 8 encoding Cre recombinase under the hepatocyte-specific thyroid binding globulin promoter (AAV8-TBG-Cre) (Penn Vector Core) followed by a 12 days (12d) washout period. To generate WT2 mice, the same AAV8-TBG-Cre was injected into or *Ctnnb1*$^{+/+}$;*Rosa-stop*$^{flox/flox}$*-EYFP* mice. To label BECs, *Krt19-Cre*^{ERT};*Rosa-stop*$^{flox/flox}$*-tdTomato* mice were given 3 doses of 12.5 mg/kg tamoxifen during postnatal week 1, followed by 2 weeks (2W) washout. For the liver injury time point, 4–5w-old mice were given choline-deficient diet (Envigo Teklad Diets) supplemented with 0.15% ethionine drinking water (Acros Organics, 146170100) for 2-3w (*Krt19-Cre*^{ERT};*Rosa-stop*$^{flox/flox}$*-tdTomato* mice). For recovery time points, animals were switched back to normal chow diet for 3d up to 6 months (6m) after 2W of CDE diet. For *in vivo* knockdown of β-catenin expression, both C57BL6/NJ (Charles River) and *Krt19-Cre*^{ERT}; *Rosa-stop*$^{flox/flox}$*-tdTomato* mice were given biweekly or weekly subcutaneous injections of 5 mg/kg GalXC-*Ctnnb1* (Dicerna Pharmaceuticals) starting 1W prior to CDE diet administration and continuing throughout CDE

diet and recovery periods. GalXC is a Dicerna Pharmaceuticals *Ctnnb1* RNAi conjugated to hepatocyte targeting ligand N-acetylgalactosamine, which allows for hepatocyte-specific knockdown of target gene expression (280). Serum biochemistry analysis was performed by automated methods at the University of Pittsburgh Medical Center clinical chemistry laboratory. All studies were performed according to the guidelines of the National Institutes of Health and the University of Pittsburgh Institutional Animal Use and Care Committee.

3.3.2 Immunohistochemistry

Tissue samples were drop-fixed in 10% buffered formalin for 48 hours prior to paraffin embedding. Samples were cut into 4 μm sections, deparaffinized, and washed with PBS. For antigen retrieval, samples were microwaved for 12 minutes in pH6 sodium citrate buffer (Cyclin D1, PanCK, GS, CD45) or Tris-EDTA buffer (Ki67), or were pressure cooked for 20 minutes in pH6 sodium citrate buffer (β-catenin), Dako Target Retrieval Solution (Dako, S1699) (CK19, EpCAM), or pH9 EDTA buffer (αSMA). After cooling, samples were placed in 3% H_2O_2 for 10 minutes to quench endogenous peroxide activity. After washing with PBS, slides were blocked with Super Block (ScyTek Laboratories, AAA500) for 10 minutes or 10% goat serum in PBS for 10 minutes (GS, p21). The primary antibodies were incubated at the following concentrations in antibody diluent (PBS + 1% BSA (Fisher BioReagents, BP1605-100) with 0.1% Tween™ 20 (Fisher BioReagents, BP337-500)): GS (Sigma G2781, 1:1500), Ki67 (Thermo Scientific RM-9106-S, 1:100), PanCK (Dako Z0622, 1:200), Cyclin D1 (Abcam ab134175, 1:200), β-catenin (Abcam ab32572, 1:100) for one hour at room temperature or at 4°C overnight: p21 (Santa Cruz sc-471, 1:25), EpCAM (Biolegend 118201, 1:50), CK19 (DSHB TROMA III, 1:10). Samples were washed with PBS three times and incubated with the appropriate biotinylated secondary antibody

(Vector Laboratories) diluted 1:500 or 1:1000 (GS) in antibody diluent for 30 minutes at room temperature. Samples were washed with PBS three times and sensitized with the Vectastain® ABC kit (Vector Laboratories, PK-6101) for 30 minutes. Following three washes with PBS color was developed with DAB Peroxidase Substrate Kit (Vector Laboratories, SK-4100), followed by quenching in distilled water for five minutes. Slides were counterstained with hematoxylin (Thermo Scientific, 7211), dehydrated to xylene and coverslips applied with Cytoseal™ XYL (Thermo Scientific, 8312-4). For H&E staining, samples were deparaffinized and stained with hematoxylin (Thermo Scientific, 7211) and eosin (Thermo Scientific, 71204), followed by dehydration to xylene and application of a coverslip. For Sirius Red staining, samples were deparaffinized and incubated for one hour in Picro-Sirius Red Stain (American MasterTech, STPSRPT), washed twice in 0.5% acetic acid water, dehydrated to xylene, and coversliped. Images were taken on a Zeiss Axioskop 40 inverted brightfield microscope. Images for tiling were taken on a Zeiss Axio Observer.Z1 microscope and assembled utilizing ZEN Imaging software.

3.3.3 Immunofluorescence

Tissue samples were drop fixed in 10% buffered formalin overnight, cryopreserved in 30% sucrose in PBS overnight, frozen in OCT compound (Sakura, 4583) and stored at -80°C or alternatively were paraffin embedded after formalin fixation. Cryopreserved samples were cut into 5 µm sections, allowed to air-dry, and then washed in PBS, while paraffin-embedded samples were cut into 4 µm sections and deparaffinized to PBS. Antigen retrieval was performed through pressure cooking for 20 minutes with Dako Target Retrieval Solution (Dako, S1699) or through microwaving in pH 6 sodium citrate buffer (PanCK, RFP, CYP2D6, GS, CK19). After cooling, slides were washed with PBS and permeabilized with 0.1% Triton X-100 in PBS for 20 minutes

at room temperature. Samples were washed three times with PBS and then blocked with 2% Donkey serum in 0.1% Tween™ 20 in PBS (antibody diluent) for 30 minutes at room temperature. Antibodies were diluted as follows: β-catenin (Abcam ab32572, 1:100), PanCK (Dako Z0622, 1:200), Hnf4α (Santa Cruz sc-6556, 1:50), GFP (Abcam ab13970, 1:200), CK19 (DSHB TROMA-III-s, 29 µg/ml), PCNA (Santa Cruz sc-56, 1:1000), RFP (Rockland 600-401-379, 1:200), GS (Abcam ab73593, 1/200), CYP2D6 (Gift from R. Wolfe, University of Dundee, 1/500) in antibody diluent and incubated at 4℃ overnight. Samples were washed three times in PBS and incubated with the proper fluorescent secondary antibody (AlexaFluor 488/555/647, Invitrogen) diluted 1:800 in antibody diluent for two hours at room temperature. Samples were washed three times with PBS and incubated with DAPI (Sigma, B2883) for 1 minute. Samples were washed three times with PBS and mounted with fluromount (SouthernBiotech) or ProLong™ Gold antifade reagent (Invitrogen, P10144). Images were taken on a Nikon Eclipse Ti epifluorescence microscope or a Zeiss LSM700 confocal microscope.

3.3.4 Western Blotting

To extract protein, whole liver tissue was homogenized in RIPA buffer as previously described (74). Protein was separated on pre-cast 4-20% or 7.5% polyacrylamide gels (Bio-Rad) and transferred to a nitrocellulose membrane using the Trans-Blot Turbo Transfer System (Bio-Rad). Membranes were blocked for 30 minutes with 5% skim milk (LabScientific, Cat# M0841) or 5% BSA in Blotto buffer (0.15 M NaCl, 0.02 M Tris pH 7.5, 0.1% Tween in dH2O), and incubated with primary antibodies at 4℃ overnight at the following concentrations: β-catenin (BD Biosciences 610154, 1:1000 in 5% milk), Active β-catenin (Cell Signaling cs-4270, 1:800 in 5% BSA), Cyclin D1 (Thermo Fisher RB-9041-P, 1:200 in 5% milk), GS (Santa Cruz sc-74430,

1:2000 in 5% milk), p21 (Santa Cruz sc-271532, 1:50 in 5% milk), αSMA (Abcam ab5694, 1:1000 in 5% milk), GAPDH (Santa Cruz sc-25778, 1:1000 in 5% milk). Membranes were washed in Blotto buffer and incubated with the appropriate HRP-conjugated secondary antibody for 1 – 3 hours at room temperature. Membranes were washed with Blotto buffer, and bands were developed utilizing SuperSignal® West Pico Chemiluminescent Substrate (Thermo Scientific, Prod# 34080) and visualized by autoradiography.

3.3.5 RT-PCR

Whole liver was homogenized in TRIzol™ (Thermo Scientific, Cat# 15596026), treated with chloroform, and nucleic acid was precipitated with isopropanol. Cellular DNA was digested with DNA-free™ Kit (ambion, AM1906), and RNA was reverse-transcribed into cDNA using SuperScript® III (Invitrogen, 18080-044). Real-time PCR was performed in technical triplicate on a StepOnePlus™ Real-Time PCR System (Applied Biosystems, Cat# 4376600) using the Power SYBR® Green PCR Master Mix (Applied Biosystems, 4367660). Target gene expression was normalized to the average of two housekeeping genes (*Gapdh* and *Rn18s*), and fold change was calculated utilizing the ΔΔ-Ct method. Primers are listed in Table 3.

Table 3: List of primers used in the Hepatology study

Gene	Forward Primer (5' – 3')	Reverse Primer (5' – 3')
Ccnd1	TTTCTTTCCAGAGTCATCAAGTGT	TGACTCCAGAAGGGCTTCAA
Ctnnb1	ACTTGCCACACGTGCAATTC	AAGGTTGTGCAGAGTCCCAG
Col1a1	TCCGGCTCCTGCTCCTCTTA	GTATGCAGCTGACTTCAGGGATGT
Acta2	CCGAGATCTCACCGACTACC	TCCAGAGCGACATAGCACAG
Sox9	GTGCAAGCTGGCAAAGTTGA	TGCTCAGTTCACCGATGTCC
Krt19	CCAGGAAGCCCACTACAACAA	TCGAGGGAGGGGTTAGAGTAAA
Gapdh	AACTTTGGCATTGTGGAAGG	ACACATTGGGGGTAGGAACA
Rn18s	GTAACCCGTTGAACCCCATT	CCATCCAATCGGTAGTAGCG

3.3.6 Statistics

For analysis of serum biochemistry between two groups, a two-tailed t-test was performed. For analysis of gene expression data between more than two groups, a one-way ANOVA was performed. For analysis of cell counts, such as proliferating hepatocytes, a Mann-Whitney U Test was performed. For analysis of change in body weight over time, a two-way ANOVA was performed. A $p<0.05$ was considered significant, and plots are mean ±SD. All statistical analysis and graph generation was performed using GraphPad Prism 7 software.

3.4 Results

3.4.1 β-catenin is Important for LR after CDE Diet-Induced Liver Injury

To test whether lack of β-catenin in hepatocytes impairs hepatocyte proliferation in a chronic liver injury setting, we placed KO1 mice (74) lacking β-catenin in hepatocytes and BECs, and WT1 mice on CDE diet for 2W (Fig. 17A). KO1 showed severe histological abnormalities including steatohepatitis (Fig. 17F), with gross liver morphology displaying pale and smaller livers (Fig. 17B). Serum liver injury markers, alanine aminotransferase (ALT) (Fig. 17C), serum aspartate aminotransferase (AST) (Fig. 18D), and bilirubin (Fig. 17D) were significantly elevated in KO1 compared to WT1 on CDE diet. There was no difference in serum alkaline phosphatase (ALP) levels in WT1 and KO1 mice (Fig. 18E). Both WT1 and KO1 displayed characteristic expansion of reactive BECs, which are positive for BEC-marker CK19 (Fig. 18A), although KO1 displayed a more robust BEC expansion as determined by increased expression of BEC markers

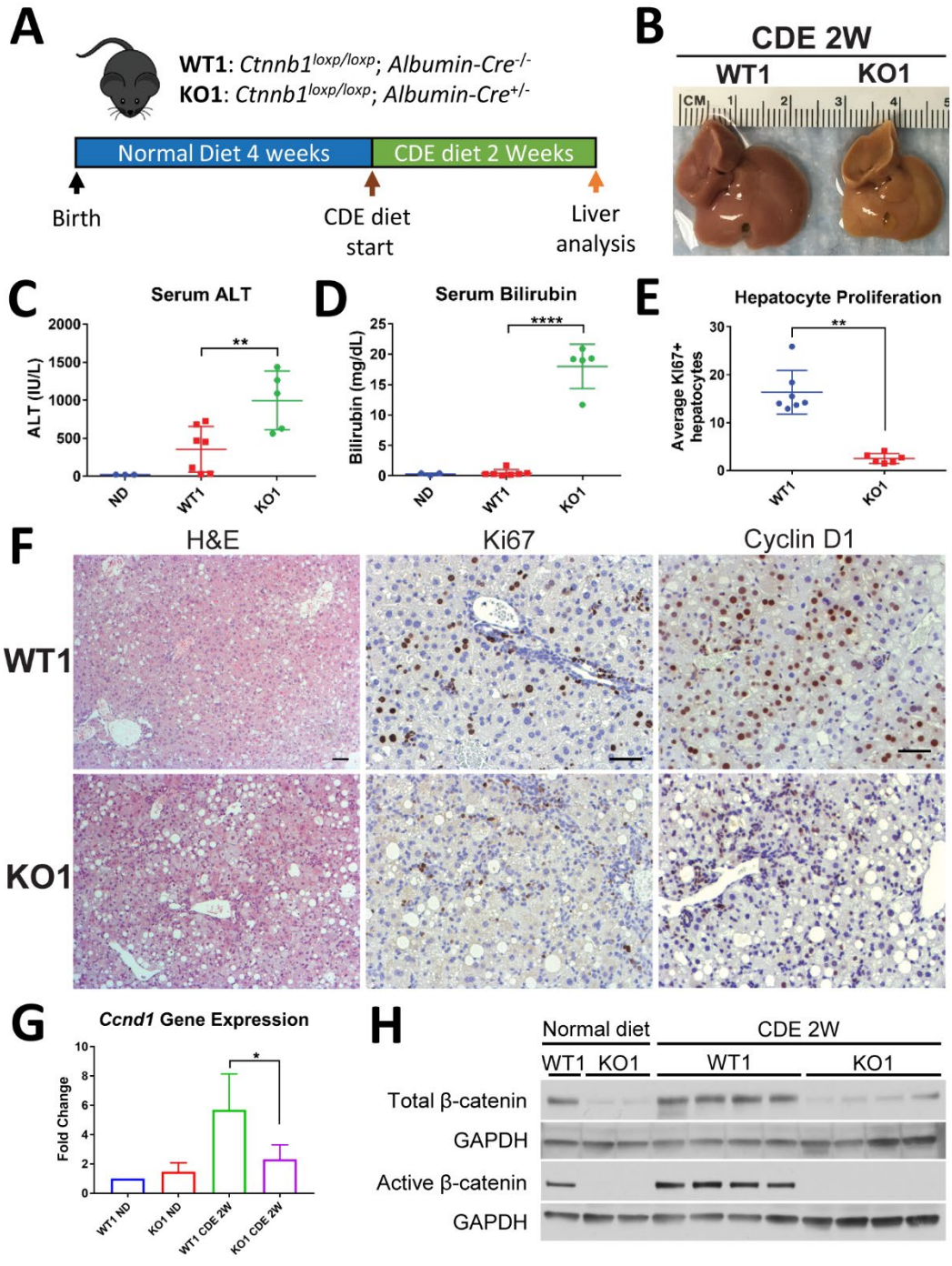

Figure 17: KO1 mice display severe liver injury and impaired hepatocyte proliferation after CDE diet.

(*a)* Four-week-old male WT1 and KO1 mice were placed on CDE diet for 2W to induce liver injury. (*b)* Gross liver morphology reveals small and pale livers in KO1 mice after 2W of CDE diet. (*c)* Serum liver injury marker alanine aminotransferase (ALT) is significantly elevated in KO1 mice after CDE diet compared to both WT1 mice and baseline normal diet (ND) levels (t-test, ** = $p < 0.01$). (*d)* Serum bilirubin is significantly elevated in KO1 mice after CDE diet compared to both WT1 mice and baseline normal diet (ND) levels (t-test, **** = $p < 0.0001$). (*e)*

Quantification of hepatocyte proliferation in mice after 2W of CDE diet reveals significantly impaired hepatocyte proliferation in KO1 mice (Mann-Whitney U test, ** = $p < 0.01$). (*f)* KO1 mice display prominent steatohepatitis and few Ki67 or Cyclin D1-positive hepatocytes (scale bar 50 μm). (*g)* Hepatic *Ccnd1* gene expression is upregulated after 2W of CDE diet, but is impaired in KO1 mice (One-way ANOVA, * = $p < 0.05$). (*h)* Whole liver lysates display dramatically reduced levels of β-catenin and active β-catenin in KO1 mice while WT1 animals exhibit upregulation of both proteins after CDE diet.

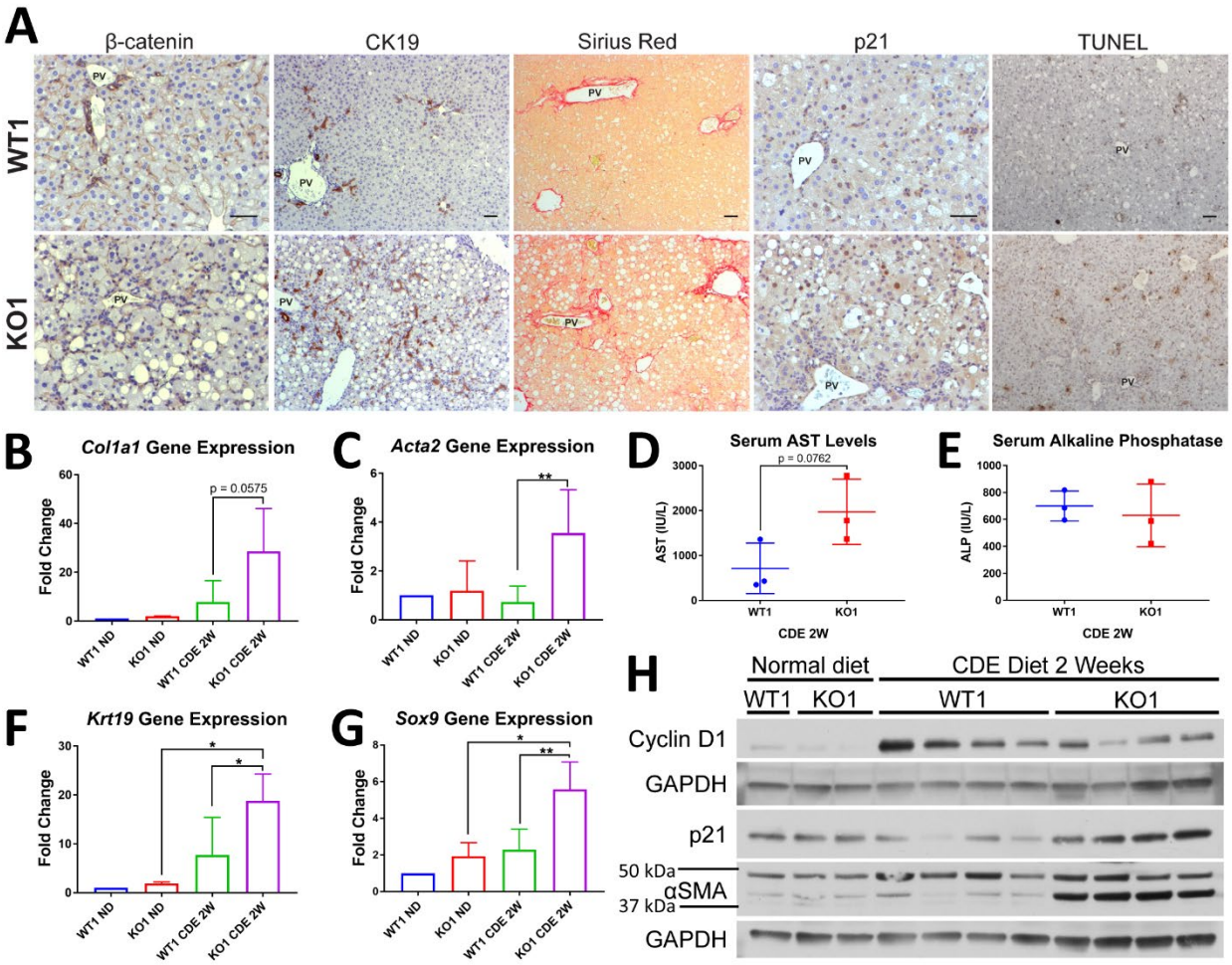

Figure 18: KO1 mice develop fibrosis and a robust BEC response after two weeks of CDE diet.

(*a)* IHC staining reveals loss of β-catenin expression in both hepatocytes and BECs in KO1 mice. Additionally, KO1 mice display robust expansion of BECs by CK19 staining, fibrosis by Sirius Red, an increase in p21-positive hepatocytes compared to WT1 mice, and TUNEL-positive cells in both WT1 and KO1 mice after two weeks of CDE diet (scale bar 50 μm). PV = portal vein. (*b*) KO1 mice display an increase in *Col1a1* gene expression (one-way ANOVA, $p = 0.0575$). (*c*) KO1 mice display a significant increase in *Acta2* (α-smooth muscle actin) gene expression compared to WT1 mice (one-way ANOVA, $p < 0.01$). (*d)* Elevated serum AST levels in KO1 mice compared to WT1 mice after two weeks of CDE diet (t-test, $p = 0.0762$). (*e)* No difference in serum ALP levels in KO1 and WT1 mice after two weeks of CDE diet. (*f)* KO1 mice display a significant increase in *Krt19* gene expression compared to WT1 mice (one-way ANOVA, $p < 0.05$) and KO1 mice on normal diet (one-way ANOVA, $p < 0.05$). (*g*) KO1 mice display a significant increase in *Sox9* gene expression compared to WT1 mice (one-way ANOVA, $p < 0.01$) and KO2 mice on normal diet (one-way ANOVA, $p < 0.05$). (*h*) KO1 mice on CDE diet for two weeks express less Cyclin D1, more p21, and more α-smooth muscle actin (molecular weight 42 kDa) compared to WT1 littermates.

Krt19 and *Sox9* (Fig. 18F, G). KO1 also displayed increased fibrosis by Sirius Red staining (Fig. 18A) and increased expression of pro-fibrotic genes *Col1a1* (Fig. 18B) and *Acta2* (Fig. 18C, H). We detected increased cell death as evidenced by TUNEL staining (Fig. 18A) and increased hepatocyte senescence in KO1 as evidenced by an increase in p21-positive hepatocytes (Fig. 18A) and increased levels of p21 protein (Fig. 18H) compared to WT1. Collectively, we detect severe liver injury in KO1 mice on CDE diet.

To determine if there was a defect in LR in KO1, we assessed hepatocyte proliferation via Ki67 and Cyclin D1 IHC (Fig. 17F). While WT1 displayed robust hepatocyte proliferation and Cyclin D1 expression especially in periportal hepatocytes, KO1 displayed significantly impaired hepatocyte proliferation (Fig. 17E) and reduced *Ccnd1* expression (Fig. 17G) and protein (Fig. 18H). As expected, low levels of β-catenin protein were observed in KO1 livers, likely due to non-parenchymal cells (Fig. 17H). However, there was no expression of active-β-catenin (hypophosphorylated) in KO1 mice even after CDE diet (Fig. 17H). Alternatively, there was increased total and active-β-catenin levels in WT1 mice on CDE diet compared to normal diet (Fig. 17H). This suggests activation of β-catenin signaling is contributing to hepatocyte proliferation, and deletion of β-catenin leads to impaired hepatocyte proliferation and defective LR after CDE diet.

3.4.2 Lack of β-catenin in Hepatocytes Impairs Hepatocyte Proliferation and Promotes Injury from the CDE Diet

As KO1 mice on CDE diet displayed severe liver injury, impaired hepatocyte proliferation, and robust expansion of BECs, we hypothesized BEC differentiation to hepatocytes would be activated to mediate restoration of hepatocyte mass. To test this hypothesis we generated KO2

mice (186). Genes in the *Rosa* locus are ubiquitously expressed, but prior to Cre recombination a floxed stop codon inactivates expression of the *Rosa*-driven enhanced yellow fluorescence protein (EYFP) reporter gene (281). AAV8 infects only hepatocytes, and greater than 99% of hepatocytes can be permanently labeled with EYFP after AAV8-TBG-Cre injection (186, 189, 190). We administered a single injection of AAV8-TBG-Cre and allowed 12d washout before administering CDE diet (Fig. 19A) to allow for clearance of residual viral genome (282). In KO2, hepatocytes lack β-catenin expression and are permanently labeled with EYFP (Fig. 19B). Importantly, BECs are not infected with AAV8 and thus retain β-catenin and do not express EYFP. Therefore, hepatocytes originating from BECs will be negative for EYFP and express β-catenin (Fig. 19F). As controls, WT2 mice showed EYFP-labeled hepatocytes that retain β-catenin expression. IHC confirmed β-catenin expression in hepatocytes in WT2 mice but not in KO2 mice (Fig. 20A).

KO2 on CDE diet, like KO1, showed severe liver injury reflected by significantly increased serum AST (Fig. 19C), serum ALT (Fig. 20D), and bilirubin levels (Fig. 19D) as compared to WT2. WT2 mice on CDE diet initially lost weight but began to recover after 5–7d. In contrast, KO2 mice continued to lose weight over the course of CDE diet administration (Fig. 19E), suggesting failure to recover from injury. Both WT2 and KO2 mice displayed expansion of BECs (Fig. 20A), confirmed by increased *Krt19* (Fig. 20F) and *Sox9* (Fig. 20G) expression. KO2 and WT2 mice developed fibrosis after 2W of CDE diet evident by increased Sirius Red staining (Fig. 20A) and increased expression of Col1a1 (Fig. 20B) and Acta2 (Fig. 20C). KO2 mice on CDE diet also displayed increased p21-positive hepatocytes (Fig. 20A) and overall p21 protein levels (Fig. 20H).

When hepatocyte proliferation was assessed by Ki67 staining, WT2 mice also displayed robust periportal hepatocyte proliferation, which was nearly absent in KO2 mice (Fig. 19G-H).

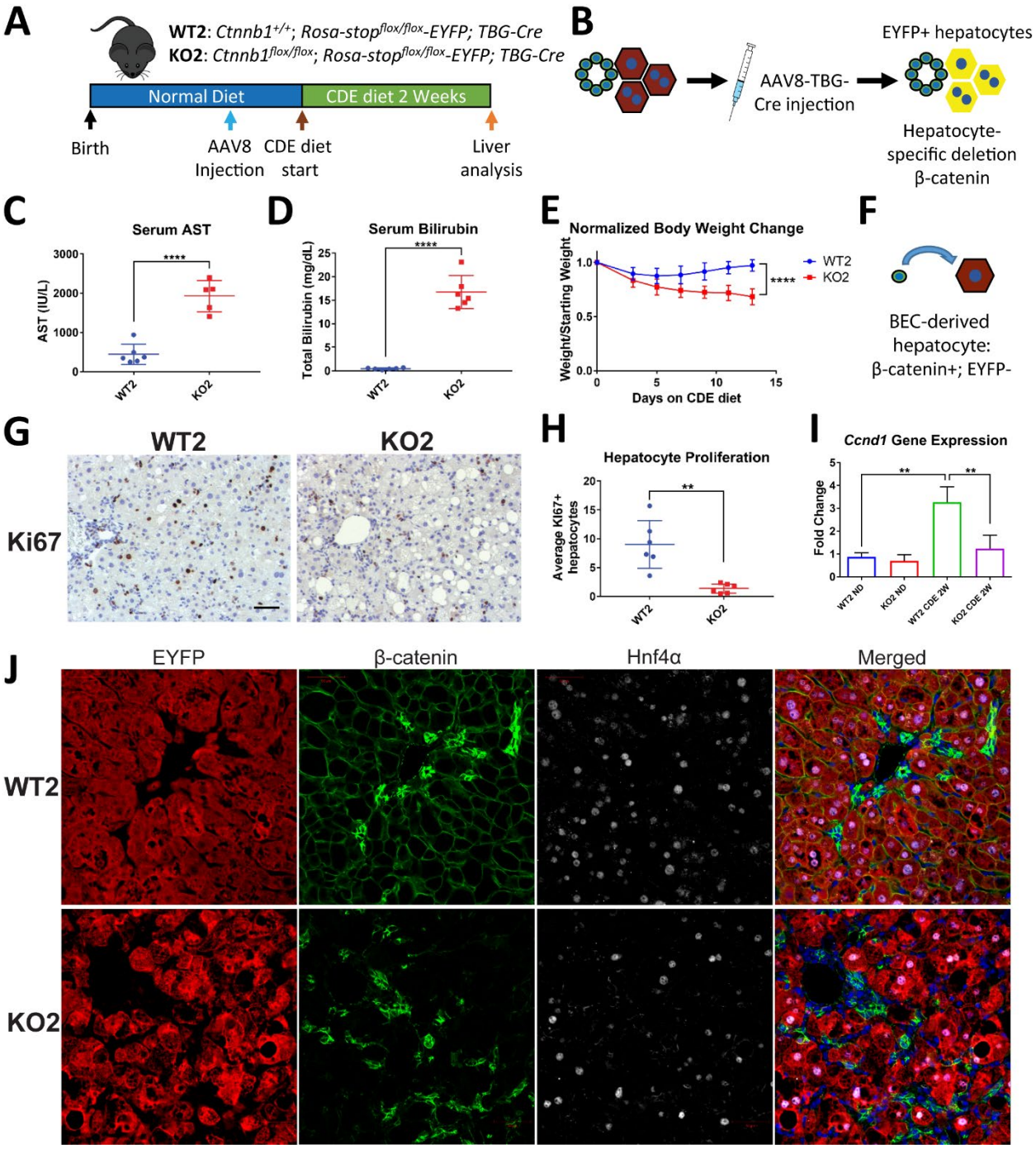

Figure 19: KO2 mice display severe liver injury and impaired hepatocyte proliferation after CDE diet-induced liver injury.

(*a*) 24-25 day old male *Ctnnb1$^{flox/flox}$; Rosa-stop$^{flox/flox}$-EYFP or Ctnnb1$^{+/+}$; Rosa-stop$^{flox/flox}$-EYFP* mice were injected with AAV8-TBG-Cre to generate KO2 and WT2 mice respectively, followed by 12ds of wash-out on normal diet before 2W of CDE diet. (*b*) Schematic of cell labeling after AAV8-TBG-Cre injection, only hepatocytes (maroon hexagons) will be labeled with EYFP and

will lose β-catenin expression (black outline). BECs (green circles) will not be altered by AAV8-TBG-Cre injection. (*c*) Serum liver injury marker aspartate aminotransferase (AST) is significantly elevated in KO2 mice after CDE diet compared to WT2 mice (t-test, **** = $p < 0.0001$). (*d*) Serum bilirubin is significantly elevated in KO2 mice after CDE diet compared to WT2 mice (t-test, **** = $p < 0.0001$). (*e*) KO2 mice lose significantly more body weight compared to WT2 mice after CDE diet (WT2 n = 22, KO2 n =11, Two-way ANOVA, **** = $p < 0.0001$). (*f*) Schematic of fate-tracing showing that any BECs that give rise to hepatocytes will be negative for EYFP and will express β-catenin. (*g*) IHC shows many Ki67-positive hepatocytes in WT2 mice but not in KO2 after CDE diet (scale bar 50 μm). (*h*) Quantification reveals fewer Ki67-positive hepatocytes in KO2 mice after CDE diet (Mann-Whitney U Test, ** = $p < 0.01$). (*i*) Hepatic *Ccnd1* gene expression is significantly elevated in WT2 mice after CDE diet, but impaired in KO2 mice (One-way ANOVA, ** = $p < 0.01$). (*j*) No BEC-derived hepatocytes (EYFP-negative, β-catenin-positive) were evident in either WT2 or KO2 mice after 2W of CDE diet (scale bar 50 μm).

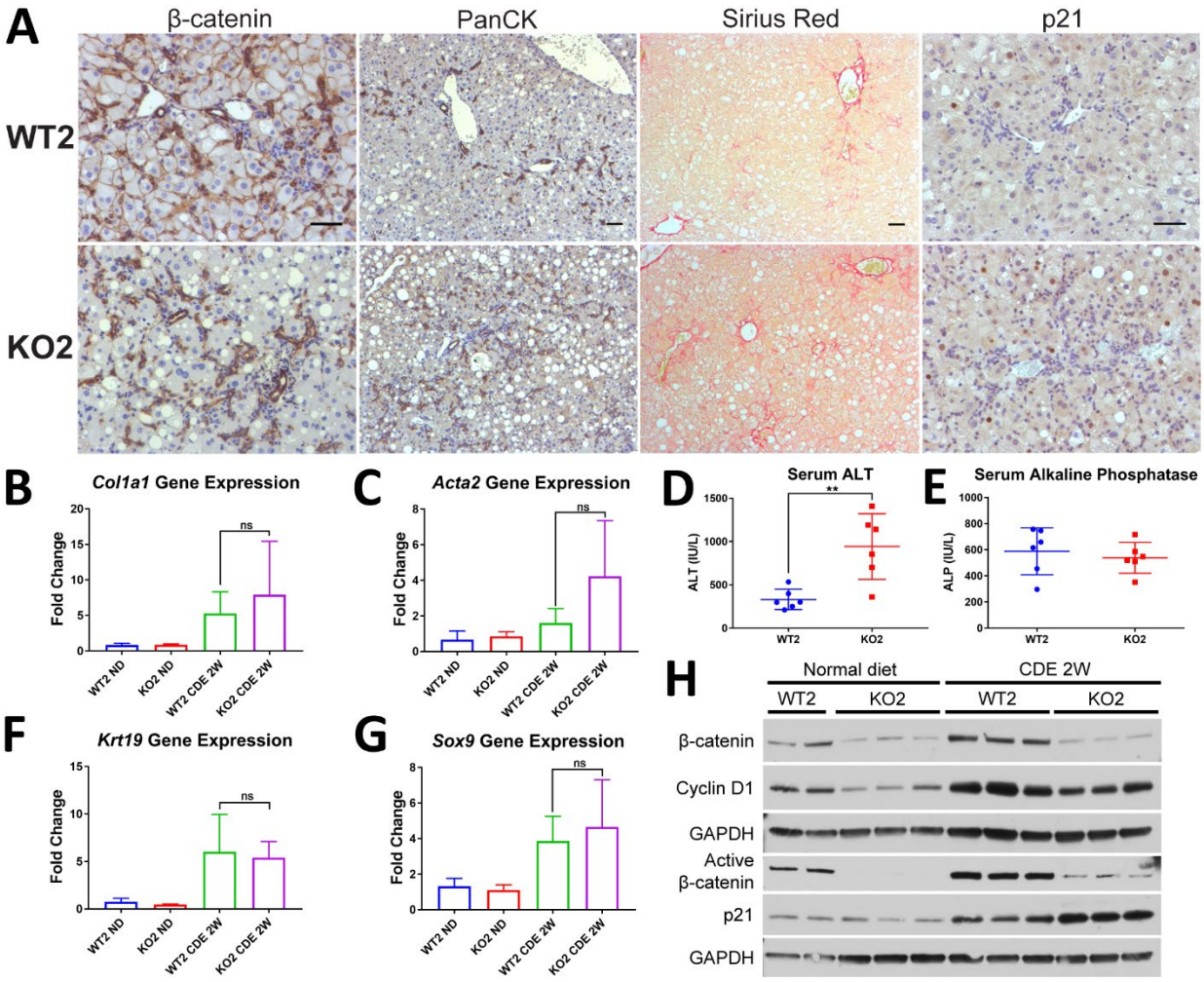

Figure 20: KO2 mice develop fibrosis and a robust BEC response after two weeks of CDE diet.

(*a*) IHC staining reveals a lack of β-catenin expression in hepatocytes in KO2 mice. Additionally, Pan-cytokeratin staining reveals a robust BEC response, Sirius Red the development of fibrosis, and p21 staining reveals an increase in p21-positive hepatocytes in KO2 mice after two weeks of CDE diet compared to WT2 mice (scale bar 50 μm). (*b*) WT2 and KO2 mice display an increase in *Col1a1* gene expression of two weeks of CDE diet. (*c*) WT2 and KO2 mice display an increase in *Acta2* (α-smooth muscle actin) gene expression after two weeks of CDE diet. (*d*) Significantly elevated serum ALT levels in KO2 mice after two weeks of CDE diet (t-test, $p < 0.01$). (*e*) No difference in serum ALP levels in WT2 and KO2 mice after two weeks of CDE diet. (*f*) WT2 and KO2 mice display an increase in *Krt19* gene expression after two weeks of CDE diet. (*g*) WT2 and KO2 mice display an increase in *Sox9* gene expression after two weeks of CDE diet. (*h*) KO2 mice do not display an increase in total β-catenin levels but do show an increase in active β-catenin after two weeks of CDE diet compared to KO2 mice on normal diet. KO2 mice also display less Cyclin D1 and more p21 expression compared to WT2 mice after two weeks of CDE diet.

WT2 mice, like WT1, displayed increased *Ccnd1* gene (Fig. 19I) and protein expression (Fig. 20H) after CDE diet, which was significantly abrogated in KO2. This suggests severely impaired hepatocyte proliferation in KO2 mice after 2W of CDE diet. We did not detect any β-catenin-positive, EYFP-negative hepatocytes in KO2 (Fig. 19J), suggesting no BEC-derived hepatocytes (Fig. 19F) were present at this time. Corroborating this observation, we did not detect an increase in total β-catenin levels in KO2 mice after 2W of CDE diet in comparison to KO2 mice left on normal diet. However, we did detect active β-catenin in KO2 mice on CDE diet, which was absent in KO2 mice on normal diet (Fig. 20H). This suggests active-β-catenin is present in β-catenin-positive BEC compartment, and that BEC differentiation into hepatocytes had yet to occur.

3.4.3 Defective Hepatocyte Proliferation in KO2 Mice Drives BEC-to-Hepatocyte Differentiation after CDE Diet-Induced Hepatic Injury

To facilitate BEC-driven repair, we next administered CDE diet to WT2 and KO2 mice for 2W followed by recovery on normal diet for 2W (184, 187, 191) (Fig. 21A). Both WT2 and KO2 displayed normal serum ALT (Fig. 21C), although KO2 displayed slightly elevated serum bilirubin (Fig. 21D) and ALP (Fig. 21E) compared to WT2. Excitingly, in KO2 mice we detected clusters of β-catenin-positive, EYFP-negative cells which stained positively for hepatocyte marker Hnf4α (Fig. 21G), indicating BEC-derived hepatocytes (Fig. 21B). We did not detect expansion of EYFP-negative hepatocytes in WT2 mice, suggesting that BECs do not give rise to hepatocytes in animals when hepatocyte proliferation is not impaired, consistent with previous reports (190, 214, 278). An alternative explanation for these cells is that they were hepatocytes which escaped initial Cre recombination, which could result in EYFP-negative, β-catenin-positive hepatocytes. However, we would predict the efficiency of AAV8-TBG-Cre to be the same in both WT2 and KO2 mice.

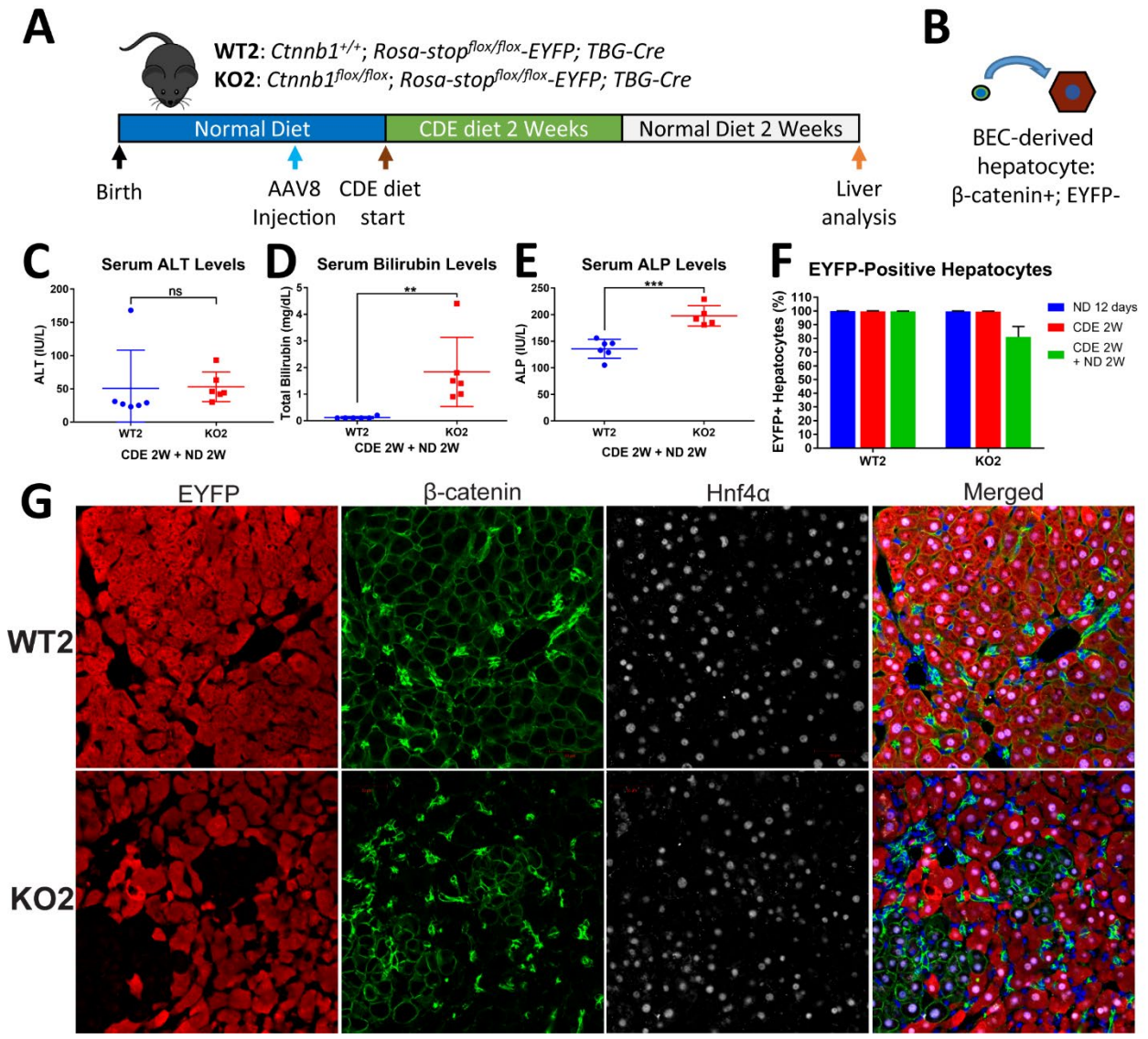

Figure 21: BEC-derived hepatocytes appear in KO2 but not WT2 mice following recovery after CDE diet.

(*a*) 24-25 day old male *Ctnnb1$^{flox/flox}$; Rosa-stop$^{flox/flox}$-EYFP or Ctnnb1$^{+/+}$; Rosa-stop$^{flox/flox}$-EYFP* mice were injected with AAV8-TBG-Cre to generate KO2 and WT2 mice respectively, followed by 12ds of wash-out on normal diet before 2W of CDE diet followed by another 2W of recovery on normal chow. (*b*) Schematic of fate tracing depicting BECs that give rise to hepatocytes will be negative for EYFP and will express β-catenin. (*c*) Serum ALT levels normalize after 2W of recovery post-CDE diet in both WT2 and KO2 mice. (*d*) Serum bilirubin levels are reduced in KO2 mice compared to immediate post-CDE diet injury levels, but still significantly elevated in comparison to WT2 mice following 2W of recovery (t-test, ** = $p < 0.01$). (*e*) Serum ALP levels are significantly elevated in KO2 compared to WT2 mice after CDE 2W and 2W of recovery (t-test, *** = $p < 0.001$). (*f*) Over 99% of hepatocytes are EYFP-positive in WT2 and KO2 mice both prior to injury (Normal Diet 12ds) and after 2W of CDE diet-induced liver injury (CDE 2W). After recovery on normal diet following CDE diet, approximately 20% of periportal hepatocytes are EYFP-negative in KO2 mice while there is no reduction in EYFP-positive hepatocytes in WT2

mice. (*g*) Hnf4α-positive hepatocytes which are negative for EYFP and positive for β-catenin appear in KO2 mice after CDE diet and recovery. No EYFP-negative hepatocytes are apparent in WT2 mice (scale bar 50 μm).

Therefore, we quantified the number of EYFP-positive/negative hepatocytes in our WT2 and KO2 mice over the course of CDE diet injury and recovery (Fig. 21F). First, we quantified the number of EYFP-positive hepatocytes in WT2 and KO2 mice 12d after injection with AAV8-TBG-Cre, corresponding to the initial labeling efficiency before the onset of liver injury. We found that greater than 99% of hepatocytes were EYFP-positive, consistent with previous reports (190, 278). After 2W of CDE diet, the percentage of EYFP-negative hepatocytes was not significantly increased in either WT2 or KO2. However, after 2W of recovery after CDE diet-induced liver injury, in KO2 mice approximately 20% of periportal hepatocytes were EYFP-negative, whereas the percentage of EYFP-negative hepatocytes in WT2 mice did not increase (Fig. 21F).

Correspondingly, tiled images (and serial higher magnification images from a representative area) from KO2 mice of representative lobes stained for β-catenin revealed no clusters of β-catenin-positive hepatocytes after 2W of CDE diet (Fig. 22A, B), whereas after 2W of CDE diet followed by 2W of recovery on normal diet many clusters of β-catenin-positive hepatocytes were evident across the entire lobe (and serial higher magnification images from a representative area) (Fig. 22C, D). Likewise, hepatic *Ctnnb1* expression tended to increase in KO2 mice after CDE diet and recovery, although it was still significantly lower than WT2 mice. In age- matched control mice left on normal diet for 6W after AAV8-TBG-Cre injection, hepatic gene expression of *Ctnnb1* was greatly reduced in KO2 mice compared to WT2 mice (Fig. 22E), indicating lack of repopulation of β-catenin-positive hepatocytes in the absence of liver injury. These results, in combination with lack of expansion of EYFP-negative hepatocytes in WT2 after CDE diet injury and recovery, support BEC-to-hepatocyte conversion in KO2 over expansion of Cre-recombinase escaped cells.

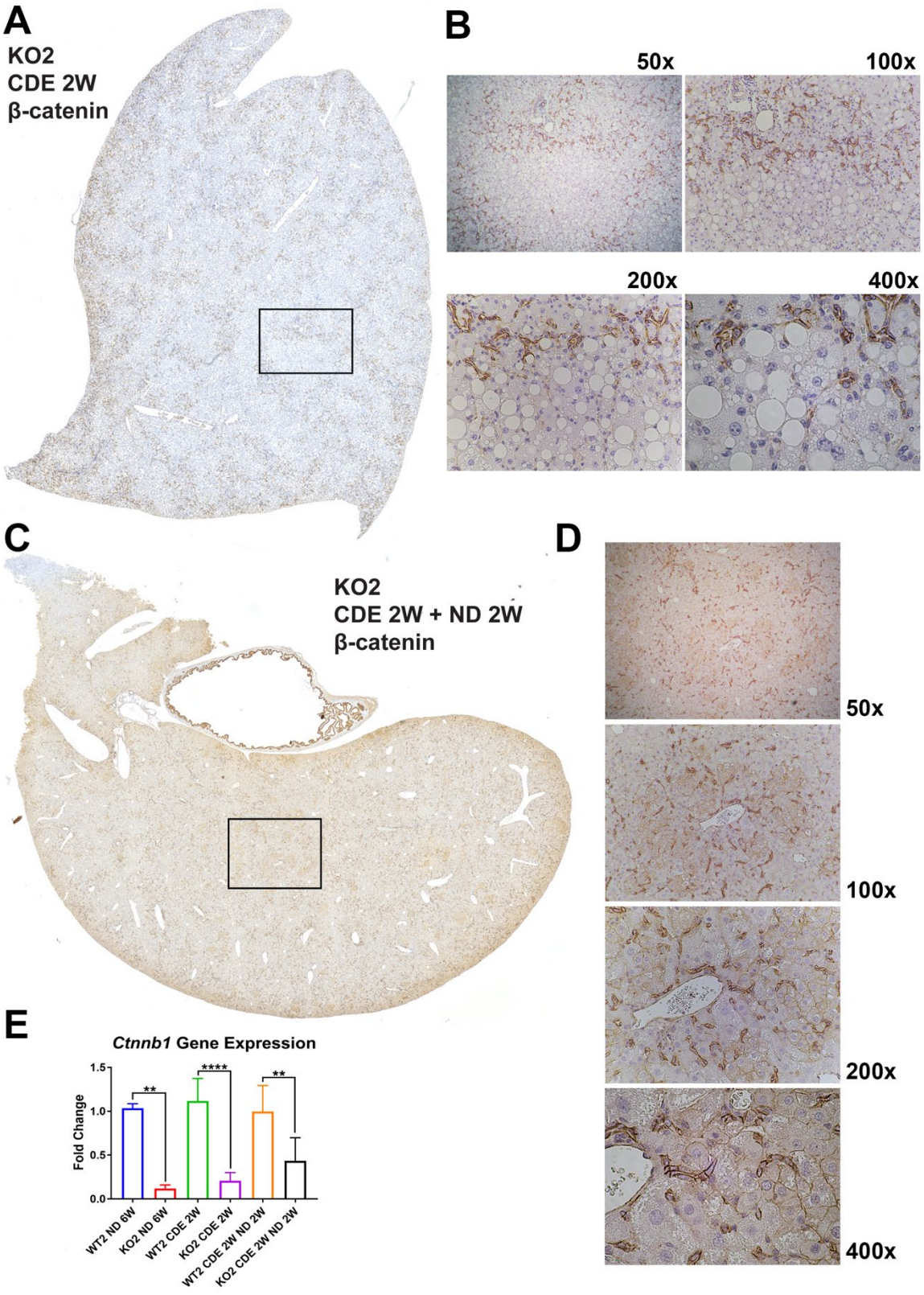

Figure 22: Expansion of β-catenin-positive hepatocytes occurs only after recovery on normal diet.

(*a*) Tiled β-catenin IHC staining of an entire lobe from the liver of a KO2 mouse after 2 weeks of CDE diet reveals dramatic expansion of β-catenin-positive BECs, but no clusters of β-catenin-positive hepatocytes. (*b*) Serial magnifications of a representative area from Figure S3A (open box) verifies dramatic expansion of β-catenin-positive BECs, but no clusters of β-catenin-positive hepatocytes (50x, 100x, 200x, 400x). (*c*) Tiled β-catenin IHC staining of an entire lobe from the liver of a KO2 mouse after 2 weeks of CDE diet followed by 2 weeks of recovery on normal diet reveals clusters of β-catenin-positive hepatocytes appearing across the entire lobe. (*d*) Serial magnifications of a representative area from Figure S3C (open box) verifies clusters of β-catenin-positive hepatocytes appearing in close association with ductules (50x, 100x, 200x, 400x). (*e*) Expression of *Ctnnb1* is dramatically reduced in KO2 mice compared to WT2 mice on normal diet for 6 weeks. After 2 weeks of CDE diet followed by 2 weeks of recovery on normal diet, expression of *Ctnnb1* is trending upward in KO2 mice, although it is still significantly reduced compared to WT2 levels (one-way ANOVA, ** = $p < 0.01$. **** = $p < 0.0001$).

3.4.4 BEC-Derived β-catenin-Positive Hepatocytes are More Proliferative than Endogenous Hepatocytes

Analysis of hepatic sections from KO2 mice after 2W of recovery on normal chow following 2W of CDE diet showed that nearly all β-catenin-positive hepatocytes were located in clusters adjacent to BECs in the periportal region (Fig. 22B). This may also explain the lack of reappearance of pericentral β-catenin target glutamine synthetase (GS) (68, 283) in KO2 mice at this time (Fig. 23C). The reactive BEC response was extensive after 2W of CDE diet and recovery, as evidenced by large numbers of EpCAM-positive BECs (Fig. 24A). The extent of BEC expansion was similar in WT2 and KO2, as indicated by comparable hepatic expression of BEC markers *Krt19* (Fig. 24B) and *Sox9* (Fig. 24C). There was ongoing fibrosis in both WT2 and KO2 as evidenced by Sirius Red staining even after 2W recovery on normal diet (Fig. 24A), which is likely due to ongoing reactive BEC response, which is known to secrete profibrogenic cytokines (127). This level of fibrosis also indicated that repair of CDE diet-induced liver injury was not complete after 2W of recovery on normal diet.

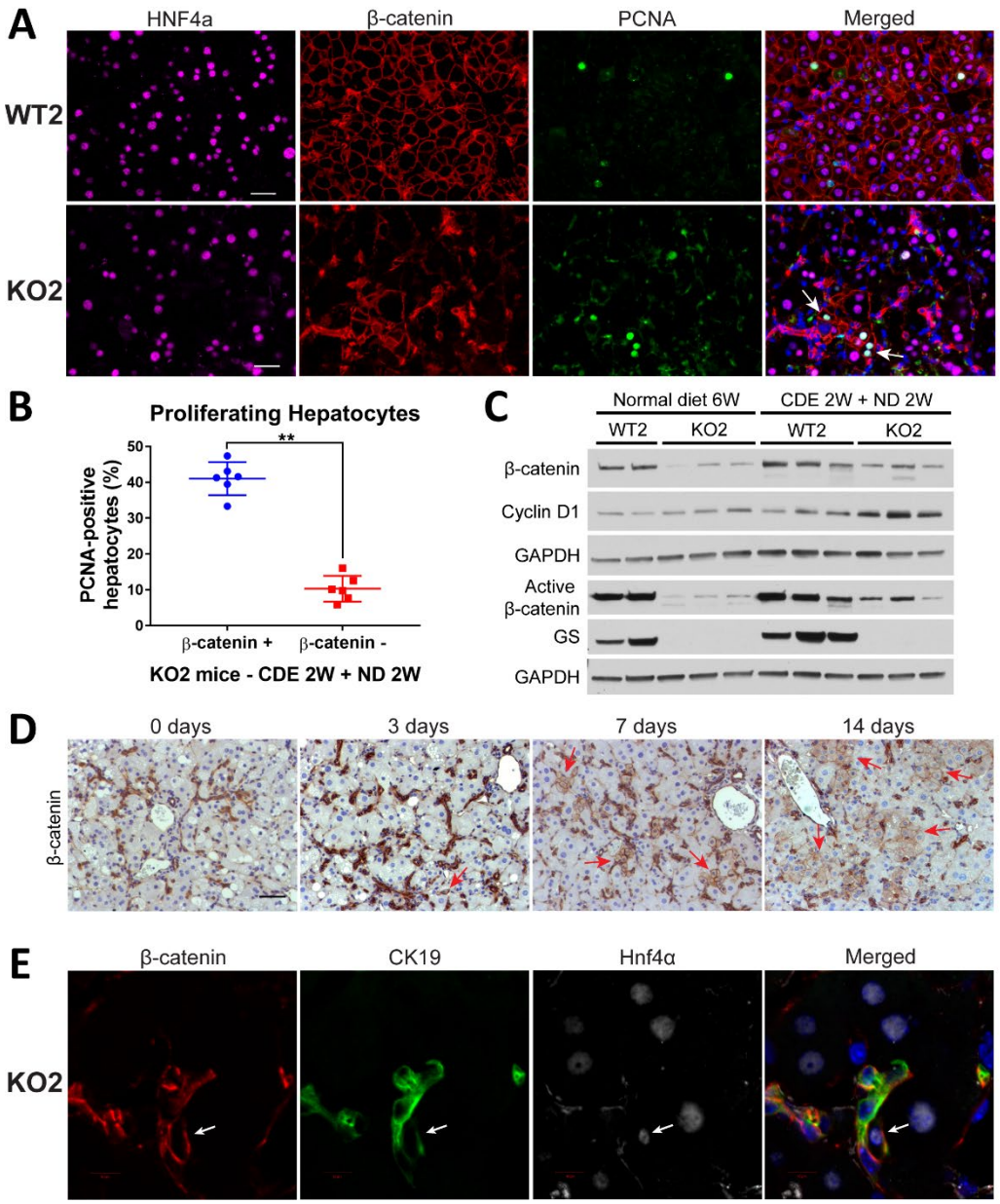

Figure 23: β-catenin-positive hepatocytes preferentially proliferate to restore lost hepatocyte mass.

(*a*) The majority of BEC-derived β-catenin-positive hepatocytes in a given cluster are PCNA-positive (scale bar 50 μm). (*b*) Quantification of PCNA reveals β-catenin-positive hepatocytes are significantly more proliferative than surrounding β-catenin-negative hepatocytes (Mann-Whitney U test, ** = $p < 0.01$). (*c*) There is an increase in total β-catenin, active β-catenin, and Cyclin D1 levels in KO2 mice after CDE diet and recovery compared to KO2 mice left on normal diet. Since all BEC-derived hepatocytes are located in the periportal region, there is no re-expression of pericentral β-catenin target GS. (*d*) IHC staining for β-catenin reveals no β-catenin-positive hepatocytes in KO2 mice after 2W on CDE diet with 0 days of recovery. However, a few β-catenin-positive hepatocytes are visible after 3 days of recovery (red arrow), with clusters of β-catenin-positive hepatocytes increasing in size from 7 days recovery to 14 days recovery on normal diet

(scale bar 50 μm). (*e*) β-catenin-positive cells which express both BEC marker CK19 and hepatocyte marker Hnf4α can be found in KO2 mice after 2W on CDE diet followed by 7 days of recovery on normal diet (scale bar 10 μm).

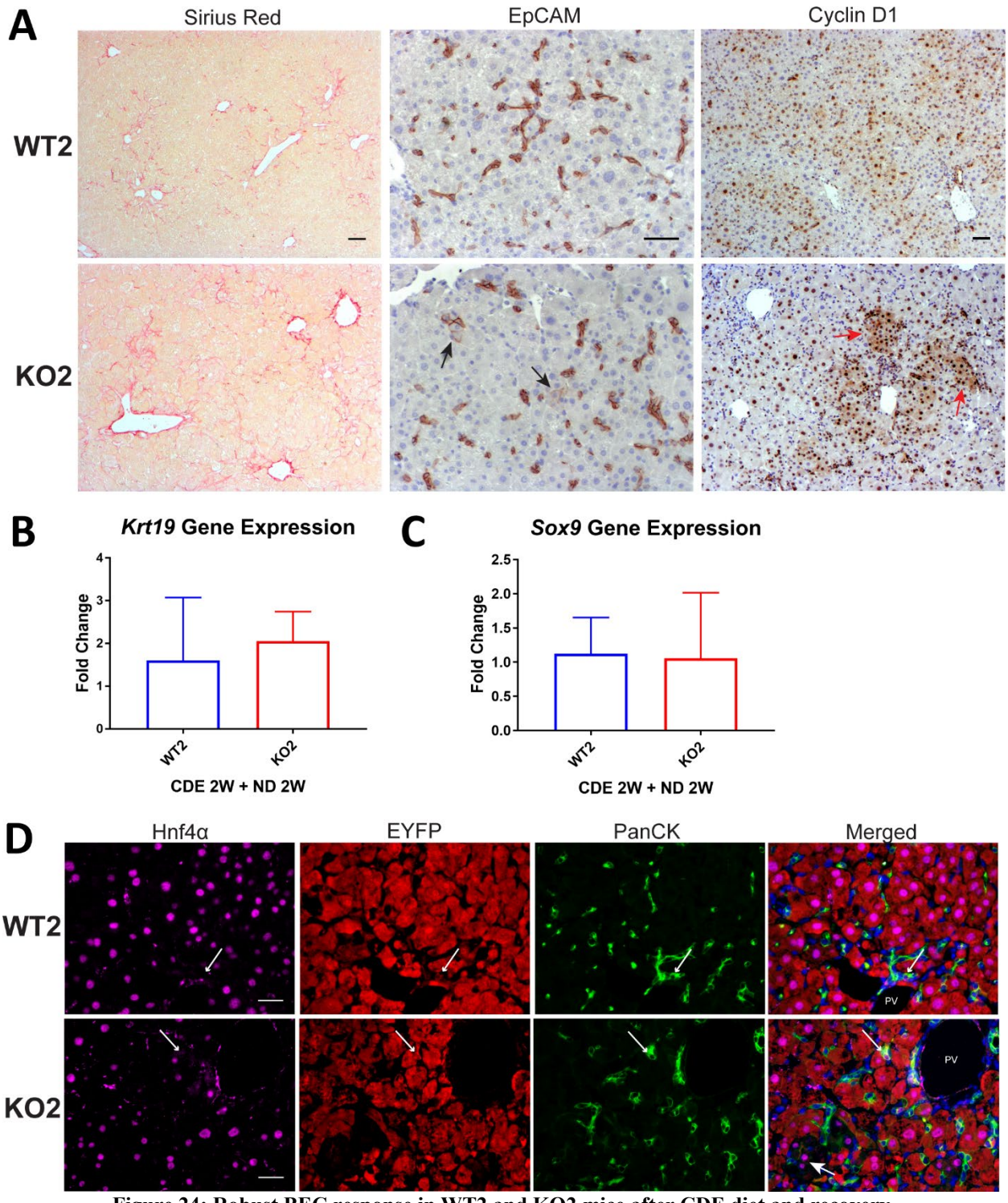

Figure 24: Robust BEC response in WT2 and KO2 mice after CDE diet and recovery.

(*a*) There is sustained fibrosis and a continued BEC response in both WT2 and KO2 mice after CDE diet and recovery. Rare EpCAM-positive cells with hepatocyte morphology are detectable in KO2 mice (black arrows). Additionally, clusters of presumable BEC-derived hepatocytes (red arrows) are strongly Cyclin D1 positive in KO2 mice (scale bar 50 µm). (*b*) The level of *Krt19* gene expression is comparable between WT2 and KO2 mice after 2 weeks of CDE diet followed

by 2 weeks of recovery on normal diet. (*c*) The level of *Sox9* gene expression is comparable between WT2 and KO2 mice after 2 weeks of CDE diet followed by 2 weeks of recovery on normal diet. (*d*) The majority of BECs are negative for EYFP in WT2 and KO2 mice after CDE diet and recovery. However, rare EYFP cells positive for BEC markers are detectable in both WT2 and KO2 mice, potentially suggesting hepatocyte-to-BEC transdifferentiation (scale bar 50 μm). PV = portal vein.

To determine if BEC-derived, β-catenin-positive hepatocytes were driving restoration of hepatocyte mass in KO2 mice after CDE diet-induced liver injury, we performed triple immunofluorescence for Hnf4α, β-catenin, and proliferating cell nuclear antigen (PCNA) (Fig. 23A). Within a given cluster of β-catenin-positive hepatocytes in KO2, the majority of β-catenin-positive hepatocytes stained positively for PCNA. Indeed, periportal β-catenin-positive hepatocytes were significantly more proliferative than surrounding β-catenin-negative hepatocytes in KO2 (Fig. 23B). Likewise, clusters of periportal hepatocytes in KO2 were strongly Cyclin D1-positive in comparison to surrounding hepatocytes (Fig. 24A, red arrows). KO2 also displayed increased total Cyclin D1 protein compared to WT2 after 2W of CDE diet and recovery (Fig. 23C). There was also a noticeable increase in total and active-β-catenin in KO2 after recovery in comparison to age-matched KO2 left on normal diet for 6W (Fig. 23C), indicating repopulation by β-catenin-positive cells in KO2 during repair. Collectively, these results demonstrate BEC-derived β-catenin-positive hepatocytes are preferentially proliferating to replenish lost hepatic mass in KO2 mice.

3.4.5 BEC Differentiation to Hepatocytes Occurs Early in Recovery on Normal Diet

To determine if the BEC-derived hepatocytes after 2W of recovery on normal diet express BEC markers, we performed triple immunofluorescence with a wide-spectrum cytokeratin antibody (PanCK) in addition to EYFP and hepatocyte marker Hnf4α (Fig. 24D). EYFP-negative

hepatocytes were PanCK-negative (Fig. 24D, white arrowhead), and as expected the majority of cytokeratin-positive BECs were negative for EYFP. Interestingly, rare EYFP-positive BECs were observed in both WT2 and KO2 mice (Fig. 24D, white arrows), potentially indicating hepatocyte-to-BEC transdifferentiation after CDE diet-induced liver injury. When we performed staining for a second BEC marker, EpCAM, we observed rare cells with hepatocyte-like morphology which were EpCAM-positive in KO2 mice (Fig. 24A, black arrows). This finding correlates with the observations of EpCAM-positive hepatocytes in human patients with BEC expansion after severe liver injury (104). These results demonstrate that after 2W of recovery on normal diet, the majority of BEC-derived hepatocytes in KO2 mice do not express BEC markers.

To further explore the timing of BEC-to-hepatocyte differentiation during recovery from CDE diet, we harvested KO2 mice after 3d or 7d of recovery on normal diet post-CDE diet (Fig. 25A). Excitingly, very few small β-catenin-positive hepatocyte-like cells are evident after 3d recovery, which grow into small clusters of β-catenin-positive cells with hepatocyte morphology after 7d recovery (Fig. 23D, red arrows). These clusters are even larger following 2W of recovery on normal diet, suggesting potential clonal expansion of BEC-derived, β-catenin-positive hepatocytes. Interestingly, serum ALT levels are dramatically reduced following 3d of recovery on normal diet (Fig. 25B), while both serum bilirubin and ALP levels remain elevated after 3d of recovery and only begin to normalize after 7d or 14d of recovery, respectively (Fig. 25C-D), potentially suggesting abatement of acute liver injury may be required for expansion of these cells. Similar serum liver injury profiles and appearance of small β-catenin-positive hepatocytes were also observed in female KO2 mice after CDE diet and three days of recovery (data not shown), suggesting BEC-to-hepatocyte differentiation also occurs in female mice following recovery from CDE diet-induced liver injury.

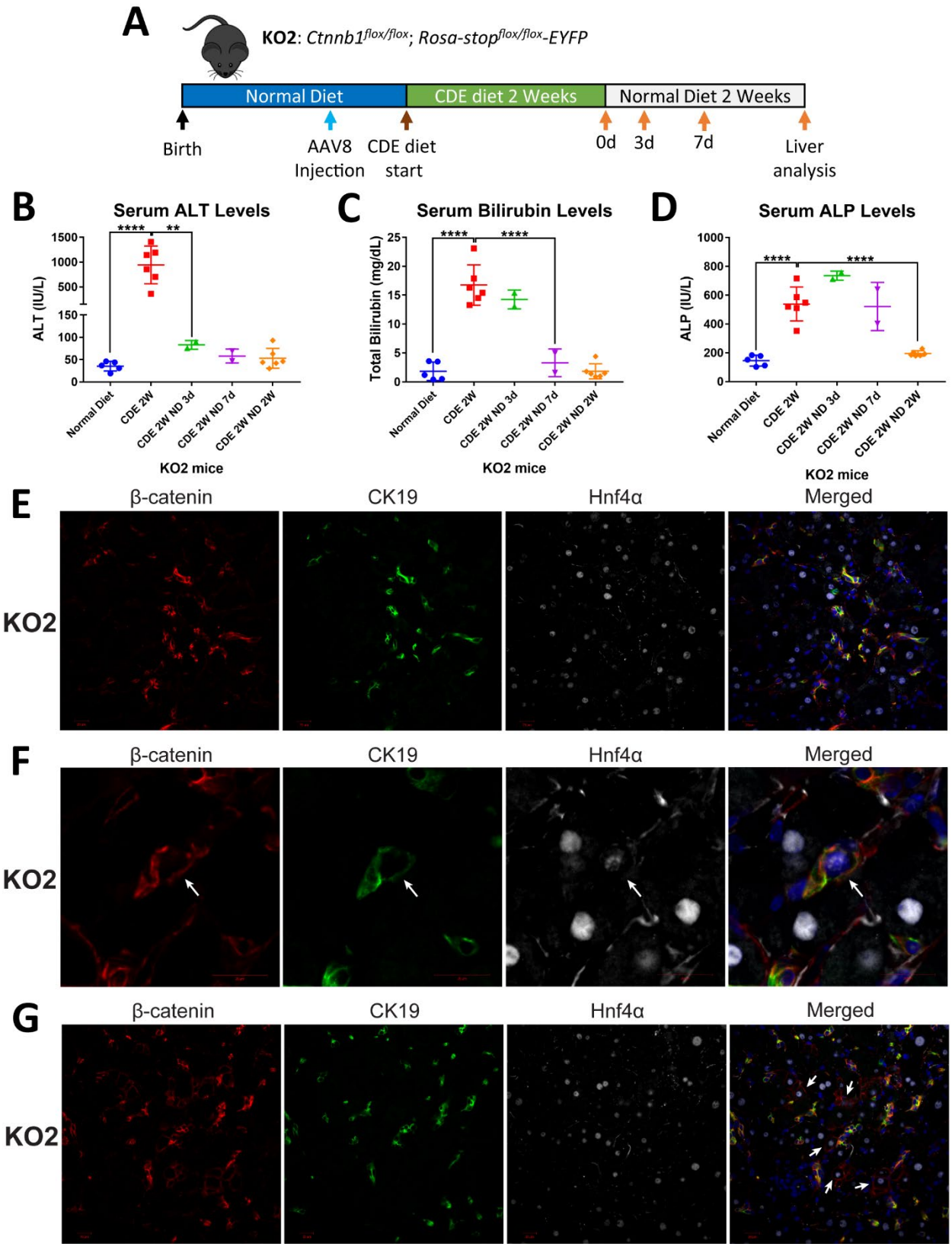

Figure 25: Expansion of BEC-derived, β-catenin-positive hepatocytes during early recovery on normal diet.

(*a*) Schematic of KO2 mice placed on normal diet for two weeks and then allowed to recovery on normal diet for either 0, 3, 7, or 14 days. (*b*) Serum ALT levels are elevated in KO2 mice on CDE diet for 2 weeks, but are dramatically reduced as early as 3 days after recovery on normal diet (One-way ANOVA, ** $p < 0.01$, **** $p < 0.0001$). (*c*) Serum bilirubin levels are elevated in KO2 mice on CDE diet for 2 weeks, and only begin to show a reduction after 7 days of recovery on normal diet (One-way ANOVA, **** $p < 0.0001$). (*d*) Serum ALP levels are elevated in KO2 mice on CDE diet for 2 weeks and begin to show a reduction after two weeks of recovery on normal diet (One-way ANOVA, **** $p < 0.0001$). (*e*) After 2 weeks of CDE diet, β-catenin-positive cells are positive for BEC-marker CK19 but negative for Hnf4α (scale bar 20 μm). (*f*) As early as 3 days of recovery following CDE diet-induced liver injury, β-catenin-positive cells which express CK19 and weakly express Hnf4α (white arrow) can be detected (scale bar 20 μm). (*g*) After 7 days of recovery on normal diet following CDE diet-induced liver injury, there are clusters containing multiple β-catenin-positive, Hnf4α-positive hepatocytes (white arrows, scale bar 20 μm).

We next investigated the expression of Hnf4α in these putative transdifferentiating BECs over time. After 2W of CDE diet, virtually all β-catenin-positive cells were positive for CK19 and negative for Hnf4α (Fig. 25E). However, as early as after 3d of recovery we detected β-catenin-positive cells which were CK19-positive and weakly positive for Hnf4α (Fig. 25F). After 7d of recovery on normal diet, rare β-catenin-positive cells were observed which were strongly positive for both CK19 and Hnf4α (Fig. 23E). At this time point, clusters containing β-catenin+/Hnf4α+/CK19+ hepatocytes were evident (Fig. 25G). The rarity of the β-catenin+/Hnf4α+/CK19+ cells in combination with the increased proliferation of β-catenin-positive hepatocytes suggests that few BECs differentiate into hepatocytes, which subsequently proliferate to restore lost hepatocyte mass in KO2 mice.

3.4.6 BEC-Derived Hepatocytes Repopulate the Liver during Long-Term Recovery

Previous studies have demonstrated that transdifferentiated cells, such as hepatocyte-derived BECs, may revert back to their original cell type when liver injury has abated (214).

Alternatively, it has been shown that with persistent need for transdifferentiated cells, such as in mice which lack the intrahepatic biliary system, hepatocyte-to-BEC conversion is permanent and stable for life (215). To determine if BEC-derived hepatocytes would persist and further repopulate the liver, KO2 mice were allowed to recover on normal diet for either 3 or 6 months (6m) after CDE diet (Fig. 26A). As a control, we traced WT2 and KO2 mice for 6m on normal diet to determine the persistence of EYFP labeling in the absence of injury. Serum ALT levels were normal in both WT2 and KO2 (Fig. 26B, C). Interestingly, KO2 mice left on normal diet for 6m showed minor elevation of bilirubin compared to WT2 (Fig. 26C). KO2 mice after long-term recovery from CDE diet showed extensive expansion of EYFP-negative, β-catenin-positive hepatocytes (Fig. 26E), as evidenced by central veins that were partially or completely GS-positive (Fig. 27A). When we quantified the number of EYFP-positive hepatocytes, we found that in control WT2 and KO2 left on normal diet for 6m there was no significant expansion of EYFP-negative hepatocytes, similar to WT2 after long-term recovery from CDE diet (Fig. 26D). However, in KO2 after 3m of recovery from CDE diet up to 70% of hepatocytes were EYFP-negative, and this number remained stable after 6m of recovery. In control KO2 mice left on normal diet for 6m, virtually all EYFP-positive hepatocytes were β-catenin-negative (Fig. 27B) as confirmed by β-catenin IHC (Fig. 27C). Hepatic expression of *Ctnnb1* was significantly reduced in KO2 mice left on normal diet for 6m compared to control WT2 mice, while expression of *Ctnnb1* in KO2 after recovery from CDE diet began to approach WT2 levels (Fig. 27D). The lack of expansion of EYFP-negative hepatocytes in WT2 mice even after 6m of recovery post-CDE diet, combined with the lack of expansion of EYFP-negative hepatocytes in KO2 left on normal diet, further supports our hypothesis that BEC-derived hepatocytes repopulate the liver in KO2 after CDE diet-induced liver injury.

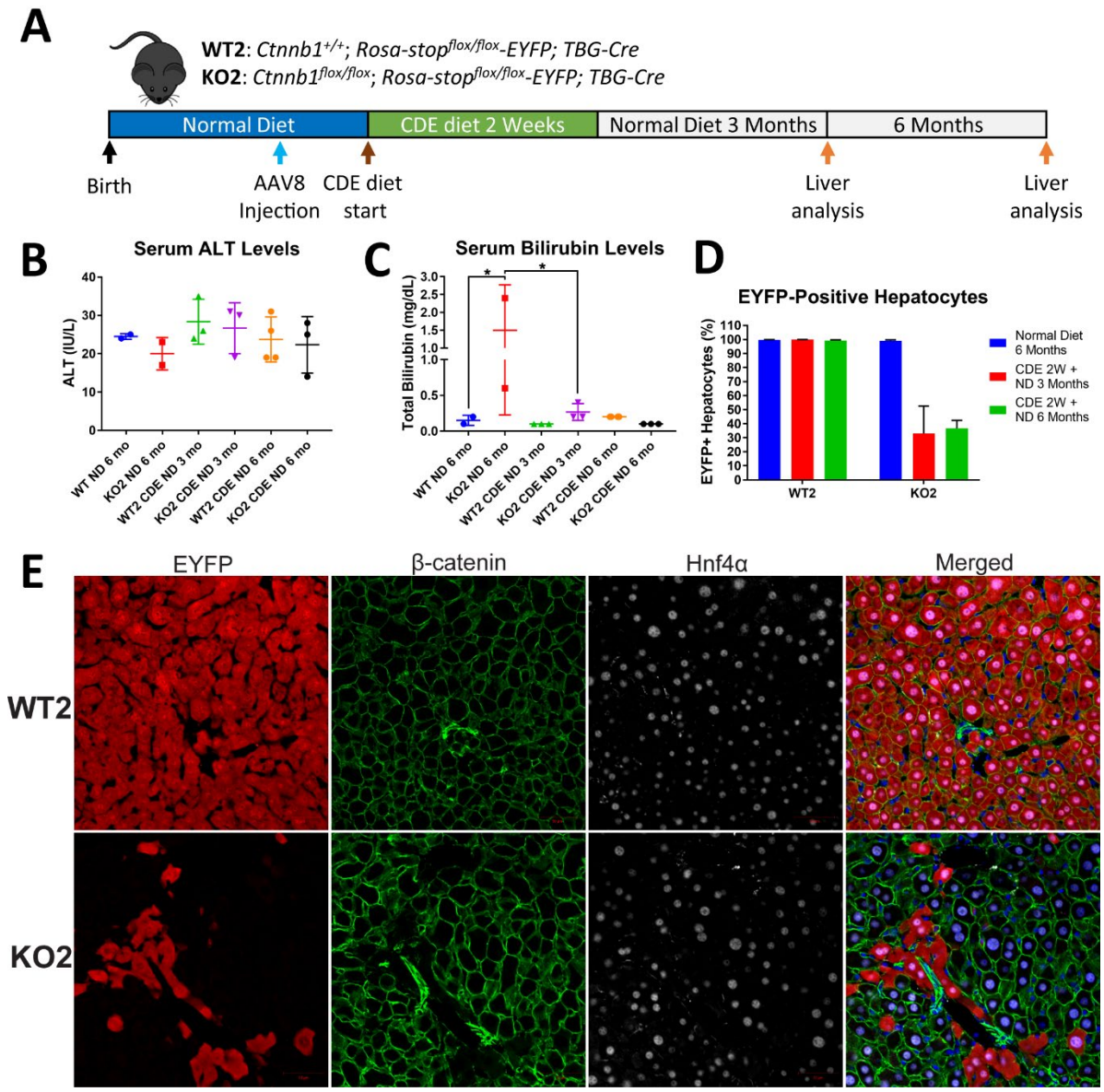

Figure 26: β-catenin-positive hepatocytes repopulate the majority of the liver during long-term recovery.

(*a*) After CDE diet treatment, WT2 and KO2 mice were allowed to recover on normal diet for either 3 or 6 months. As a control, WT2 and KO2 mice which were never exposed to CDE diet were traced for 6 months after AAV8 injection. (*b*) Serum ALT levels are normal in both WT2 and KO2 mice after long-term recovery on normal diet. (*c*) Serum bilirubin levels are normal in both WT2 and KO2 mice on long-term recovery on normal diet, although serum bilirubin is slightly elevated in control KO2 mice kept on normal diet for 6 months (one-way ANOVA, * = $p < 0.05$). (*d*) There is no significant expansion of EYFP-negative hepatocytes in control WT2 and KO2 mice left on normal diet for 6 months (blue bars), or in WT2 mice exposed to CDE diet for 2W and allowed to recover on normal diet for up to 6 months. However, in KO2 mice up to 70% of hepatocytes are EYFP negative after 6 months of recovery on normal diet following CDE diet-

induced liver injury. (*e*) Expansion of EYFP-negative hepatocytes is only evident in KO2, not WT2, mice after 6 months of recovery on normal diet following CDE diet-induced liver injury.

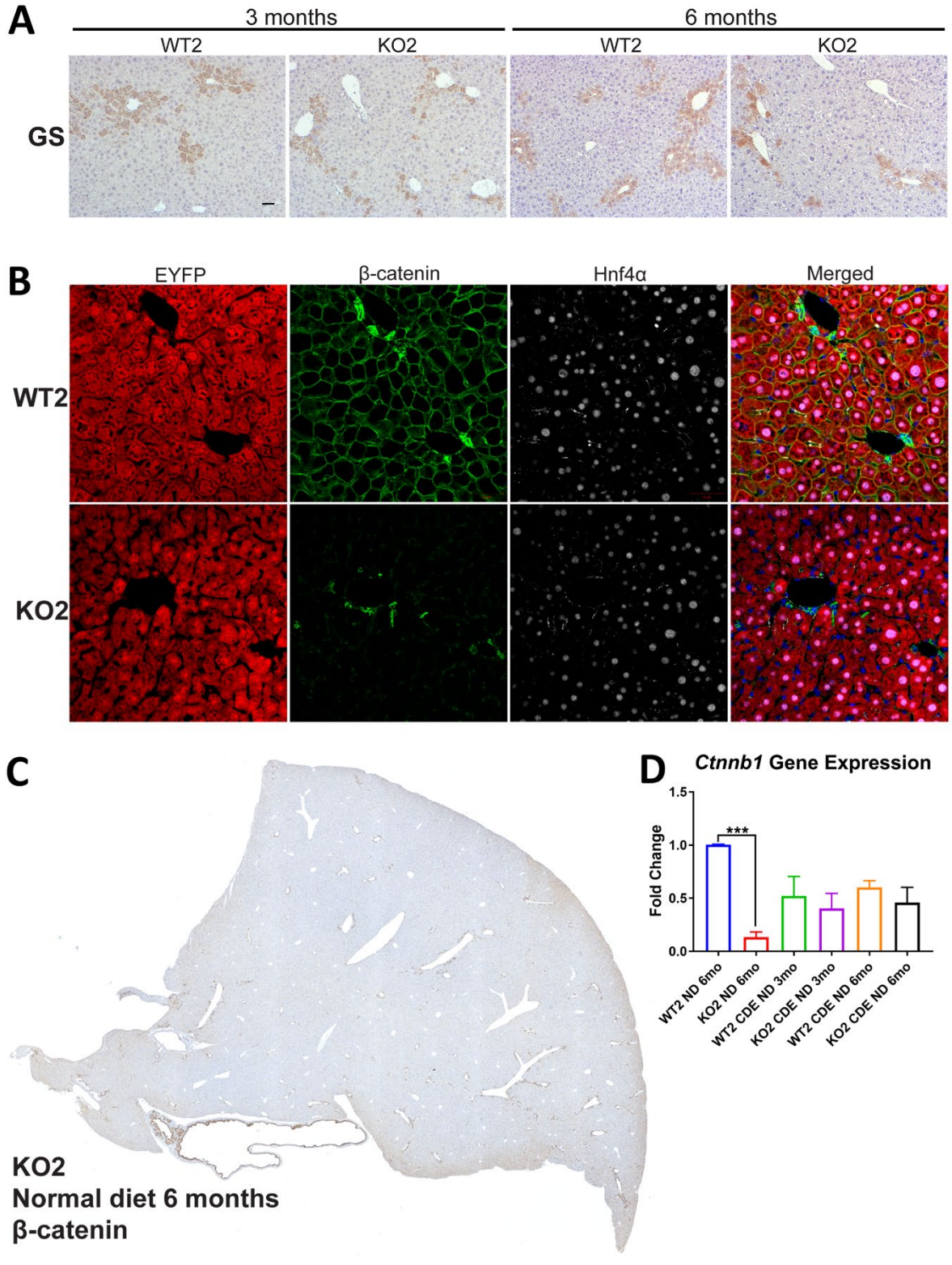

Figure 27: Expansion of EYFP-negative hepatocytes occurs only after exposure to CDE diet in KO2 mice.

(*a*) Expression of GS partially reappears in KO2 mice after CDE diet-induced liver injury and either 3 or 6 months of recovery on normal diet. (*b*) Virtually all hepatocytes are EYFP-positive in both control WT2 and KO2 mice left on normal diet for 6 months (scale bar 50 μm). (*c*) Tiled IHC β-catenin staining of a lobe from a KO2 mouse left on normal diet for 6 months after AAV8 injection reveals virtually no β-catenin-positive hepatocytes. (*d*) There is dramatically reduced hepatic *Ctnnb1* expression in control KO2 mice left on normal diet for 6 months compared to WT2 controls. However, in KO2 mice placed on CDE diet followed by up to 6 months of recovery on normal diet the level of hepatic *Ctnnb1* expression is approaching WT2 levels (one-way ANOVA, *** = $p < 0.001$).

3.4.7 *In Vivo Ctnnb1* RNAi Impairs Hepatocyte Proliferation after CDE Diet-Induced Liver Injury

To prove BECs were indeed giving rise to hepatocytes in our model, we sought to perform direct lineage tracing of BECs utilizing tamoxifen-inducible *Krt19-Cre* to label BECs with the reporter tdTomato. However, usage of Cre recombinase to label BECs precluded the usage of Cre recombinase to delete *Ctnnb1* specifically in hepatocytes. To achieve labeling of BECs with a reporter and simultaneous knockdown of *Ctnnb1* expression in hepatocytes, we utilized GalXC (280). To validate that GalXC injection would recapitulate the phenotype of CDE diet-fed mice with genetic hepatocyte-specific *Ctnnb1* deletion, we performed weekly subcutaneous injections of GalXC in mice fed CDE diet. The first injection was performed 1W before CDE diet exposure to ensure reduced β-catenin levels in hepatocytes at the time of CDE diet administration (Fig. 28A).

Real-time PCR analysis demonstrated significant reduction of hepatic *Ctnnb1* gene expression in GalXC-injected mice compared to PBS-injected control mice on CDE diet (Fig. 28B). GalXC-injected mice fed CDE diet for 2W displayed significantly elevated serum ALT (Fig. 28C), AST (Fig. 28D), and bilirubin levels (Fig. 28F) compared to control PBS-injected mice. We

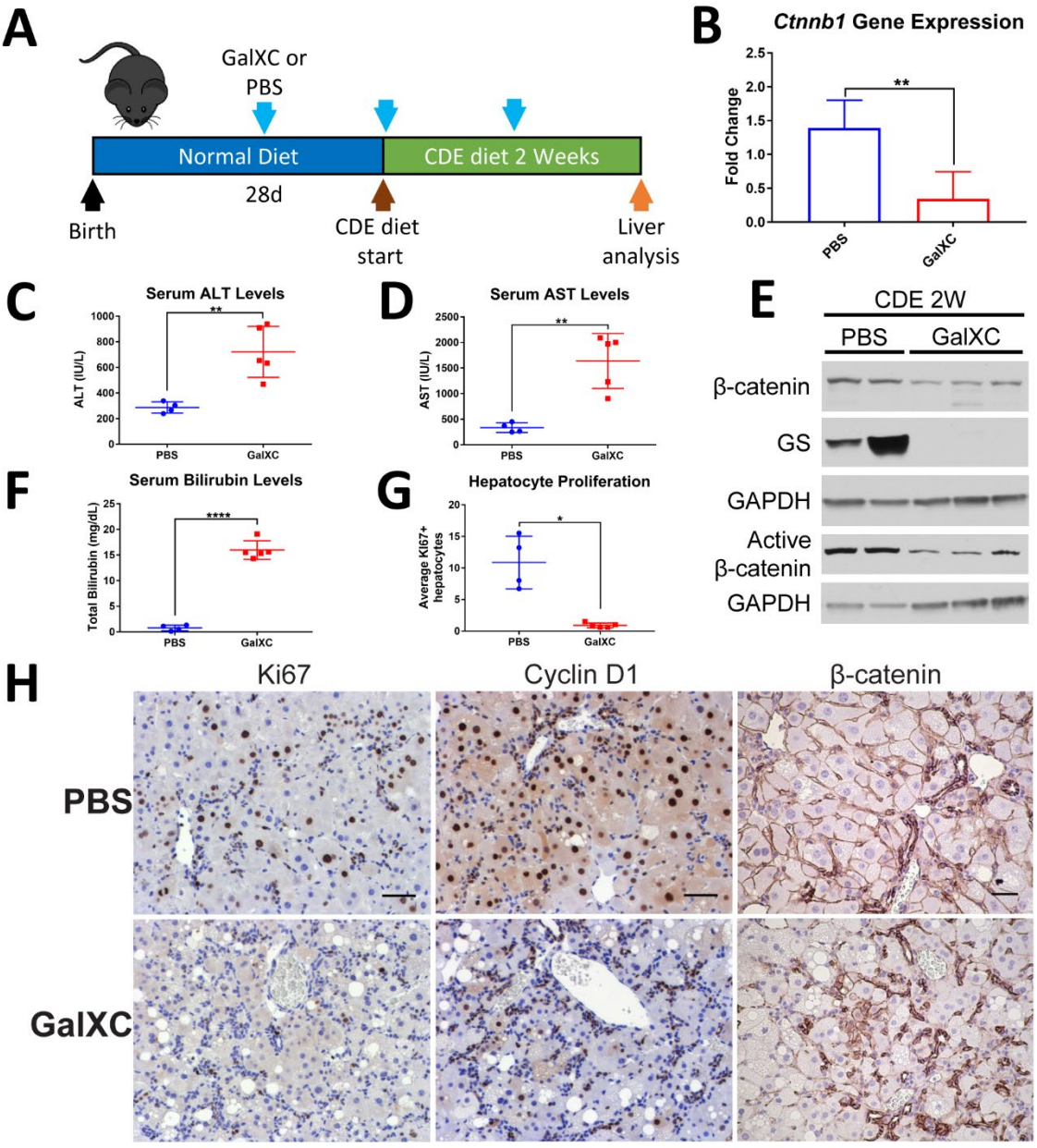

Figure 28: Hepatocyte-specific *in vivo Ctnnb1* RNAi induces severe liver injury and a block of hepatocyte proliferation in CDE diet-fed mice.

(*a*) C57BL6/NJ mice were placed on CDE diet for 2W. Mice were given weekly subcutaneous injections of GalXC or PBS one week prior to CDE diet administration and throughout the course of CDE diet feeding. (*b*) RT-PCR analysis of *Ctnnb1* gene expression in whole liver lysates of GalXC or PBS-injected mice on CDE diet (t-test, ** = $p < 0.01$). (*c*) Significantly elevated serum ALT levels in GalXC-injected mice compared to PBS controls (t-test, ** = $p < 0.01$). (*d*) Significantly elevated serum AST levels in GalXC-injected mice compared to PBS controls (t-test, ** = $p < 0.01$). (*e*) Whole liver lysate reveals reduction in total β-catenin and active β-catenin, as well as complete loss of β-catenin-target GS in GalXC-injected mice on CDE diet. (*f*) Significantly

elevated serum bilirubin levels in GalXC-injected mice compared to PBS controls (t-test, **** = $p < 0.0001$). (*g*) Quantification reveals significantly fewer Ki67-positive hepatocytes in GalXC-injected mice compared to PBS-injected controls (Mann-Whitney U test, * = $p < 0.05$). (*h*) IHC staining reveals robust Ki67 staining of hepatocytes in PBS but not GalXC-injected animals. Cyclin D1 staining is significantly reduced in GalXC-injected mice, which also display a lack of hepatocyte-specific β-catenin staining (scale bar 50 μm).

additionally confirmed reduction in both total and active β-catenin protein levels, as well as loss of expression of β-catenin downstream target GS, in GalXC-injected mice on CDE diet (Fig. 28E). Staining for Ki67 displayed robust hepatocyte proliferation in PBS-injected controls but not GalXC-injected mice on CDE diet (Fig. 28H), which was confirmed by quantification (Fig. 28G). There was also a notable decrease in Cyclin D1 staining in the livers of GalXC-injected mice on CDE diet (Fig. 28H). Finally, IHC for β-catenin confirmed loss of β-catenin expression specifically in hepatocytes of GalXC-injected mice (Fig. 28H). Collectively, these results demonstrate that GalXC-injected mice display increased liver injury and impairment of hepatocyte proliferation.

3.4.8 BECs Give Rise to Hepatocytes in *Ctnnb1* RNAi-Treated Mice after CDE Diet-Induced Liver Injury

Having proven that injection of GalXC was sufficient to block hepatocyte proliferation in mice on CDE diet, we developed a mouse model of *Krt19*-Cre$^{ERT+/-}$-driven BEC lineage tracing (191) in combination with hepatocyte-specific *Ctnnb1* knockdown. To label BECs, tamoxifen was injected in *Krt19*-Cre$^{ERT+/-}$ mice during postnatal week one, followed by a two-week washout period to ensure elimination of any residual tamoxifen (Fig. 29A). Next, these mice were given weekly injections of GalXC throughout the course of CDE diet and recovery (Fig. 29A). In this model, BEC-derived hepatocytes can be directly traced as they will be tdTomato-positive (Fig. 29B). Prior to CDE diet administration, we verified that early postnatal tamoxifen

administration labeled only BECs and not surrounding hepatocytes (Fig. 30A), implying that any tdTomato-positive hepatocytes would have to arise from a pre-existing tdTomato-positive BEC. We additionally determined the *Krt19*-Cre$^{ERT+/-}$ recombination efficiency in BECs in this model to be approximately 50% (Fig. 30B). After CDE diet and recovery, serum liver injury markers were approaching normal levels in both PBS and GalXC-injected mice (Fig. 30B-D). Excitingly, clusters of tdTomato-positive hepatocytes which were also Hnf4α-positive (Fig. 29C) and CYP2D6-positive (Fig. 31A) were evident in the GalXC-injected mice but not in the mice injected with PBS as a control. Quantification revealed that approximately 6% of hepatocytes were tdTomato-positive in GalXC-injected mice after CDE diet and recovery (Fig. 29D).

Immunofluorescence of β-catenin was strongly detected in the hepatocytes of PBS-injected mice but was significantly reduced in GalXC-injected mice (Fig. 29E). Importantly, tdTomato-positive hepatocytes were located adjacent to clusters of β-catenin-positive BECs in GalXC-injected mice. Finally, clusters of tdTomato-positive hepatocytes in GalXC-injected mice would occasionally extend all the way to the central vein, resulting in localized re-expression of β-catenin target GS (Fig. 31B). All together, these results demonstrate that BECs give rise to hepatocytes when hepatocyte proliferation is impaired, which was achieved in our model through the loss of β-catenin expression in hepatocytes in mice exposed to CDE diet-induced liver injury (Fig. 31C).

3.5 Discussion

The role of BECs in mediating LR has remained controversial, as several studies have reported a limited role for BEC differentiation to hepatocytes (150, 190, 278). Recent studies have demonstrated widespread hepatocyte senescence (191), hepatocyte ablation (232), impaired

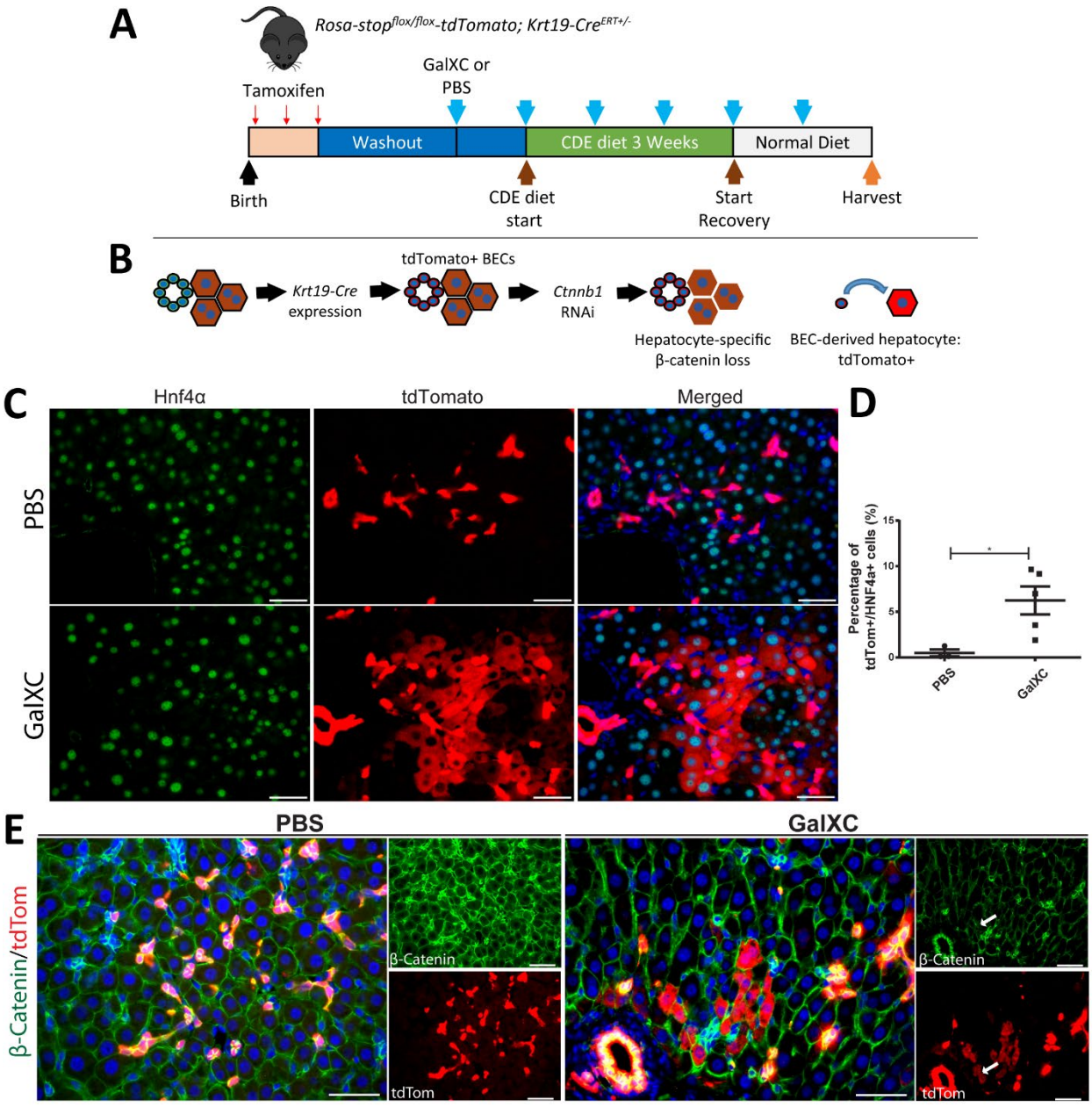

Figure 29: BEC-derived hepatocytes appear in GalXC but not PBS treated mice following recovery period after CDE diet.

(*a*) *Krt19*-Cre$^{ERT+/-}$ mice were given tamoxifen during postnatal week 1, followed by a 2 week washout. Mice were given subcutaneous injections of either GalXC or PBS one week prior to CDE diet administration, and injected weekly throughout the course of the experiment. Mice remained on CDE diet for 3 weeks followed by a 2 week recovery on normal diet. (*b*) After tamoxifen administration, BECs will be labeled with tdTomato, and GalXC injections induce hepatocyte-specific knockdown of *Ctnnb1* expression. Therefore, a BEC-derived hepatocyte will be tdTomato-positive and re-express β-catenin. (*c*) In control PBS-injected mice after CDE diet and recovery, BECs but not hepatocytes are tdTomato-positive. In GalXC-injected mice clusters of

tdTomato-positive, Hnf4α-positive hepatocytes are evident, demonstrating BEC-to-hepatocyte conversion (scale bar 100 μm). (*d*) Quantification of tdTomato, Hnf4α double-positive cells reveals significantly more BEC-derived hepatocytes in GalXC-injected mice compared to PBS-injected controls (t-test, * = $p < 0.05$). (*e*) In control PBS-injected mice, both BECs and hepatocytes are β-catenin-positive, but only BECs are tdTomato-positive. In GalXC-injected mice, hepatocytes lose cytoplasmic β-catenin-staining and clusters of tdTomato-positive hepatocytes (white arrows) are located periportally (scale bar 100 μm).

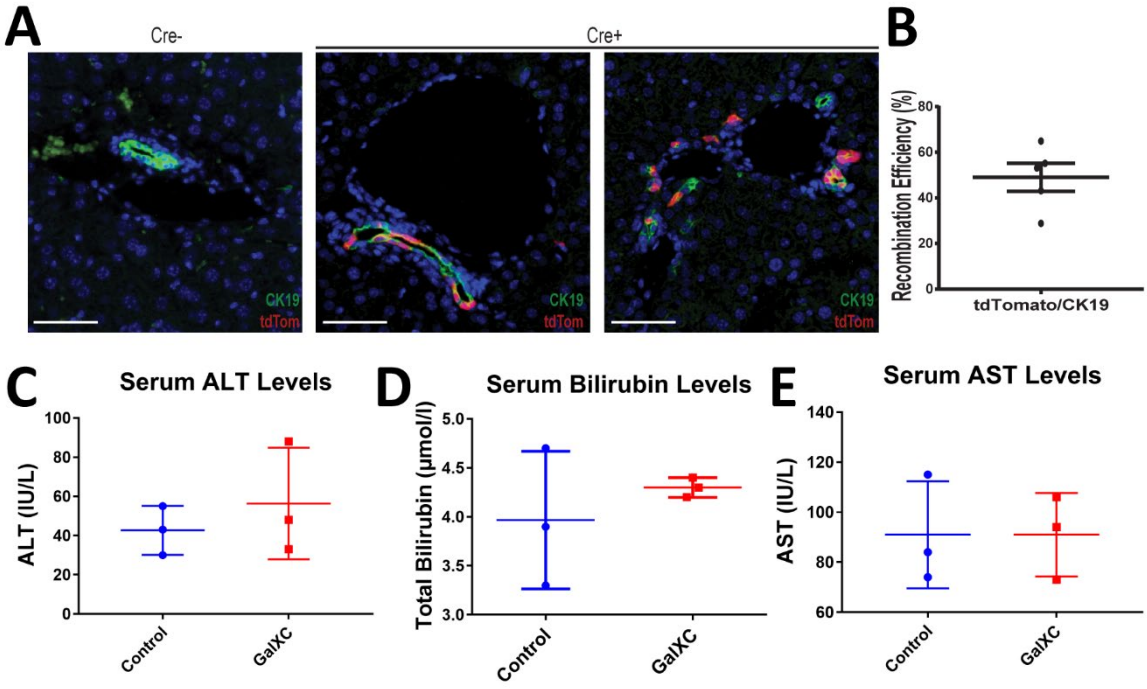

Figure 30: BEC-derived hepatocytes begin to repopulate the liver in GalXC-injected mice.

(*a*) After tamoxifen administration, only CK19-positive BECs are labeled with tdTomato. Expression of tdTomato is not detected in mice that do not express Cre recombinase (scale bar 100 μm). (*b*) Quantification of recombination efficiency of CK19-positive cells following tamoxifen injections. (*c*) Serum ALT levels are normalizing in GalXC-injected mice after CDE diet and recovery. (*d*) Serum Bilirubin levels are normalizing in GalXC-injected mice after CDE diet and recovery. (*e*) Serum AST levels are normalizing in GalXC-injected mice after CDE diet and recovery.

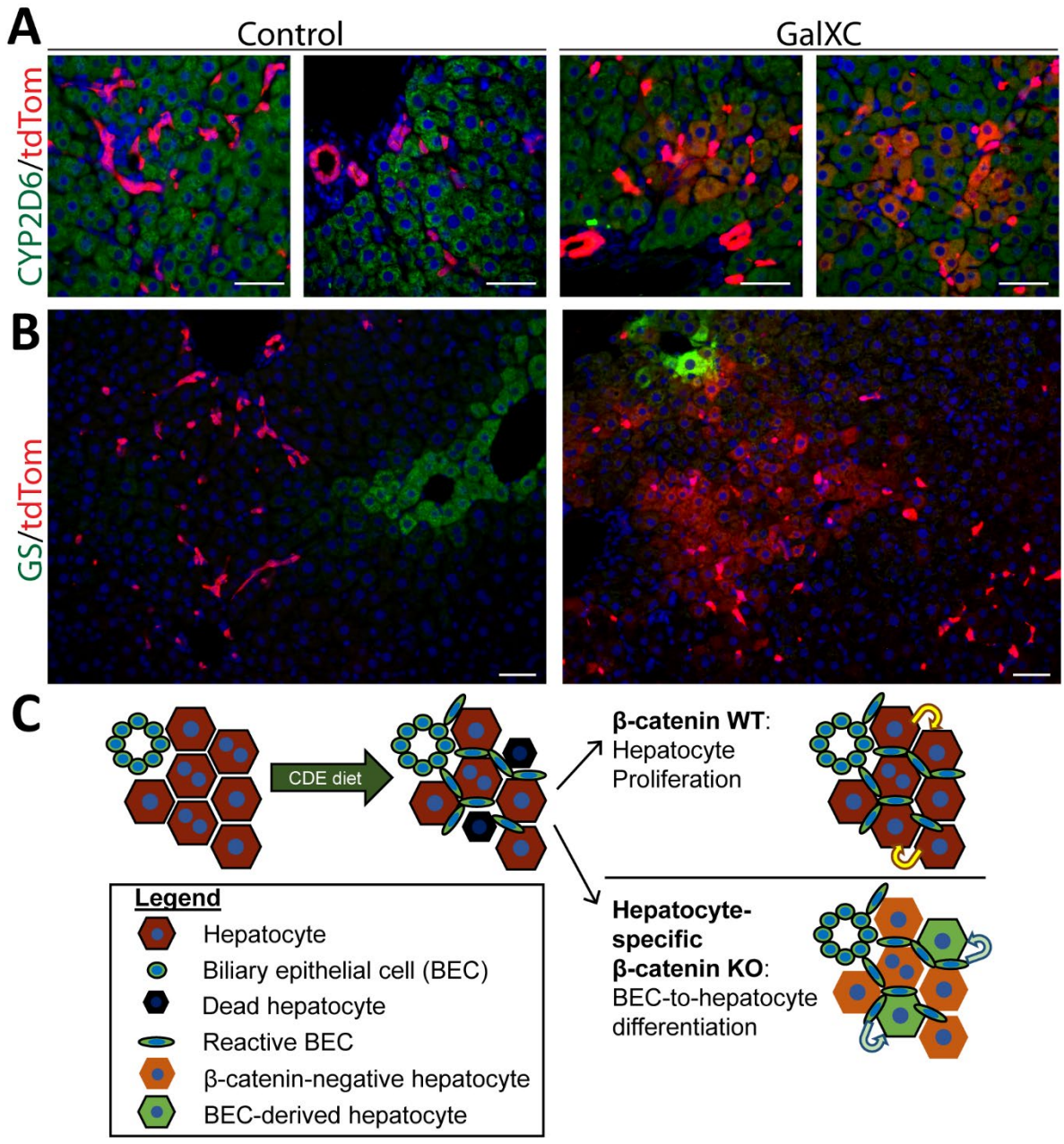

Figure 31: BEC-derived hepatocytes express mature hepatocyte markers.

(*a*) BEC-derived tdTomato-positive hepatocytes are positive for hepatocyte marker CYP2D6 in GalXC-injected mice (scale bar 100 μm). (*b*) BEC-derived tdTomato-positive hepatocytes in GalXC-injected mice extend all the way to the central vein, resulting in re-expression of β-catenin-target GS (scale bar 100 μm). (*c*) Schematic illustrating key findings: when hepatocyte proliferation is intact (β-catenin WT hepatocytes) after CDE diet-induced liver injury, liver regeneration is driven by hepatocyte proliferation. When mice with hepatocyte-specific loss of β-catenin are subjected to CDE diet, BEC-to-hepatocyte differentiation occurs to facilitate liver regeneration.

hepatocyte proliferation (187), or prolonged exposure to severe liver injury (195) can trigger differentiation of BECs to hepatocytes. Interestingly, a previous study reported ductular reaction and BEC-to-hepatocyte differentiation in aged *Albumin*-Cre β-catenin KO livers (284), suggesting expression of β-catenin in hepatocytes is important for long-term liver health. Here, we demonstrate that hepatocyte-specific loss of β-catenin expression in combination with CDE diet-induced liver injury triggers severe impairment of hepatocyte proliferation and leads to unequivocal repopulation of liver with BEC-derived hepatocytes.

Genetic loss of β-catenin in hepatocytes led to extensive injury in the CDE diet model with robust expansion of BECs in both male and female mice (data not shown). Further, knockdown of *Ctnnb1* expression in hepatocytes via siRNA also impaired hepatocyte proliferation after CDE diet. Intriguingly, BEC expansion occurred normally despite β-catenin loss in these cells in *Albumin-Cre Ctnnb1* KO mice on CDE diet. However, the appearance of active-β-catenin in KO2 mice, which retained β-catenin expression in BECs, suggests activation of β-catenin signaling in this compartment during CDE diet. This observation is in accordance with previous findings that activation of β-catenin in reactive BECs promotes differentiation towards the hepatocyte lineage (210). In our model, appearance of BEC-derived hepatocytes was evident as early as 3d of recovery on basal diet after 2W of CDE diet, when cells positive for both BEC and hepatocyte markers could be observed. Excitingly, Hnf4α+/CK19+ cells have also been observed in a recent study demonstrating BEC-derived hepatocytes during long-term severe liver injury (195). Our results suggest that differentiation of BECs to hepatocytes is limited or impaired during ongoing injury and that a period of recovery is necessary to allow BEC differentiation to hepatocytes, as also shown elsewhere (184, 187, 191).

Greater than 99% of hepatocytes were labeled with EYFP after AAV8-TBG-Cre injection, and after 6 months of normal diet the numbers of EYFP-negative hepatocytes in both WT2 and KO2 mice were not significantly increased. Additionally, over 99% of hepatocytes were still EYFP-positive in both WT2 and KO2 mice after 2W of CDE diet, suggesting no significant population of hepatocytes escaping initial Cre-recombination, as these cells would express β-catenin and would be expected to have a proliferative advantage during CDE diet-induced liver injury. In this negative tracing model, we found that after recovery, approximately 20% of periportal hepatocytes were BEC-derived. Interestingly, in our positive lineage tracing model, we found only 6% of hepatocytes were BEC-derived. This is attributable to the fact that initially only around 50% of BECs were labeled with tdTomato in this model, suggesting potentially 12% of hepatocytes were BEC-derived in our model after factoring in the limited recombination efficiency. Furthermore, newly BEC-derived hepatocytes may be susceptible to GalXC-mediated *Ctnnb1* knockdown, potentially reducing their proliferation during recovery from CDE diet, further reducing tdTomato-positive hepatocyte numbers.

Although our data convincingly proves the differentiation and long-term survival of BEC-derived hepatocytes, much remains to be elucidated about both the long-term effects of BEC-derived hepatocytes on liver health and the mechanisms underlying BEC-to-hepatocyte differentiation. For instance, it will be interesting to determine if BEC-derived hepatocytes are equally as adept at promoting resolution of liver injury, such as resolution of fibrosis. Additionally, while factors that promote ductular reaction are better known (285), our knowledge of the factors promoting BEC differentiation to hepatocytes is much more limited. Since our model establishes a clear timeline for BEC differentiation to hepatocytes, it will be invaluable in determining the factors that underlie this process. For example, as we have demonstrated the importance of β-

catenin signaling in LR, this would potentially allow promotion of BEC-to-hepatocyte differentiation while circumventing activation of oncogenic β-catenin signaling in patients. Additionally, it will be important to determine the threshold of hepatic impairment that triggers BEC-to-hepatocyte differentiation, as this may lead to the development of biomarkers for patients with severe liver disease that are amenable to such treatments. These would be important steps in developing regenerative medicine therapies for the treatment of chronic liver disease.

4.0 Concluding Remarks and General Discussion

4.1 Significance

Chronic liver disease is a major public health concern which is growing in magnitude. In 2013, chronic liver disease and cirrhosis was the 12th leading cause of death in the United States (286). Chronic liver disease (CLD) has many causes including viral hepatitis, alcoholic hepatitis, primary biliary cirrhosis, and non-alcoholic fatty liver disease (NAFLD) (222, 287, 288). Patients with CLD are at risk for progression to cirrhosis and/or liver failure (222, 223, 289, 290), conditions where the only available treatment is a liver transplant (222, 290). The scarcity of donor organs and mortality of patients on the waiting list means there is a great need to develop alternative treatments for CLD (291). Liver progenitor cells (LPCs), bipotent cells arising from the biliary epithelial cell (BEC) compartment, are thought to differentiate into hepatocytes to mediate liver regeneration only when hepatocyte proliferation is impaired (80, 175, 176, 218). In this dissertation, we have identified an important role for BET protein signaling in promoting hepatocyte proliferation after acute liver injury (216). This will be important knowledge to keep in mind when designing therapies involving the use of BET inhibitors, as this treatment may put patients at higher risk of developing liver failure with the use of over-the-counter medicines that contain acetaminophen.

The mechanisms of LPC-mediated liver regeneration are poorly understood. Expansion of LPCs is observed in a wide range of human patients with both chronic (116, 275, 276) and acute liver injury (292). Therapies promoting LPC differentiation to hepatocytes could have major clinical benefits, as impairment of endogenous hepatocyte proliferation is thought to promote

progression of CLD (222). β-catenin signaling, which is important for both normal liver development (70, 293, 294) and regeneration after liver injury (74, 82, 97), has been implicated in the differentiation of LPCs to hepatocytes (210). In this dissertation, we have identified lack of β-catenin in hepatocytes during exposure to severe liver injury as a mechanism of impairing hepatocyte proliferation, leading to BEC-to-hepatocyte differentiation (188). This suggests that patients with innately impaired liver Wnt/β-catenin signaling may be at a higher risk of developing severe liver injury and progressing to cirrhosis in the context of chronic liver disease, also this hypothesis remains to be tested with clinical specimens.

4.2 Future Directions: Wnt/β-catenin Signaling

As more knowledge about the role of Wnt/β-catenin signaling in liver biology is obtained, it is becoming clear that Wnt/β-catenin signaling is involved in almost every aspect of liver function, from liver development to metabolism to regeneration. This review has also illustrated the diverse roles of Wnt/β-catenin signaling in nearly every cell type in the liver. As this signaling pathway can promote both liver injury and regeneration, therapies targeting Wnt/β-catenin signaling must be carefully evaluated to consider both the disease context and the targeted cell type. The pleiotropic nature of this signaling pathway would also necessitate the development of delivery methods that would minimize off-target effects of undesirable Wnt/β-catenin signaling inhibition in non-target cell types.

Despite all that is known about Wnt/β-catenin signaling in liver biology, there is clearly still much to be discovered. For example, very little is understood about which Wnt ligands interact with which Frizzled receptors in many cell type and disease contexts. As there are 19 Wnts and 10

Frizzled receptors in the mammalian genome (39), this a problem of almost dizzying complexity. Additionally, the role of non-canonical Wnt signaling is liver homeostasis, disease, and regeneration is poorly understood. Finally, the role of Wnt/β-catenin signaling in the pathobiology of conditions such as steatohepatitis (92, 97), cholestasis (65), and hepatic fibrosis (295, 296) in human patients will need to be investigated further, as experiment evidence has implicated a role for Wnt/β-catenin signaling in the etiology of these conditions. Undoubtedly, future research will continue to identify new and exciting roles for Wnt/β-catenin signaling in liver pathobiology and regeneration.

4.3 Future Directions: BEC-to-Hepatocyte Differentiation

The current body of literature clearly indicates that there is remarkable cellular plasticity within the epithelial cells of the liver during hepatic injury, such that under specific circumstances the hepatocytes and BECs can change their cellular fate to mediate liver regeneration. Whether this cell type conversion is direct transdifferentiation or goes through a "progenitor cell" intermediate remains to be definitively elucidated. It also remains to be proven if there are certain subsets of hepatocytes and BECs which are more primed to undergo cell fate changes, and if this were the case, whether these subsets of cell are facultative stem cells or represent a progenitor cell compartment is an argument of semantics. Based on their diverse origin and their dynamic cellular fate in diseased liver, LPC-specific markers (or a marker which is absent in mature BECs and hepatocytes but expressed in a cell undergoing a cell fate conversion) are not currently available. Therefore, it is not feasible to distinguish LPC activation and BEC proliferation/hyperplasia to repair damage to biliary structures. Although several markers are suggested as LPC markers, such

as Foxl1 (184), Lgr5 (297), Trop2 (147) and Ncam (298), these genes are not usable for detecting all LPC populations, as expression of these markers is most likely context-dependent. There is no doubt that identification of LPC-specific markers would greatly advance this field; however, it remains challenging to identify concrete markers for LPCs applicable to multiple disease conditions.

It also remains to be seen if targeting LPCs for differentiation into hepatocytes represents a viable therapeutic strategy for chronic liver disease. Only a subset of patients with chronic liver disease will progress to end-stage liver disease and liver cancer, and the role or function of LPCs during disease progression remains unknown. Most studies have focused on proving the phenomena of cell fate conversion and sought to identify the molecular mechanisms underlying this process. While these experiments are essential for developing druggable targets, few studies have examined the long-term consequences of promoting LPC differentiation. Since the DR is well known to promote fibrogenesis and inflammation, is simply targeting the cells of the DR for conversion to hepatocytes enough to induce a restorative hepatic microenvironment? Can this process be achieved with enough specificity and efficiency to produce a measurable effect? Currently the technology for targeting BECs, the main cell type of the DR, is severely limited, which serves as a major roadblock to the development of new therapeutics. Many studies involved in promoting LPC differentiation to hepatocytes have removed the underlying liver injury to allow recovery and enhance LPC differentiation. This is a very unrealistic scenario in clinical practice, so more work will be necessary to determine the efficiency of LPC differentiation in the context of ongoing liver injury.

In conclusion, the liver is a remarkable organ with a diverse array of regenerative responses to hepatic injury. It remains to be determined if activation of LPCs, or activation of BECs and

hepatocytes as facultative stem cells, is a viable alternative liver regeneration mechanism to proliferation of the endogenous epithelial cells of the liver. Nonetheless, advances in this field and identification of new mechanisms of liver regeneration hold great promise towards the development of therapies for patients with chronic liver disease.

Appendix A

A.1 Publications

Russell JO, Ko S, Molina LM, Monga SP. 2019. Liver progenitor cells and cell plasticity in liver injury and repair: knowns and unknowns. Submitted to Annual Reviews of Pathology.

Russell JO, Ko S, Monga SP, Shin D. 2019. Notch Inhibition Promotes Differentiation of Liver Progenitor Cells into Hepatocytes via sox9b Repression in Zebrafish. Stem Cells International.

Min Q, Molina L, Li J, Adebayo Michael AO, **Russell JO**, Preziosi ME, Singh S, Poddar M, Matz-Soja M, Ranganathan S, Bell AW, Gebhardt R, Gaunitz F, Yu J, Tao J, Monga SP. 2019. β-Catenin and yes-associated protein 1 cooperate in hepatoblastoma pathogenesis. Am J Pathol

Adebayo Michael AO, Ko S, Tao J, Moghe A, Yang H, Xu M, **Russell JO**, Pradhan-Sundd T, Liu S, Singh S, Poddar M, Monga JS, Liu P, Oertel M, Ranganathan S, Singhi A, Rebouissou S, Zucman-Rossi J, Ribback S, Calvisi D, Qvartskhava N, Görg B, Häussinger D, Chen X, Monga SP. 2019. Inhibiting Glutamine-Dependent mTORC1 Activation Ameliorates Liver Cancers Driven by β-Catenin Mutations. Cell Metab

Ko S, **Russell JO**, Tian J, Gao C, Kobayashi M, Feng R, Yuan X, Shao C, Ding H, Poddar M, Singh S, Locker J, Weng HL, Monga SP, Shin D. 2019. Hdac1 Regulates Differentiation of Bipotent Liver Progenitor Cells During Regeneration via Sox9b and Cdk8. Gastroenterology 156: 187-202.e14

Zhang R, Kikuchi AT, Nakao T, **Russell JO**, Preziosi ME, Poddar M, Singh S, Bell AW, England SG, Monga SP. 2018. Elimination of Wnt secretion from stellate cells is dispensable for zonation and development of liver fibrosis following hepatobiliary injury. Gene Expr

Russell JO, Lu WY, Okabe H, Abrams M, Oertel M, Poddar M, Singh S, Forbes SJ, Monga SP. 2018. Hepatocyte-specific β-catenin deletion during severe liver injury provokes cholangiocytes to differentiate into hepatocytes. Hepatology

Pradhan-Sundd T, Vats R, **Russell JO**, Singh S, Michael AA, Molina L, Kakar S, Cornuet P, Poddar M, Watkins SC, Nejak-Bowen KN, Monga SP, Sundd P. 2018. Dysregulated bile transporters and impaired tight junctions during chronic liver injury in mice. Gastroenterology

Russell JO, Ko S, Saggi HS, Singh S, Poddar M, Shin D, Monga SP. 2018. Bromodomain and Extraterminal (BET) Proteins Regulate Hepatocyte Proliferation in Hepatocyte-Driven Liver Regeneration. Am J Pathol 188: 1389-405

Russell JO, Monga SP. 2018. Wnt/β-Catenin Signaling in Liver Development, Homeostasis, and Pathobiology. Annu Rev Pathol 13: 351-78

Pradhan-Sundd T, Zhou L, Vats R, Jiang A, Molina L, Singh S, Poddar M, **Russell J**, Stolz DB, Oertel M, Apte U, Watkins S, Ranganathan S, Nejak-Bowen KN, Sundd P, Monga SP. 2018. Dual catenin loss in murine liver causes tight junctional deregulation and progressive intrahepatic cholestasis. Hepatology 67: 2320-37

Ko S, Choi TY, **Russell JO**, So J, Monga SPS, Shin D. 2016. Bromodomain and extraterminal (BET) proteins regulate biliary-driven liver regeneration. J Hepatol 64: 316-25

Cranz-Mileva S, MacTaggart B, **Russell J**, Hitchcock-DeGregori SE. 2015. Evolutionarily conserved sites in yeast tropomyosin function in cell polarity, transport and contractile ring formation. Biol Open 4: 1040-51

Delgado E, Okabe H, Preziosi M, **Russell JO**, Alvarado TF, Oertel M, Nejak-Bowen KN, Zhang Y, Monga SP. 2015. Complete response of Ctnnb1-mutated tumours to β-catenin suppression by locked nucleic acid antisense in a mouse hepatocarcinogenesis model. J Hepatol 62: 380-7

Cranz-Mileva S, Pamula MC, Barua B, Desai B, Hong YH, **Russell J**, Trent R, Wang J, Walworth NC, Hitchcock-DeGregori SE. 2013. A molecular evolution approach to study the roles of tropomyosin in fission yeast. PLoS One 8: e76726

A.2 Funding

- T32 training grant: Cellular Approaches to Tissue Engineering and Regeneration (NIH T32EB0010216), 2015-2017

- F31 fellowship: Elucidating the role of β-catenin signaling in liver progenitor cell-mediated liver regeneration (NIH/NIDDK 1F31DK115017-01), 2017-2019

Bibliography

1. Russell JO, Monga SS. 2017. Wnt/β-Catenin Signaling in Liver Development, Homeostasis, and Pathobiology. *Annu Rev Pathol*

2. Dhalluin C, Carlson JE, Zeng L, He C, Aggarwal AK, Zhou MM. 1999. Structure and ligand of a histone acetyltransferase bromodomain. *Nature* 399: 491-6

3. Shi J, Vakoc CR. 2014. The mechanisms behind the therapeutic activity of BET bromodomain inhibition. *Mol Cell* 54: 728-36

4. Jiang YW, Veschambre P, Erdjument-Bromage H, Tempst P, Conaway JW, Conaway RC, Kornberg RD. 1998. Mammalian mediator of transcriptional regulation and its possible role as an end-point of signal transduction pathways. *Proc Natl Acad Sci U S A* 95: 8538-43

5. Wu SY, Chiang CM. 2007. The double bromodomain-containing chromatin adaptor Brd4 and transcriptional regulation. *J Biol Chem* 282: 13141-5

6. Zhou Q, Li T, Price DH. 2012. RNA polymerase II elongation control. *Annu Rev Biochem* 81: 119-43

7. Adelman K, Lis JT. 2012. Promoter-proximal pausing of RNA polymerase II: emerging roles in metazoans. *Nat Rev Genet* 13: 720-31

8. Lovén J, Hoke HA, Lin CY, Lau A, Orlando DA, Vakoc CR, Bradner JE, Lee TI, Young RA. 2013. Selective inhibition of tumor oncogenes by disruption of super-enhancers. *Cell* 153: 320-34

9. Anand P, Brown JD, Lin CY, Qi J, Zhang R, Artero PC, Alaiti MA, Bullard J, Alazem K, Margulies KB, Cappola TP, Lemieux M, Plutzky J, Bradner JE, Haldar SM. 2013. BET bromodomains mediate transcriptional pause release in heart failure. *Cell* 154: 569-82

10. Zhang W, Prakash C, Sum C, Gong Y, Li Y, Kwok JJ, Thiessen N, Pettersson S, Jones SJ, Knapp S, Yang H, Chin KC. 2012. Bromodomain-containing protein 4 (BRD4) regulates RNA polymerase II serine 2 phosphorylation in human CD4+ T cells. *J Biol Chem* 287: 43137-55

11. Filippakopoulos P, Qi J, Picaud S, Shen Y, Smith WB, Fedorov O, Morse EM, Keates T, Hickman TT, Felletar I, Philpott M, Munro S, McKeown MR, Wang Y, Christie AL, West N, Cameron MJ, Schwartz B, Heightman TD, La Thangue N, French CA, Wiest O, Kung AL, Knapp S, Bradner JE. 2010. Selective inhibition of BET bromodomains. *Nature* 468: 1067-73

12. Delmore JE, Issa GC, Lemieux ME, Rahl PB, Shi J, Jacobs HM, Kastritis E, Gilpatrick T, Paranal RM, Qi J, Chesi M, Schinzel AC, McKeown MR, Heffernan TP, Vakoc CR, Bergsagel PL, Ghobrial IM, Richardson PG, Young RA, Hahn WC, Anderson KC, Kung AL, Bradner JE, Mitsiades CS. 2011. BET bromodomain inhibition as a therapeutic strategy to target c-Myc. *Cell* 146: 904-17

13. Dawson MA, Prinjha RK, Dittmann A, Giotopoulos G, Bantscheff M, Chan WI, Robson SC, Chung CW, Hopf C, Savitski MM, Huthmacher C, Gudgin E, Lugo D, Beinke S, Chapman TD, Roberts EJ, Soden PE, Auger KR, Mirguet O, Doehner K, Delwel R, Burnett AK, Jeffrey P, Drewes G, Lee K, Huntly BJ, Kouzarides T. 2011. Inhibition of BET recruitment to chromatin as an effective treatment for MLL-fusion leukaemia. *Nature* 478: 529-33

14. Zuber J, Shi J, Wang E, Rappaport AR, Herrmann H, Sison EA, Magoon D, Qi J, Blatt K, Wunderlich M, Taylor MJ, Johns C, Chicas A, Mulloy JC, Kogan SC, Brown P, Valent P, Bradner JE, Lowe SW, Vakoc CR. 2011. RNAi screen identifies Brd4 as a therapeutic target in acute myeloid leukaemia. *Nature* 478: 524-8

15. Wang YH, Sui XM, Sui YN, Zhu QW, Yan K, Wang LS, Wang F, Zhou JH. 2015. BRD4 induces cell migration and invasion in HCC cells through MMP-2 and MMP-9 activation mediated by the Sonic hedgehog signaling pathway. *Oncol Lett* 10: 2227-32

16. Ding N, Hah N, Yu RT, Sherman MH, Benner C, Leblanc M, He M, Liddle C, Downes M, Evans RM. 2015. BRD4 is a novel therapeutic target for liver fibrosis. *Proc Natl Acad Sci U S A* 112: 15713-8

17. Ko S, Choi TY, Russell JO, So J, Monga SPS, Shin D. 2016. Bromodomain and extraterminal (BET) proteins regulate biliary-driven liver regeneration. *J Hepatol* 64: 316-25

18. Kimelman D, Xu W. 2006. beta-catenin destruction complex: insights and questions from a structural perspective. *Oncogene* 25: 7482-91

19. Behrens J, Jerchow BA, Würtele M, Grimm J, Asbrand C, Wirtz R, Kühl M, Wedlich D, Birchmeier W. 1998. Functional interaction of an axin homolog, conductin, with beta-catenin, APC, and GSK3beta. *Science* 280: 596-9

20. Liu C, Li Y, Semenov M, Han C, Baeg GH, Tan Y, Zhang Z, Lin X, He X. 2002. Control of beta-catenin phosphorylation/degradation by a dual-kinase mechanism. *Cell* 108: 837-47

21. Amit S, Hatzubai A, Birman Y, Andersen JS, Ben-Shushan E, Mann M, Ben-Neriah Y, Alkalay I. 2002. Axin-mediated CKI phosphorylation of beta-catenin at Ser 45: a molecular switch for the Wnt pathway. *Genes Dev* 16: 1066-76

22. Aberle H, Bauer A, Stappert J, Kispert A, Kemler R. 1997. beta-catenin is a target for the ubiquitin-proteasome pathway. *EMBO J* 16: 3797-804

23. Hart M, Concordet JP, Lassot I, Albert I, del los Santos R, Durand H, Perret C, Rubinfeld B, Margottin F, Benarous R, Polakis P. 1999. The F-box protein beta-TrCP associates with phosphorylated beta-catenin and regulates its activity in the cell. *Curr Biol* 9: 207-10

24. Barrott JJ, Cash GM, Smith AP, Barrow JR, Murtaugh LC. 2011. Deletion of mouse Porcn blocks Wnt ligand secretion and reveals an ectodermal etiology of human focal dermal hypoplasia/Goltz syndrome. *Proc Natl Acad Sci U S A* 108: 12752-7

25. Zhai L, Chaturvedi D, Cumberledge S. 2004. Drosophila wnt-1 undergoes a hydrophobic modification and is targeted to lipid rafts, a process that requires porcupine. *J Biol Chem* 279: 33220-7

26. Bänziger C, Soldini D, Schütt C, Zipperlen P, Hausmann G, Basler K. 2006. Wntless, a conserved membrane protein dedicated to the secretion of Wnt proteins from signaling cells. *Cell* 125: 509-22

27. Bartscherer K, Pelte N, Ingelfinger D, Boutros M. 2006. Secretion of Wnt ligands requires Evi, a conserved transmembrane protein. *Cell* 125: 523-33

28. Bhanot P, Brink M, Samos CH, Hsieh JC, Wang Y, Macke JP, Andrew D, Nathans J, Nusse R. 1996. A new member of the frizzled family from Drosophila functions as a Wingless receptor. *Nature* 382: 225-30

29. Wehrli M, Dougan ST, Caldwell K, O'Keefe L, Schwartz S, Vaizel-Ohayon D, Schejter E, Tomlinson A, DiNardo S. 2000. arrow encodes an LDL-receptor-related protein essential for Wingless signalling. *Nature* 407: 527-30

30. Pinson KI, Brennan J, Monkley S, Avery BJ, Skarnes WC. 2000. An LDL-receptor-related protein mediates Wnt signalling in mice. *Nature* 407: 535-8

31. Tamai K, Semenov M, Kato Y, Spokony R, Liu C, Katsuyama Y, Hess F, Saint-Jeannet JP, He X. 2000. LDL-receptor-related proteins in Wnt signal transduction. *Nature* 407: 530-5

32. Tamai K, Zeng X, Liu C, Zhang X, Harada Y, Chang Z, He X. 2004. A mechanism for Wnt coreceptor activation. *Mol Cell* 13: 149-56

33. MacDonald BT, Tamai K, He X. 2009. Wnt/beta-catenin signaling: components, mechanisms, and diseases. *Dev Cell* 17: 9-26

34. Carmon KS, Gong X, Lin Q, Thomas A, Liu Q. 2011. R-spondins function as ligands of the orphan receptors LGR4 and LGR5 to regulate Wnt/beta-catenin signaling. *Proc Natl Acad Sci U S A* 108: 11452-7

35. de Lau W, Barker N, Low TY, Koo BK, Li VS, Teunissen H, Kujala P, Haegebarth A, Peters PJ, van de Wetering M, Stange DE, van Es JE, Guardavaccaro D, Schasfoort RB, Mohri Y, Nishimori K, Mohammed S, Heck AJ, Clevers H. 2011. Lgr5 homologues associate with Wnt receptors and mediate R-spondin signalling. *Nature* 476: 293-7

36. Hao HX, Xie Y, Zhang Y, Charlat O, Oster E, Avello M, Lei H, Mickanin C, Liu D, Ruffner H, Mao X, Ma Q, Zamponi R, Bouwmeester T, Finan PM, Kirschner MW, Porter JA, Serluca FC, Cong F. 2012. ZNRF3 promotes Wnt receptor turnover in an R-spondin-sensitive manner. *Nature* 485: 195-200

37. Koo BK, Spit M, Jordens I, Low TY, Stange DE, van de Wetering M, van Es JH, Mohammed S, Heck AJ, Maurice MM, Clevers H. 2012. Tumour suppressor RNF43 is a stem-cell E3 ligase that induces endocytosis of Wnt receptors. *Nature* 488: 665-9

38. Cadigan KM, Nusse R. 1997. Wnt signaling: a common theme in animal development. *Genes Dev* 11: 3286-305

39. Vincan E, Barker N. 2008. The upstream components of the Wnt signalling pathway in the dynamic EMT and MET associated with colorectal cancer progression. *Clin Exp Metastasis* 25: 657-63

40. Oishi I, Suzuki H, Onishi N, Takada R, Kani S, Ohkawara B, Koshida I, Suzuki K, Yamada G, Schwabe GC, Mundlos S, Shibuya H, Takada S, Minami Y. 2003. The receptor tyrosine kinase Ror2 is involved in non-canonical Wnt5a/JNK signalling pathway. *Genes Cells* 8: 645-54

41. Sastre-Perona A, Santisteban P. 2012. Role of the wnt pathway in thyroid cancer. *Front Endocrinol (Lausanne)* 3: 31

42. Pez F, Lopez A, Kim M, Wands JR, Caron de Fromentel C, Merle P. 2013. Wnt signaling and hepatocarcinogenesis: molecular targets for the development of innovative anticancer drugs. *J Hepatol* 59: 1107-17

43. Nishita M, Enomoto M, Yamagata K, Minami Y. 2010. Cell/tissue-tropic functions of Wnt5a signaling in normal and cancer cells. *Trends Cell Biol* 20: 346-54

44. Topol L, Jiang X, Choi H, Garrett-Beal L, Carolan PJ, Yang Y. 2003. Wnt-5a inhibits the canonical Wnt pathway by promoting GSK-3-independent beta-catenin degradation. *J Cell Biol* 162: 899-908

45. Acebron SP, Karaulanov E, Berger BS, Huang YL, Niehrs C. 2014. Mitotic wnt signaling promotes protein stabilization and regulates cell size. *Mol Cell* 54: 663-74

46. Fuentealba LC, Eivers E, Ikeda A, Hurtado C, Kuroda H, Pera EM, De Robertis EM. 2007. Integrating patterning signals: Wnt/GSK3 regulates the duration of the BMP/Smad1 signal. *Cell* 131: 980-93

47. Kim NG, Xu C, Gumbiner BM. 2009. Identification of targets of the Wnt pathway destruction complex in addition to beta-catenin. *Proc Natl Acad Sci U S A* 106: 5165-70

48. Koch S, Acebron SP, Herbst J, Hatiboglu G, Niehrs C. 2015. Post-transcriptional Wnt Signaling Governs Epididymal Sperm Maturation. *Cell* 163: 1225-36

49. Xu C, Kim NG, Gumbiner BM. 2009. Regulation of protein stability by GSK3 mediated phosphorylation. *Cell Cycle* 8: 4032-9

50. Kim H, Vick P, Hedtke J, Ploper D, De Robertis EM. 2015. Wnt Signaling Translocates Lys48-Linked Polyubiquitinated Proteins to the Lysosomal Pathway. *Cell Rep* 11: 1151-9

51. Taelman VF, Dobrowolski R, Plouhinec JL, Fuentealba LC, Vorwald PP, Gumper I, Sabatini DD, De Robertis EM. 2010. Wnt signaling requires sequestration of glycogen synthase kinase 3 inside multivesicular endosomes. *Cell* 143: 1136-48

52. Vinyoles M, Del Valle-Perez B, Curto J, Vinas-Castells R, Alba-Castellon L, Garcia de Herreros A, Dunach M. 2014. Multivesicular GSK3 sequestration upon Wnt signaling is controlled by p120-catenin/cadherin interaction with LRP5/6. *Mol Cell* 53: 444-57

53. Acebron SP, Niehrs C. 2016. beta-Catenin-Independent Roles of Wnt/LRP6 Signaling. *Trends Cell Biol* 26: 956-67

54. Inoki K, Ouyang H, Zhu T, Lindvall C, Wang Y, Zhang X, Yang Q, Bennett C, Harada Y, Stankunas K, Wang CY, He X, MacDougald OA, You M, Williams BO, Guan KL. 2006. TSC2 integrates Wnt and energy signals via a coordinated phosphorylation by AMPK and GSK3 to regulate cell growth. *Cell* 126: 955-68

55. Wheelock MJ, Johnson KR. 2003. Cadherins as modulators of cellular phenotype. *Annu Rev Cell Dev Biol* 19: 207-35

56. D'Souza-Schorey C. 2005. Disassembling adherens junctions: breaking up is hard to do. *Trends Cell Biol* 15: 19-26

57. Hinck L, Näthke IS, Papkoff J, Nelson WJ. 1994. Dynamics of cadherin/catenin complex formation: novel protein interactions and pathways of complex assembly. *J Cell Biol* 125: 1327-40

58. Chen YT, Stewart DB, Nelson WJ. 1999. Coupling assembly of the E-cadherin/beta-catenin complex to efficient endoplasmic reticulum exit and basal-lateral membrane targeting of E-cadherin in polarized MDCK cells. *J Cell Biol* 144: 687-99

59. Huber AH, Stewart DB, Laurents DV, Nelson WJ, Weis WI. 2001. The cadherin cytoplasmic domain is unstructured in the absence of beta-catenin. A possible mechanism for regulating cadherin turnover. *J Biol Chem* 276: 12301-9

60. Lilien J, Balsamo J. 2005. The regulation of cadherin-mediated adhesion by tyrosine phosphorylation/dephosphorylation of beta-catenin. *Curr Opin Cell Biol* 17: 459-65

61. Monga SP, Mars WM, Pediaditakis P, Bell A, Mulé K, Bowen WC, Wang X, Zarnegar R, Michalopoulos GK. 2002. Hepatocyte growth factor induces Wnt-independent nuclear translocation of beta-catenin after Met-beta-catenin dissociation in hepatocytes. *Cancer Res* 62: 2064-71

62. Zeng G, Apte U, Micsenyi A, Bell A, Monga SP. 2006. Tyrosine residues 654 and 670 in beta-catenin are crucial in regulation of Met-beta-catenin interactions. *Exp Cell Res* 312: 3620-30

63. Kojima T, Yamamoto T, Murata M, Chiba H, Kokai Y, Sawada N. 2003. Regulation of the blood-biliary barrier: interaction between gap and tight junctions in hepatocytes. *Med Electron Microsc* 36: 157-64

64. Rajasekaran AK, Hojo M, Huima T, Rodriguez-Boulan E. 1996. Catenins and zonula occludens-1 form a complex during early stages in the assembly of tight junctions. *J Cell Biol* 132: 451-63

65. Yeh TH, Krauland L, Singh V, Zou B, Devaraj P, Stolz DB, Franks J, Monga SP, Sasatomi E, Behari J. 2010. Liver-specific β-catenin knockout mice have bile canalicular abnormalities, bile secretory defect, and intrahepatic cholestasis. *Hepatology* 52: 1410-9

66. Son S, Kojima T, Decaens C, Yamaguchi H, Ito T, Imamura M, Murata M, Tanaka S, Chiba H, Hirata K, Sawada N. 2009. Knockdown of tight junction protein claudin-2 prevents bile canalicular formation in WIF-B9 cells. *Histochem Cell Biol* 131: 411-24

67. Gordillo M, Evans T, Gouon-Evans V. 2015. Orchestrating liver development. *Development* 142: 2094-108

68. Yang J, Mowry LE, Nejak-Bowen KN, Okabe H, Diegel CR, Lang RA, Williams BO, Monga SP. 2014. β-catenin signaling in murine liver zonation and regeneration: a Wnt-Wnt situation! *Hepatology* 60: 964-76

69. Behari J. 2010. The Wnt/β-catenin signaling pathway in liver biology and disease. *Expert Rev Gastroenterol Hepatol* 4: 745-56

70. Lemaigre FP. 2009. Mechanisms of liver development: concepts for understanding liver disorders and design of novel therapies. *Gastroenterology* 137: 62-79

71. Jungermann K, Katz N. 1989. Functional specialization of different hepatocyte populations. *Physiol Rev* 69: 708-64

72. Jho EH, Zhang T, Domon C, Joo CK, Freund JN, Costantini F. 2002. Wnt/beta-catenin/Tcf signaling induces the transcription of Axin2, a negative regulator of the signaling pathway. *Mol Cell Biol* 22: 1172-83

73. Sekine S, Lan BY, Bedolli M, Feng S, Hebrok M. 2006. Liver-specific loss of beta-catenin blocks glutamine synthesis pathway activity and cytochrome p450 expression in mice. *Hepatology* 43: 817-25

74. Tan X, Behari J, Cieply B, Michalopoulos GK, Monga SP. 2006. Conditional deletion of beta-catenin reveals its role in liver growth and regeneration. *Gastroenterology* 131: 1561-72

75. Planas-Paz L, Orsini V, Boulter L, Calabrese D, Pikiolek M, Nigsch F, Xie Y, Roma G, Donovan A, Marti P, Beckmann N, Dill MT, Carbone W, Bergling S, Isken A, Mueller M, Kinzel B, Yang Y, Mao X, Nicholson TB, Zamponi R, Capodieci P, Valdez R, Rivera D, Loew A, Ukomadu C, Terracciano LM, Bouwmeester T, Cong F, Heim MH, Forbes SJ, Ruffner H, Tchorz JS. 2016. The RSPO-LGR4/5-ZNRF3/RNF43 module controls liver zonation and size. *Nat Cell Biol* 18: 467-79

76. Gougelet A, Torre C, Veber P, Sartor C, Bachelot L, Denechaud PD, Godard C, Moldes M, Burnol AF, Dubuquoy C, Terris B, Guillonneau F, Ye T, Schwarz M, Braeuning A, Perret C, Colnot S. 2014. T-cell factor 4 and β-catenin chromatin occupancies pattern zonal liver metabolism in mice. *Hepatology* 59: 2344-57

77. Benhamouche S, Decaens T, Godard C, Chambrey R, Rickman DS, Moinard C, Vasseur-Cognet M, Kuo CJ, Kahn A, Perret C, Colnot S. 2006. Apc tumor suppressor gene is the "zonation-keeper" of mouse liver. *Dev Cell* 10: 759-70

78. Stanulović VS, Kyrmizi I, Kruithof-de Julio M, Hoogenkamp M, Vermeulen JL, Ruijter JM, Talianidis I, Hakvoort TB, Lamers WH. 2007. Hepatic HNF4alpha deficiency induces periportal expression of glutamine synthetase and other pericentral enzymes. *Hepatology* 45: 433-44

79. Fitamant J, Kottakis F, Benhamouche S, Tian HS, Chuvin N, Parachoniak CA, Nagle JM, Perera RM, Lapouge M, Deshpande V, Zhu AX, Lai A, Min B, Hoshida Y, Avruch J, Sia D, Campreciós G, McClatchey AI, Llovet JM, Morrissey D, Raj L, Bardeesy N. 2015. YAP Inhibition Restores Hepatocyte Differentiation in Advanced HCC, Leading to Tumor Regression. *Cell Rep*

80. Thorgeirsson SS. 1996. Hepatic stem cells in liver regeneration. *FASEB J* 10: 1249-56

81. Michalopoulos GK, DeFrances MC. 1997. Liver regeneration. *Science* 276: 60-6

82. Monga SP, Pediaditakis P, Mule K, Stolz DB, Michalopoulos GK. 2001. Changes in WNT/beta-catenin pathway during regulated growth in rat liver regeneration. *Hepatology* 33: 1098-109

83. Nelsen CJ, Rickheim DG, Timchenko NA, Stanley MW, Albrecht JH. 2001. Transient expression of cyclin D1 is sufficient to promote hepatocyte replication and liver growth in vivo. *Cancer Res* 61: 8564-8

84. Yang J, Cusimano A, Monga JK, Preziosi ME, Pullara F, Calero G, Lang R, Yamaguchi TP, Nejak-Bowen KN, Monga SP. 2015. WNT5A inhibits hepatocyte proliferation and concludes β-catenin signaling in liver regeneration. *Am J Pathol* 185: 2194-205

85. Hinson JA, Roberts DW, James LP. 2010. Mechanisms of acetaminophen-induced liver necrosis. *Handb Exp Pharmacol*: 369-405

86. Zaher H, Buters JT, Ward JM, Bruno MK, Lucas AM, Stern ST, Cohen SD, Gonzalez FJ. 1998. Protection against acetaminophen toxicity in CYP1A2 and CYP2E1 double-null mice. *Toxicol Appl Pharmacol* 152: 193-9

87. Apte U, Singh S, Zeng G, Cieply B, Virji MA, Wu T, Monga SP. 2009. Beta-catenin activation promotes liver regeneration after acetaminophen-induced injury. *Am J Pathol* 175: 1056-65

88. Kaidi A, Williams AC, Paraskeva C. 2007. Interaction between beta-catenin and HIF-1 promotes cellular adaptation to hypoxia. *Nat Cell Biol* 9: 210-7

89. Lehwald N, Tao GZ, Jang KY, Sorkin M, Knoefel WT, Sylvester KG. 2011. Wnt-β-catenin signaling protects against hepatic ischemia and reperfusion injury in mice. *Gastroenterology* 141: 707-18, 18.e1-5

90. Mani A, Radhakrishnan J, Wang H, Mani MA, Nelson-Williams C, Carew KS, Mane S, Najmabadi H, Wu D, Lifton RP. 2007. LRP6 mutation in a family with early coronary disease and metabolic risk factors. *Science* 315: 1278-82

91. Go GW, Srivastava R, Hernandez-Ono A, Gang G, Smith SB, Booth CJ, Ginsberg HN, Mani A. 2014. The combined hyperlipidemia caused by impaired Wnt-LRP6 signaling is reversed by Wnt3a rescue. *Cell Metab* 19: 209-20

92. Lehwald N, Tao GZ, Jang KY, Papandreou I, Liu B, Pysz MA, Willmann JK, Knoefel WT, Denko NC, Sylvester KG. 2012. β-Catenin regulates hepatic mitochondrial function and energy balance in mice. *Gastroenterology* 143: 754-64

93. Essers MA, de Vries-Smits LM, Barker N, Polderman PE, Burgering BM, Korswagen HC. 2005. Functional interaction between beta-catenin and FOXO in oxidative stress signaling. *Science* 308: 1181-4

94. Liu H, Fergusson MM, Wu JJ, Rovira II, Liu J, Gavrilova O, Lu T, Bao J, Han D, Sack MN, Finkel T. 2011. Wnt signaling regulates hepatic metabolism. *Sci Signal* 4: ra6

95. Russell DW. 2003. The enzymes, regulation, and genetics of bile acid synthesis. *Annu Rev Biochem* 72: 137-74

96. Gebhardt R. 1992. Metabolic zonation of the liver: regulation and implications for liver function. *Pharmacol Ther* 53: 275-354

97. Behari J, Yeh TH, Krauland L, Otruba W, Cieply B, Hauth B, Apte U, Wu T, Evans R, Monga SP. 2010. Liver-specific beta-catenin knockout mice exhibit defective bile acid and cholesterol homeostasis and increased susceptibility to diet-induced steatohepatitis. *Am J Pathol* 176: 744-53

98. Stoick-Cooper CL, Moon RT, Weidinger G. 2007. Advances in signaling in vertebrate regeneration as a prelude to regenerative medicine. *Genes Dev* 21: 1292-315

99. Cordero-Espinoza L, Huch M. 2018. The balancing act of the liver: tissue regeneration versus fibrosis. *J Clin Invest* 128: 85-96

100. Vivien CJ, Hudson JE, Porrello ER. 2016. Evolution, comparative biology and ontogeny of vertebrate heart regeneration. *NPJ Regen Med* 1: 16012

101. Ferretti P, Zhang F, O'Neill P. 2003. Changes in spinal cord regenerative ability through phylogenesis and development: lessons to be learnt. *Dev Dyn* 226: 245-56

102. Wynn TA. 2008. Cellular and molecular mechanisms of fibrosis. *J Pathol* 214: 199-210

103. Forbes SJ, Newsome PN. 2016. Liver regeneration - mechanisms and models to clinical application. *Nat Rev Gastroenterol Hepatol* 13: 473-85

104. Michalopoulos GK, Khan Z. 2015. Liver Stem Cells: Experimental Findings and Implications for Human Liver Disease. *Gastroenterology* 149: 876-82

105. Fausto N, Campbell JS. 2003. The role of hepatocytes and oval cells in liver regeneration and repopulation. *Mech Dev* 120: 117-30

106. Tabibian JH, Masyuk AI, Masyuk TV, O'Hara SP, LaRusso NF. 2013. Physiology of cholangiocytes. *Compr Physiol* 3: 541-65

107. Roskams TA, Theise ND, Balabaud C, Bhagat G, Bhathal PS, Bioulac-Sage P, Brunt EM, Crawford JM, Crosby HA, Desmet V, Finegold MJ, Geller SA, Gouw AS, Hytiroglou P, Knisely AS, Kojiro M, Lefkowitch JH, Nakanuma Y, Olynyk JK, Park YN, Portmann B, Saxena R, Scheuer PJ, Strain AJ, Thung SN, Wanless IR, West AB. 2004. Nomenclature of the finer branches of the biliary tree: canals, ductules, and ductular reactions in human livers. *Hepatology* 39: 1739-45

108. Sato K, Marzioni M, Meng F, Francis H, Glaser S, Alpini G. 2019. Ductular Reaction in Liver Diseases: Pathological Mechanisms and Translational Significances. *Hepatology* 69: 420-30

109. Kim WR, Lake JR, Smith JM, Schladt DP, Skeans MA, Harper AM, Wainright JL, Snyder JJ, Israni AK, Kasiske BL. 2018. OPTN/SRTR 2016 Annual Data Report: Liver. *Am J Transplant* 18 Suppl 1: 172-253

110. Katoonizadeh A, Nevens F, Verslype C, Pirenne J, Roskams T. 2006. Liver regeneration in acute severe liver impairment: a clinicopathological correlation study. *Liver Int* 26: 1225-33

111. Weng HL, Cai X, Yuan X, Liebe R, Dooley S, Li H, Wang TL. 2015. Two sides of one coin: massive hepatic necrosis and progenitor cell-mediated regeneration in acute liver failure. *Front Physiol* 6: 178

112. Stueck AE, Wanless IR. 2015. Hepatocyte buds derived from progenitor cells repopulate regions of parenchymal extinction in human cirrhosis. *Hepatology* 61: 1696-707

113. Dechêne A, Sowa JP, Gieseler RK, Jochum C, Bechmann LP, El Fouly A, Schlattjan M, Saner F, Baba HA, Paul A, Dries V, Odenthal M, Gerken G, Friedman SL, Canbay A. 2010. Acute liver failure is associated with elevated liver stiffness and hepatic stellate cell activation. *Hepatology* 52: 1008-16

114. Williams MJ, Clouston AD, Forbes SJ. 2014. Links between hepatic fibrosis, ductular reaction, and progenitor cell expansion. *Gastroenterology* 146: 349-56

115. Lowes KN, Brennan BA, Yeoh GC, Olynyk JK. 1999. Oval cell numbers in human chronic liver diseases are directly related to disease severity. *Am J Pathol* 154: 537-41

116. Gouw AS, Clouston AD, Theise ND. 2011. Ductular reactions in human liver: diversity at the interface. *Hepatology* 54: 1853-63

117. Machado MV, Michelotti GA, Pereira TA, Xie G, Premont R, Cortez-Pinto H, Diehl AM. 2015. Accumulation of duct cells with activated YAP parallels fibrosis progression in non-alcoholic fatty liver disease. *J Hepatol* 63: 962-70

118. Guldiken N, Kobazi Ensari G, Lahiri P, Couchy G, Preisinger C, Liedtke C, Zimmermann HW, Ziol M, Boor P, Zucman-Rossi J, Trautwein C, Strnad P. 2016. Keratin 23 is a stress-inducible marker of mouse and human ductular reaction in liver disease. *J Hepatol* 65: 552-9

119. Helal TESA, Ehsan NA, Radwan NA, Abdelsameea E. 2018. Relationship between hepatic progenitor cells and stellate cells in chronic hepatitis C genotype 4. *APMIS* 126: 14-20

120. El-Araby HA, Ehsan NA, Konsowa HA, Abd-Elaati BM, Sira AM. 2015. Hepatic progenitor cells in children with chronic hepatitis C: correlation with histopathology, viremia, and treatment response. *Eur J Gastroenterol Hepatol* 27: 561-9

121. Richardson MM, Jonsson JR, Powell EE, Brunt EM, Neuschwander-Tetri BA, Bhathal PS, Dixon JB, Weltman MD, Tilg H, Moschen AR, Purdie DM, Demetris AJ, Clouston AD. 2007. Progressive fibrosis in nonalcoholic steatohepatitis: association with altered regeneration and a ductular reaction. *Gastroenterology* 133: 80-90

122. Gadd VL, Skoien R, Powell EE, Fagan KJ, Winterford C, Horsfall L, Irvine K, Clouston AD. 2014. The portal inflammatory infiltrate and ductular reaction in human nonalcoholic fatty liver disease. *Hepatology* 59: 1393-405

123. Zhao L, Westerhoff M, Pai RK, Choi WT, Gao ZH, Hart J. 2018. Centrilobular ductular reaction correlates with fibrosis stage and fibrosis progression in non-alcoholic steatohepatitis. *Mod Pathol* 31: 150-9

124. Carpino G, Nobili V, Renzi A, De Stefanis C, Stronati L, Franchitto A, Alisi A, Onori P, De Vito R, Alpini G, Gaudio E. 2016. Macrophage Activation in Pediatric Nonalcoholic Fatty Liver Disease (NAFLD) Correlates with Hepatic Progenitor Cell Response via Wnt3a Pathway. *PLoS One* 11: e0157246

125. Carpino G, Cardinale V, Folseraas T, Overi D, Floreani A, Franchitto A, Onori P, Cazzagon N, Berloco PB, Karlsen TH, Alvaro D, Gaudio E. 2018. Hepatic Stem/Progenitor Cell Activation Differs between Primary Sclerosing and Primary Biliary Cholangitis. *Am J Pathol* 188: 627-39

126. Govaere O, Cockell S, Van Haele M, Wouters J, Van Delm W, Van den Eynde K, Bianchi A, van Eijsden R, Van Steenbergen W, Monbaliu D, Nevens F, Roskams T. 2018. High-throughput sequencing identifies aetiology-dependent differences in ductular reaction in human chronic liver disease. *J Pathol*

127. Svegliati-Baroni G, De Minicis S, Marzioni M. 2008. Hepatic fibrogenesis in response to chronic liver injury: novel insights on the role of cell-to-cell interaction and transition. *Liver Int* 28: 1052-64

128. Aguilar-Bravo B, Rodrigo-Torres D, Ariño S, Coll M, Pose E, Blaya D, Graupera I, Perea L, Vallverdú J, Rubio-Tomás T, Dubuquoy L, Armengol C, Lo Nigro A, Stärkel P, Mathurin P, Bataller R, Caballería J, Lozano JJ, Ginès P, Sancho-Bru P. 2018. Ductular reaction cells display an inflammatory profile and recruit neutrophils in alcoholic hepatitis. *Hepatology*

129. Elßner C, Goeppert B, Longerich T, Scherr AL, Stindt J, Nanduri LK, Rupp C, Kather JN, Schmitt N, Kautz N, Breuhahn K, Ismail L, Heide D, Hetzer J, García-Beccaria M, Hövelmeyer N, Waisman A, Urbanik T, Mueller S, Gdynia G, Banales JM, Roessler S, Schirmacher P, Jäger D, Schölch S, Keitel V, Heikenwalder M, Schulze-Bergkamen H, Köhler BC. 2018. Nuclear Translocation of RELB is Increased in Diseased Human Liver and Promotes Ductular Reaction and Biliary Fibrosis in Mice. *Gastroenterology*

130. Yu LX, Ling Y, Wang HY. 2018. Role of nonresolving inflammation in hepatocellular carcinoma development and progression. *NPJ Precis Oncol* 2: 6

131. Sia D, Villanueva A, Friedman SL, Llovet JM. 2017. Liver Cancer Cell of Origin, Molecular Class, and Effects on Patient Prognosis. *Gastroenterology* 152: 745-61

132. Roskams T. 2006. Liver stem cells and their implication in hepatocellular and cholangiocarcinoma. *Oncogene* 25: 3818-22

133. Ye F, Jing YY, Guo SW, Yu GF, Fan QM, Qu FF, Gao L, Yang Y, Wu D, Meng Y, Yu FH, Wei LX. 2014. Proliferative ductular reactions correlate with hepatic progenitor cell and predict recurrence in HCC patients after curative resection. *Cell Biosci* 4: 50

134. Xu M, Xie F, Qian G, Jing Y, Zhang S, Gao L, Zheng T, Wu M, Yang J, Wei L. 2014. Peritumoral ductular reaction: a poor postoperative prognostic factor for hepatocellular carcinoma. *BMC Cancer* 14: 65

135. Cai X, Zhai J, Kaplan DE, Zhang Y, Zhou L, Chen X, Qian G, Zhao Q, Li Y, Gao L, Cong W, Zhu M, Yan Z, Shi L, Wu D, Wei L, Shen F, Wu M. 2012. Background progenitor activation is associated with recurrence after hepatectomy of combined hepatocellular-cholangiocarcinoma. *Hepatology* 56: 1804-16

136. Gérard C, Tys J, Lemaigre FP. 2017. Gene regulatory networks in differentiation and direct reprogramming of hepatic cells. *Semin Cell Dev Biol* 66: 43-50

137. Suzuki A, Zheng YW, Kaneko S, Onodera M, Fukao K, Nakauchi H, Taniguchi H. 2002. Clonal identification and characterization of self-renewing pluripotent stem cells in the developing liver. *J Cell Biol* 156: 173-84

138. Tanimizu N, Nishikawa M, Saito H, Tsujimura T, Miyajima A. 2003. Isolation of hepatoblasts based on the expression of Dlk/Pref-1. *J Cell Sci* 116: 1775-86

139. Nava S, Westgren M, Jaksch M, Tibell A, Broomé U, Ericzon BG, Sumitran-Holgersson S. 2005. Characterization of cells in the developing human liver. *Differentiation* 73: 249-60

140. Schmelzer E, Zhang L, Bruce A, Wauthier E, Ludlow J, Yao HL, Moss N, Melhem A, McClelland R, Turner W, Kulik M, Sherwood S, Tallheden T, Cheng N, Furth ME, Reid LM. 2007. Human hepatic stem cells from fetal and postnatal donors. *J Exp Med* 204: 1973-87

141. Dan YY, Riehle KJ, Lazaro C, Teoh N, Haque J, Campbell JS, Fausto N. 2006. Isolation of multipotent progenitor cells from human fetal liver capable of differentiating into liver and mesenchymal lineages. *Proc Natl Acad Sci U S A* 103: 9912-7

142. Oertel M, Menthena A, Dabeva MD, Shafritz DA. 2006. Cell competition leads to a high level of normal liver reconstitution by transplanted fetal liver stem/progenitor cells. *Gastroenterology* 130: 507-20; quiz 90

143. Turner R, Lozoya O, Wang Y, Cardinale V, Gaudio E, Alpini G, Mendel G, Wauthier E, Barbier C, Alvaro D, Reid LM. 2011. Human hepatic stem cell and maturational liver lineage biology. *Hepatology* 53: 1035-45

144. Cardinale V, Wang Y, Carpino G, Cui CB, Gatto M, Rossi M, Berloco PB, Cantafora A, Wauthier E, Furth ME, Inverardi L, Dominguez-Bendala J, Ricordi C, Gerber D, Gaudio E, Alvaro D, Reid L. 2011. Multipotent stem/progenitor cells in human biliary tree give rise to hepatocytes, cholangiocytes, and pancreatic islets. *Hepatology* 54: 2159-72

145. Isse K, Lesniak A, Grama K, Maier J, Specht S, Castillo-Rama M, Lunz J, Roysam B, Michalopoulos G, Demetris AJ. 2013. Preexisting epithelial diversity in normal human livers: a tissue-tethered cytometric analysis in portal/periportal epithelial cells. *Hepatology* 57: 1632-43

146. Kamiya A, Kakinuma S, Yamazaki Y, Nakauchi H. 2009. Enrichment and clonal culture of progenitor cells during mouse postnatal liver development in mice. *Gastroenterology* 137: 1114-26, 26.e1-14

147. Okabe M, Tsukahara Y, Tanaka M, Suzuki K, Saito S, Kamiya Y, Tsujimura T, Nakamura K, Miyajima A. 2009. Potential hepatic stem cells reside in EpCAM+ cells of normal and injured mouse liver. *Development* 136: 1951-60

148. Dorrell C, Erker L, Schug J, Kopp JL, Canaday PS, Fox AJ, Smirnova O, Duncan AW, Finegold MJ, Sander M, Kaestner KH, Grompe M. 2011. Prospective isolation of a bipotential clonogenic liver progenitor cell in adult mice. *Genes Dev* 25: 1193-203

149. Tanimizu N, Kobayashi S, Ichinohe N, Mitaka T. 2014. Downregulation of miR122 by grainyhead-like 2 restricts the hepatocytic differentiation potential of adult liver progenitor cells. *Development* 141: 4448-56

150. Tarlow BD, Finegold MJ, Grompe M. 2014. Clonal tracing of Sox9+ liver progenitors in mouse oval cell injury. *Hepatology* 60: 278-89

151. Li B, Dorrell C, Canaday PS, Pelz C, Haft A, Finegold M, Grompe M. 2017. Adult Mouse Liver Contains Two Distinct Populations of Cholangiocytes. *Stem Cell Reports* 9: 478-89

152. Kuwahara R, Kofman AV, Landis CS, Swenson ES, Barendswaard E, Theise ND. 2008. The hepatic stem cell niche: identification by label-retaining cell assay. *Hepatology* 47: 1994-2002

153. Kordes C, Häussinger D. 2013. Hepatic stem cell niches. *J Clin Invest* 123: 1874-80

154. Sicklick JK, Li YX, Melhem A, Schmelzer E, Zdanowicz M, Huang J, Caballero M, Fair JH, Ludlow JW, McClelland RE, Reid LM, Diehl AM. 2006. Hedgehog signaling maintains resident hepatic progenitors throughout life. *Am J Physiol Gastrointest Liver Physiol* 290: G859-70

155. Español-Suñer R, Carpentier R, Van Hul N, Legry V, Achouri Y, Cordi S, Jacquemin P, Lemaigre F, Leclercq IA. 2012. Liver progenitor cells yield functional hepatocytes in response to chronic liver injury in mice. *Gastroenterology* 143: 1564-75.e7

156. Clayton E, Forbes SJ. 2009. The isolation and in vitro expansion of hepatic Sca-1 progenitor cells. *Biochem Biophys Res Commun* 381: 549-53

157. Lorenzini S, Bird TG, Boulter L, Bellamy C, Samuel K, Aucott R, Clayton E, Andreone P, Bernardi M, Golding M, Alison MR, Iredale JP, Forbes SJ. 2010. Characterisation of a stereotypical cellular and extracellular adult liver progenitor cell niche in rodents and diseased human liver. *Gut* 59: 645-54

158. Van Hul NK, Abarca-Quinones J, Sempoux C, Horsmans Y, Leclercq IA. 2009. Relation between liver progenitor cell expansion and extracellular matrix deposition in a CDE-induced murine model of chronic liver injury. *Hepatology* 49: 1625-35

159. Factor VM, Radaeva SA, Thorgeirsson SS. 1994. Origin and fate of oval cells in dipin-induced hepatocarcinogenesis in the mouse. *Am J Pathol* 145: 409-22

160. FARBER E. 1956. Similarities in the sequence of early histological changes induced in the liver of the rat by ethionine, 2-acetylamino-fluorene, and 3'-methyl-4-dimethylaminoazobenzene. *Cancer Res* 16: 142-8

161. Dempo K, Chisaka N, Yoshida Y, Kaneko A, Onoé T. 1975. Immunofluorescent study on alpha-fetoprotein-producing cells in the early stage of 3'-methyl-4-dimethylaminoazobenzene carcinogenesis. *Cancer Res* 35: 1282-7

162. Inaoka Y. 1967. Significance of the so-called oval cell proliferation during azo-dye hepatocarcinogenesis. *Gan* 58: 355-66

163. Ogawa K, Minase T, Onhoe T. 1974. Demonstration of glucose 6-phosphatase activity in the oval cells of rat liver and the significance of the oval cells in azo dye carcinogenesis. *Cancer Res* 34: 3379-86

164. RUBIN E. 1964. THE ORIGIN AND FATE OF PROLIFERATED BILE DUCTULAR CELLS. *Exp Mol Pathol* 3: 279-86

165. GRISHAM JW, PORTA EA. 1964. ORIGIN AND FATE OF PROLIFERATED HEPATIC DUCTAL CELLS IN THE RAT: ELECTRON MICROSCOPIC AND AUTORADIOGRAPHIC STUDIES. *Exp Mol Pathol* 3: 242-61

166. Tatematsu M, Ho RH, Kaku T, Ekem JK, Farber E. 1984. Studies on the proliferation and fate of oval cells in the liver of rats treated with 2-acetylaminofluorene and partial hepatectomy. *Am J Pathol* 114: 418-30

167. SOLT D, FARBER E. 1976. New principle for the analysis of chemical carcinogenesis. *Nature* 263: 703

168. Petersen BE, Zajac VF, Michalopoulos GK. 1997. Bile ductular damage induced by methylene dianiline inhibits oval cell activation. *Am J Pathol* 151: 905-9

169. Evarts RP, Nagy P, Marsden E, Thorgeirsson SS. 1987. A precursor-product relationship exists between oval cells and hepatocytes in rat liver. *Carcinogenesis* 8: 1737-40

170. Evarts RP, Nagy P, Nakatsukasa H, Marsden E, Thorgeirsson SS. 1989. In vivo differentiation of rat liver oval cells into hepatocytes. *Cancer Res* 49: 1541-7

171. Alison M, Golding M, Lalani EN, Nagy P, Thorgeirsson S, Sarraf C. 1997. Wholesale hepatocytic differentiation in the rat from ductular oval cells, the progeny of biliary stem cells. *J Hepatol* 26: 343-52

172. Copeland DH, Salmon WD. 1946. The Occurrence of Neoplasms in the Liver, Lungs, and Other Tissues of Rats as a Result of Prolonged Choline Deficiency. *Am J Pathol* 22: 1059-79

173. Newberne PM, Camargo JL, Clark AJ. 1982. Choline Deficiency, Partial Hepatectomy, and Liver Tumors in Rats and Mice. *Toxicol Pathol* 10: 95-106

174. Alix JH. 1982. Molecular aspects of the in vivo and in vitro effects of ethionine, an analog of methionine. *Microbiol Rev* 46: 281-95

175. Shinozuka H, Lombardi B, Sell S, Iammarino RM. 1978. Early histological and functional alterations of ethionine liver carcinogenesis in rats fed a choline-deficient diet. *Cancer Res* 38: 1092-8

176. Akhurst B, Croager EJ, Farley-Roche CA, Ong JK, Dumble ML, Knight B, Yeoh GC. 2001. A modified choline-deficient, ethionine-supplemented diet protocol effectively induces oval cells in mouse liver. *Hepatology* 34: 519-22

177. Pradhan-Sundd T, Vats R, Russell JM, Singh S, Michael AA, Molina L, Kakar S, Cornuet P, Poddar M, Watkins SC, Nejak-Bowen KN, Monga SP, Sundd P. 2018. Dysregulated bile transporters and impaired tight junctions during chronic liver injury in mice. *Gastroenterology*

178. Knight B, Matthews VB, Akhurst B, Croager EJ, Klinken E, Abraham LJ, Olynyk JK, Yeoh G. 2005. Liver inflammation and cytokine production, but not acute phase protein synthesis, accompany the adult liver progenitor (oval) cell response to chronic liver injury. *Immunol Cell Biol* 83: 364-74

179. Knight B, Akhurst B, Matthews VB, Ruddell RG, Ramm GA, Abraham LJ, Olynyk JK, Yeoh GC. 2007. Attenuated liver progenitor (oval) cell and fibrogenic responses to the choline deficient, ethionine supplemented diet in the BALB/c inbred strain of mice. *J Hepatol* 46: 134-41

180. Strick-Marchand H, Masse GX, Weiss MC, Di Santo JP. 2008. Lymphocytes support oval cell-dependent liver regeneration. *J Immunol* 181: 2764-71

181. Bird TG, Lu WY, Boulter L, Gordon-Keylock S, Ridgway RA, Williams MJ, Taube J, Thomas JA, Wojtacha D, Gambardella A, Sansom OJ, Iredale JP, Forbes SJ. 2013. Bone marrow injection stimulates hepatic ductular reactions in the absence of injury via macrophage-mediated TWEAK signaling. *Proc Natl Acad Sci U S A* 110: 6542-7

182. Karaca G, Swiderska-Syn M, Xie G, Syn WK, Krüger L, Machado MV, Garman K, Choi SS, Michelotti GA, Burkly LC, Ochoa B, Diehl AM. 2014. TWEAK/Fn14 signaling is required for liver regeneration after partial hepatectomy in mice. *PLoS One* 9: e83987

183. Carpentier R, Suñer RE, van Hul N, Kopp JL, Beaudry JB, Cordi S, Antoniou A, Raynaud P, Lepreux S, Jacquemin P, Leclercq IA, Sander M, Lemaigre FP. 2011. Embryonic ductal plate cells give rise to cholangiocytes, periportal hepatocytes, and adult liver progenitor cells. *Gastroenterology* 141: 1432-8, 8.e1-4

184. Shin S, Upadhyay N, Greenbaum LE, Kaestner KH. 2015. Ablation of Foxl1-Cre-labeled hepatic progenitor cells and their descendants impairs recovery of mice from liver injury. *Gastroenterology* 148: 192-202.e3

185. Rodrigo-Torres D, Affò S, Coll M, Morales-Ibanez O, Millán C, Blaya D, Alvarez-Guaita A, Rentero C, Lozano JJ, Maestro MA, Solar M, Arroyo V, Caballería J, van Grunsven LA, Enrich C, Ginès P, Bataller R, Sancho-Bru P. 2014. The biliary epithelium gives rise to liver progenitor cells. *Hepatology* 60: 1367-77

186. Yanger K, Knigin D, Zong Y, Maggs L, Gu G, Akiyama H, Pikarsky E, Stanger BZ. 2014. Adult hepatocytes are generated by self-duplication rather than stem cell differentiation. *Cell Stem Cell* 15: 340-9

187. Raven A, Lu WY, Man TY, Ferreira-Gonzalez S, O'Duibhir E, Dwyer BJ, Thomson JP, Meehan RR, Bogorad R, Koteliansky V, Kotelevtsev Y, Ffrench-Constant C, Boulter L, Forbes SJ. 2017. Cholangiocytes act as facultative liver stem cells during impaired hepatocyte regeneration. *Nature*

188. Russell JO, Lu WY, Okabe H, Abrams M, Oertel M, Poddar M, Singh S, Forbes SJ, Monga SP. 2018. Hepatocyte-specific β-catenin deletion during severe liver injury provokes cholangiocytes to differentiate into hepatocytes. *Hepatology*

189. Malato Y, Naqvi S, Schürmann N, Ng R, Wang B, Zape J, Kay MA, Grimm D, Willenbring H. 2011. Fate tracing of mature hepatocytes in mouse liver homeostasis and regeneration. *J Clin Invest* 121: 4850-60

190. Schaub JR, Malato Y, Gormond C, Willenbring H. 2014. Evidence against a Stem Cell Origin of New Hepatocytes in a Common Mouse Model of Chronic Liver Injury. *Cell Rep* 8: 933-9

191. Lu WY, Bird TG, Boulter L, Tsuchiya A, Cole AM, Hay T, Guest RV, Wojtacha D, Man TY, Mackinnon A, Ridgway RA, Kendall T, Williams MJ, Jamieson T, Raven A, Hay DC, Iredale JP, Clarke AR, Sansom OJ, Forbes SJ. 2015. Hepatic progenitor cells of biliary origin with liver repopulation capacity. *Nat Cell Biol* 17: 971-83

192. Fickert P, Stöger U, Fuchsbichler A, Moustafa T, Marschall HU, Weiglein AH, Tsybrovskyy O, Jaeschke H, Zatloukal K, Denk H, Trauner M. 2007. A new xenobiotic-induced mouse model of sclerosing cholangitis and biliary fibrosis. *Am J Pathol* 171: 525-36

193. Yanger K, Zong Y, Maggs LR, Shapira SN, Maddipati R, Aiello NM, Thung SN, Wells RG, Greenbaum LE, Stanger BZ. 2013. Robust cellular reprogramming occurs spontaneously during liver regeneration. *Genes Dev* 27: 719-24

194. Huch M, Dorrell C, Boj SF, van Es JH, Li VS, van de Wetering M, Sato T, Hamer K, Sasaki N, Finegold MJ, Haft A, Vries RG, Grompe M, Clevers H. 2013. In vitro expansion of single Lgr5+ liver stem cells induced by Wnt-driven regeneration. *Nature* 494: 247-50

195. Deng X, Zhang X, Li W, Feng RX, Li L, Yi GR, Zhang XN, Yin C, Yu HY, Zhang JP, Lu B, Hui L, Xie WF. 2018. Chronic Liver Injury Induces Conversion of Biliary Epithelial Cells into Hepatocytes. *Cell Stem Cell* 23: 114-22.e3

196. Aoki R, Chiba T, Miyagi S, Negishi M, Konuma T, Taniguchi H, Ogawa M, Yokosuka O, Iwama A. 2010. The polycomb group gene product Ezh2 regulates proliferation and differentiation of murine hepatic stem/progenitor cells. *J Hepatol* 52: 854-63

197. Koike H, Ouchi R, Ueno Y, Nakata S, Obana Y, Sekine K, Zheng YW, Takebe T, Isono K, Koseki H, Taniguchi H. 2014. Polycomb group protein Ezh2 regulates hepatic progenitor cell proliferation and differentiation in murine embryonic liver. *PLoS One* 9: e104776

198. Jalan-Sakrikar N, De Assuncao TM, Lu J, Almada LL, Lomberk G, Fernandez-Zapico ME, Urrutia R, Huebert RC. 2016. Hedgehog Signaling Overcomes an EZH2-Dependent Epigenetic Barrier to Promote Cholangiocyte Expansion. *PLoS One* 11: e0168266

199. Hunter AL, Holscher MA, Neal RA. 1977. Thioacetamide-induced hepatic necrosis. I. Involvement of the mixed-function oxidase enzyme system. *J Pharmacol Exp Ther* 200: 439-48

200. Müller A, Machnik F, Zimmermann T, Schubert H. 1988. Thioacetamide-induced cirrhosis-like liver lesions in rats--usefulness and reliability of this animal model. *Exp Pathol* 34: 229-36

201. Gracz AD, Fuller MK, Wang F, Li L, Stelzner M, Dunn JC, Martin MG, Magness ST. 2013. Brief report: CD24 and CD44 mark human intestinal epithelial cell populations with characteristics of active and facultative stem cells. *Stem Cells* 31: 2024-30

202. Michalopoulos GK, Bowen WC, Mulè K, Lopez-Talavera JC, Mars W. 2002. Hepatocytes undergo phenotypic transformation to biliary epithelium in organoid cultures. *Hepatology* 36: 278-83

203. Tag CG, Sauer-Lehnen S, Weiskirchen S, Borkham-Kamphorst E, Tolba RH, Tacke F, Weiskirchen R. 2015. Bile duct ligation in mice: induction of inflammatory liver injury and fibrosis by obstructive cholestasis. *J Vis Exp*

204. Michalopoulos GK, Barua L, Bowen WC. 2005. Transdifferentiation of rat hepatocytes into biliary cells after bile duct ligation and toxic biliary injury. *Hepatology* 41: 535-44

205. Yovchev MI, Locker J, Oertel M. 2016. Biliary fibrosis drives liver repopulation and phenotype transition of transplanted hepatocytes. *J Hepatol* 64: 1348-57

206. Tanimizu N, Nishikawa Y, Ichinohe N, Akiyama H, Mitaka T. 2014. Sry HMG box protein 9-positive (Sox9+) epithelial cell adhesion molecule-negative (EpCAM-) biphenotypic cells derived from hepatocytes are involved in mouse liver regeneration. *J Biol Chem* 289: 7589-98

207. Nagahama Y, Sone M, Chen X, Okada Y, Yamamoto M, Xin B, Matsuo Y, Komatsu M, Suzuki A, Enomoto K, Nishikawa Y. 2014. Contributions of hepatocytes and bile ductular cells in ductular reactions and remodeling of the biliary system after chronic liver injury. *Am J Pathol* 184: 3001-12

208. Lin S, Nascimento EM, Gajera CR, Chen L, Neuhöfer P, Garbuzov A, Wang S, Artandi SE. 2018. Distributed hepatocytes expressing telomerase repopulate the liver in homeostasis and injury. *Nature* 556: 244-8

209. Sekiya S, Suzuki A. 2014. Hepatocytes, rather than cholangiocytes, can be the major source of primitive ductules in the chronically injured mouse liver. *Am J Pathol* 184: 1468-78

210. Boulter L, Govaere O, Bird TG, Radulescu S, Ramachandran P, Pellicoro A, Ridgway RA, Seo SS, Spee B, Van Rooijen N, Sansom OJ, Iredale JP, Lowell S, Roskams T, Forbes SJ. 2012. Macrophage-derived Wnt opposes Notch signaling to specify hepatic progenitor cell fate in chronic liver disease. *Nat Med* 18: 572-9

211. Yimlamai D, Christodoulou C, Galli GG, Yanger K, Pepe-Mooney B, Gurung B, Shrestha K, Cahan P, Stanger BZ, Camargo FD. 2014. Hippo pathway activity influences liver cell fate. *Cell* 157: 1324-38

212. Font-Burgada J, Shalapour S, Ramaswamy S, Hsueh B, Rossell D, Umemura A, Taniguchi K, Nakagawa H, Valasek MA, Ye L, Kopp JL, Sander M, Carter H, Deisseroth K, Verma IM, Karin M. 2015. Hybrid Periportal Hepatocytes Regenerate the Injured Liver without Giving Rise to Cancer. *Cell* 162: 766-79

213. Okabe H, Yang J, Sylakowski K, Yovchev M, Miyagawa Y, Nagarajan S, Chikina M, Thompson M, Oertel M, Baba H, Monga SP, Nejak-Bowen KN. 2016. Wnt signaling regulates hepatobiliary repair following cholestatic liver injury in mice. *Hepatology* 64: 1652-66

214. Tarlow BD, Pelz C, Naugler WE, Wakefield L, Wilson EM, Finegold MJ, Grompe M. 2014. Bipotential adult liver progenitors are derived from chronically injured mature hepatocytes. *Cell Stem Cell* 15: 605-18

215. Schaub JR, Huppert KA, Kurial SNT, Hsu BY, Cast AE, Donnelly B, Karns RA, Chen F, Rezvani M, Luu HY, Mattis AN, Rougemont AL, Rosenthal P, Huppert SS, Willenbring H. 2018. De novo formation of the biliary system by TGFβ-mediated hepatocyte transdifferentiation. *Nature* 557: 247-51

216. Russell JO, Ko S, Saggi HS, Singh S, Poddar M, Shin D, Monga SP. 2018. Bromodomain and Extraterminal (BET) Proteins Regulate Hepatocyte Proliferation in Hepatocyte-Driven Liver Regeneration. *Am J Pathol* 188: 1389-405

217. Michalopoulos GK, Khan Z. 2015. Liver Stem Cells: Experimental Findings and Implications for Human Liver Disease. *Gastroenterology* 149: 876-82

218. Duncan AW, Dorrell C, Grompe M. 2009. Stem cells and liver regeneration. *Gastroenterology* 137: 466-81

219. Kochanek KD, Murphy SL, Xu J, Tejada-Vera B. 2016. Deaths: Final Data for 2014. *Natl Vital Stat Rep* 65: 1-122

220. Mittal S, El-Serag HB. 2013. Epidemiology of hepatocellular carcinoma: consider the population. *J Clin Gastroenterol* 47 Suppl: S2-6

221. Njei B, Rotman Y, Ditah I, Lim JK. 2015. Emerging trends in hepatocellular carcinoma incidence and mortality. *Hepatology* 61: 191-9

222. Pellicoro A, Ramachandran P, Iredale JP, Fallowfield JA. 2014. Liver fibrosis and repair: immune regulation of wound healing in a solid organ. *Nat Rev Immunol* 14: 181-94

223. Luedde T, Kaplowitz N, Schwabe RF. 2014. Cell death and cell death responses in liver disease: mechanisms and clinical relevance. *Gastroenterology* 147: 765-83.e4

224. Lockwood WW, Zejnullahu K, Bradner JE, Varmus H. 2012. Sensitivity of human lung adenocarcinoma cell lines to targeted inhibition of BET epigenetic signaling proteins. *Proc Natl Acad Sci U S A* 109: 19408-13

225. Zhang P, Dong Z, Cai J, Zhang C, Shen Z, Ke A, Gao D, Fan J, Shi G. 2015. BRD4 promotes tumor growth and epithelial-mesenchymal transition in hepatocellular carcinoma. *Int J Immunopathol Pharmacol* 28: 36-44

226. Li GQ, Guo WZ, Zhang Y, Seng JJ, Zhang HP, Ma XX, Zhang G, Li J, Yan B, Tang HW, Li SS, Wang LD, Zhang SJ. 2016. Suppression of BRD4 inhibits human hepatocellular carcinoma by repressing MYC and enhancing BIM expression. *Oncotarget* 7: 2462-74

227. Ko S, Choi TY, Russell JO, So J, Monga SP, Shin D. 2016. Bromodomain and extraterminal (BET) proteins regulate biliary-driven liver regeneration. *J Hepatol* 64: 316-25

228. Ye H, Holterman AX, Yoo KW, Franks RR, Costa RH. 1999. Premature expression of the winged helix transcription factor HFH-11B in regenerating mouse liver accelerates hepatocyte entry into S phase. *Mol Cell Biol* 19: 8570-80

229. Tan XP, Behari J, Cieply B, Michalopoulos GK, Monga SPS. 2006. Conditional deletion of beta-catenin reveals its role in liver growth and regeneration. *Gastroenterology* 131: 1561-72

230. Du Q, Zhang X, Cardinal J, Cao Z, Guo Z, Shao L, Geller DA. 2009. Wnt/beta-catenin signaling regulates cytokine-induced human inducible nitric oxide synthase expression by inhibiting nuclear factor-kappaB activation in cancer cells. *Cancer Res* 69: 3764-71

231. Westerfield M. 2007. The Zebrafish Book. A Guide for the Laboratory Use of Zebrafish (Danio rerio), 5th Edition. *University of Oregon Press, Eugene (Book)*

232. Choi TY, Ninov N, Stainier DY, Shin D. 2014. Extensive conversion of hepatic biliary epithelial cells to hepatocytes after near total loss of hepatocytes in zebrafish. *Gastroenterology* 146: 776-88

233. Ninov N, Borius M, Stainier DYR. 2012. Different levels of Notch signaling regulate quiescence, renewal and differentiation in pancreatic endocrine progenitors. *Development* 139: 1557-67

234. Shimizu N, Kawakami K, Ishitani T. 2012. Visualization and exploration of Tcf/Lef function using a highly responsive Wnt/beta-catenin signaling-reporter transgenic zebrafish. *Developmental Biology* 370: 71-85

235. McCloy RA, Rogers S, Caldon CE, Lorca T, Castro A, Burgess A. 2014. Partial inhibition of Cdk1 in G 2 phase overrides the SAC and decouples mitotic events. *Cell Cycle* 13: 1400-12

236. Choi TY, Khaliq M, Ko S, So J, Shin D. 2015. Hepatocyte-specific ablation in zebrafish to study biliary-driven liver regeneration. *J Vis Exp*: e52785

237. de Groh ED, Swanhart LM, Cosentino CC, Jackson RL, Dai W, Kitchens CA, Day BW, Smithgall TE, Hukriede NA. 2010. Inhibition of histone deacetylase expands the renal progenitor cell population. *J Am Soc Nephrol* 21: 794-802

238. Weglarz TC, Sandgren EP. 2000. Timing of hepatocyte entry into DNA synthesis after partial hepatectomy is cell autonomous. *Proc Natl Acad Sci U S A* 97: 12595-600

239. Taub R. 2004. Liver regeneration: from myth to mechanism. *Nat Rev Mol Cell Biol* 5: 836-47

240. Hall PA, Levison DA, Woods AL, Yu CC, Kellock DB, Watkins JA, Barnes DM, Gillett CE, Camplejohn R, Dover R. 1990. Proliferating cell nuclear antigen (PCNA) immunolocalization in paraffin sections: an index of cell proliferation with evidence of deregulated expression in some neoplasms. *J Pathol* 162: 285-94

241. Albrecht JH, Hu MY, Cerra FB. 1995. Distinct patterns of cyclin D1 regulation in models of liver regeneration and human liver. *Biochem Biophys Res Commun* 209: 648-55

242. Núñez KG, Gonzalez-Rosario J, Thevenot PT, Cohen AJ. 2017. Cyclin D1 in the Liver: Role of Noncanonical Signaling in Liver Steatosis and Hormone Regulation. *Ochsner J* 17: 56-65

243. Shtutman M, Zhurinsky J, Simcha I, Albanese C, D'Amico M, Pestell R, Ben-Ze'ev A. 1999. The cyclin D1 gene is a target of the beta-catenin/LEF-1 pathway. *Proc Natl Acad Sci U S A* 96: 5522-7

244. Tetsu O, McCormick F. 1999. Beta-catenin regulates expression of cyclin D1 in colon carcinoma cells. *Nature* 398: 422-6

245. Nejak-Bowen KN, Zeng G, Tan X, Cieply B, Monga SP. 2009. Beta-catenin regulates vitamin C biosynthesis and cell survival in murine liver. *J Biol Chem* 284: 28115-27

246. Ovejero C, Cavard C, Périanin A, Hakvoort T, Vermeulen J, Godard C, Fabre M, Chafey P, Suzuki K, Romagnolo B, Yamagoe S, Perret C. 2004. Identification of the leukocyte cell-derived chemotaxin 2 as a direct target gene of beta-catenin in the liver. *Hepatology* 40: 167-76

247. Albrecht JH, Poon RY, Ahonen CL, Rieland BM, Deng C, Crary GS. 1998. Involvement of p21 and p27 in the regulation of CDK activity and cell cycle progression in the regenerating liver. *Oncogene* 16: 2141-50

248. Rickheim DG, Nelsen CJ, Fassett JT, Timchenko NA, Hansen LK, Albrecht JH. 2002. Differential regulation of cyclins D1 and D3 in hepatocyte proliferation. *Hepatology* 36: 30-8

249. Delgado I, Fresnedo O, Iglesias A, Rueda Y, Syn WK, Zubiaga AM, Ochoa B. 2011. A role for transcription factor E2F2 in hepatocyte proliferation and timely liver regeneration. *Am J Physiol Gastrointest Liver Physiol* 301: G20-31

250. Hong SH, Eun JW, Choi SK, Shen Q, Choi WS, Han JW, Nam SW, You JS. 2016. Epigenetic reader BRD4 inhibition as a therapeutic strategy to suppress E2F2-cell cycle regulation circuit in liver cancer. *Oncotarget* 7: 32628-40

251. Timmers C, Sharma N, Opavsky R, Maiti B, Wu L, Wu J, Orringer D, Trikha P, Saavedra HI, Leone G. 2007. E2f1, E2f2, and E2f3 control E2F target expression and cellular proliferation via a p53-dependent negative feedback loop. *Mol Cell Biol* 27: 65-78

252. Cressman DE, Greenbaum LE, Haber BA, Taub R. 1994. Rapid activation of post-hepatectomy factor/nuclear factor kappa B in hepatocytes, a primary response in the regenerating liver. *J Biol Chem* 269: 30429-35

253. FitzGerald MJ, Webber EM, Donovan JR, Fausto N. 1995. Rapid DNA binding by nuclear factor kappa B in hepatocytes at the start of liver regeneration. *Cell Growth Differ* 6: 417-27

254. North TE, Babu IR, Vedder LM, Lord AM, Wishnok JS, Tannenbaum SR, Zon LI, Goessling W. 2010. PGE2-regulated wnt signaling and N-acetylcysteine are synergistically hepatoprotective in zebrafish acetaminophen injury. *Proc Natl Acad Sci U S A* 107: 17315-20

255. Cox AG, Saunders DC, Kelsey PB, Jr., Conway AA, Tesmenitsky Y, Marchini JF, Brown KK, Stamler JS, Colagiovanni DB, Rosenthal GJ, Croce KJ, North TE, Goessling W. 2014. S-nitrosothiol signaling regulates liver development and improves outcome following toxic liver injury. *Cell Rep* 6: 56-69

256. Jaeschke H, Xie Y, McGill MR. 2014. Acetaminophen-induced Liver Injury: from Animal Models to Humans. *J Clin Transl Hepatol* 2: 153-61

257. He JH, Guo SY, Zhu F, Zhu JJ, Chen YX, Huang CJ, Gao JM, Dong QX, Xuan YX, Li CQ. 2013. A zebrafish phenotypic assay for assessing drug-induced hepatotoxicity. *J Pharmacol Toxicol Methods* 67: 25-32

258. Nourjah P, Ahmad SR, Karwoski C, Willy M. 2006. Estimates of acetaminophen (Paracetomal)-associated overdoses in the United States. *Pharmacoepidemiol Drug Saf* 15: 398-405

259. Lorent K, Moore JC, Siekmann AF, Lawson N, Pack M. 2010. Reiterative use of the notch signal during zebrafish intrahepatic biliary development. *Dev Dyn* 239: 855-64

260. Sugiyama M, Sakaue-Sawano A, Iimura T, Fukami K, Kitaguchi T, Kawakami K, Okamoto H, Higashijima SI, Miyawaki A. 2009. Illuminating cell-cycle progression in the developing zebrafish embryo. *Proc Natl Acad Sci U S A* 106: 20812-7

261. Nicodeme E, Jeffrey KL, Schaefer U, Beinke S, Dewell S, Chung CW, Chandwani R, Marazzi I, Wilson P, Coste H, White J, Kirilovsky J, Rice CM, Lora JM, Prinjha RK, Lee K, Tarakhovsky A. 2010. Suppression of inflammation by a synthetic histone mimic. *Nature* 468: 1119-23

262. Xu Y, Vakoc CR. 2014. Brd4 is on the move during inflammation. *Trends Cell Biol* 24: 615-6

263. Chu J, Sadler KC. 2009. New school in liver development: lessons from zebrafish. *Hepatology* 50: 1656-63

264. Tao J, Calvisi DF, Ranganathan S, Cigliano A, Zhou L, Singh S, Jiang L, Fan B, Terracciano L, Armeanu-Ebinger S, Ribback S, Dombrowski F, Evert M, Chen X, Monga SP. 2014. Activation of β-catenin and Yap1 in human hepatoblastoma and induction of hepatocarcinogenesis in mice. *Gastroenterology* 147: 690-701

265. Tao J, Xu E, Zhao Y, Singh S, Li X, Couchy G, Chen X, Zucman-Rossi J, Chikina M, Monga SP. 2016. Modeling a human hepatocellular carcinoma subset in mice through coexpression of met and point-mutant β-catenin. *Hepatology* 64: 1587-605

266. Tao J, Zhang R, Singh S, Poddar M, Xu E, Oertel M, Chen X, Ganesh S, Abrams M, Monga SP. 2016. Targeting β-catenin in hepatocellular cancers induced by coexpression of mutant β-catenin and K-Ras in mice. *Hepatology*

267. Delgado E, Okabe H, Preziosi M, Russell JO, Alvarado TF, Oertel M, Nejak-Bowen KN, Zhang Y, Monga SP. 2015. Complete response of Ctnnb1-mutated tumours to β-catenin suppression by locked nucleic acid antisense in a mouse hepatocarcinogenesis model. *J Hepatol* 62: 380-7

268. Tögel L, Nightingale R, Chueh AC, Jayachandran A, Tran H, Phesse T, Wu R, Sieber OM, Arango D, Dhillon AS, Dawson MA, Diez-Dacal B, Gahman TC, Filippakopoulos P, Shiau AK, Mariadason JM. 2016. Dual Targeting of Bromodomain and Extraterminal Domain Proteins, and WNT or MAPK Signaling, Inhibits c-MYC Expression and Proliferation of Colorectal Cancer Cells. *Mol Cancer Ther* 15: 1217-26

269. Whyte WA, Orlando DA, Hnisz D, Abraham BJ, Lin CY, Kagey MH, Rahl PB, Lee TI, Young RA. 2013. Master transcription factors and mediator establish super-enhancers at key cell identity genes. *Cell* 153: 307-19

270. Parker SC, Stitzel ML, Taylor DL, Orozco JM, Erdos MR, Akiyama JA, van Bueren KL, Chines PS, Narisu N, Black BL, Visel A, Pennacchio LA, Collins FS, Program NCS, Authors NIoHISCCSP, Authors NCSP. 2013. Chromatin stretch enhancer states drive cell-specific gene regulation and harbor human disease risk variants. *Proc Natl Acad Sci U S A* 110: 17921-6

271. Hnisz D, Abraham BJ, Lee TI, Lau A, Saint-André V, Sigova AA, Hoke HA, Young RA. 2013. Super-enhancers in the control of cell identity and disease. *Cell* 155: 934-47

272. Hnisz D, Schuijers J, Lin CY, Weintraub AS, Abraham BJ, Lee TI, Bradner JE, Young RA. 2015. Convergence of developmental and oncogenic signaling pathways at transcriptional super-enhancers. *Mol Cell* 58: 362-70

273. Kennedy AL, Vallurupalli M, Chen L, Crompton B, Cowley G, Vazquez F, Weir BA, Tsherniak A, Parasuraman S, Kim S, Alexe G, Stegmaier K. 2015. Functional, chemical genomic, and super-enhancer screening identify sensitivity to cyclin D1/CDK4 pathway inhibition in Ewing sarcoma. *Oncotarget* 6: 30178-93

274. Kim WR, Lake JR, Smith JM, Skeans MA, Schladt DP, Edwards EB, Harper AM, Wainright JL, Snyder JJ, Israni AK, Kasiske BL. 2017. OPTN/SRTR 2015 Annual Data Report: Liver. *Am J Transplant* 17 Suppl 1: 174-251

275. Carpino G, Renzi A, Onori P, Gaudio E. 2013. Role of hepatic progenitor cells in nonalcoholic fatty liver disease development: cellular cross-talks and molecular networks. *Int J Mol Sci* 14: 20112-30

276. Zhang L, Theise N, Chua M, Reid LM. 2008. The stem cell niche of human livers: symmetry between development and regeneration. *Hepatology* 48: 1598-607

277. Libbrecht L, Roskams T. 2002. Hepatic progenitor cells in human liver diseases. *Semin Cell Dev Biol* 13: 389-96

278. Yanger K, Knigin D, Zong Y, Maggs L, Gu G, Akiyama H, Pikarsky E, Stanger BZ. 2014. Adult Hepatocytes Are Generated by Self-Duplication Rather than Stem Cell Differentiation. *Cell Stem Cell*

279. Monga SP. 2015. β-Catenin Signaling and Roles in Liver Homeostasis, Injury, and Tumorigenesis. *Gastroenterology* 148: 1294-310

280. Nair JK, Willoughby JL, Chan A, Charisse K, Alam MR, Wang Q, Hoekstra M, Kandasamy P, Kel'in AV, Milstein S, Taneja N, O'Shea J, Shaikh S, Zhang L, van der Sluis RJ, Jung ME, Akinc A, Hutabarat R, Kuchimanchi S, Fitzgerald K, Zimmermann T, van Berkel TJ, Maier MA, Rajeev KG, Manoharan M. 2014. Multivalent N-acetylgalactosamine-conjugated siRNA localizes in hepatocytes and elicits robust RNAi-mediated gene silencing. *J Am Chem Soc* 136: 16958-61

281. Soriano P. 1999. Generalized lacZ expression with the ROSA26 Cre reporter strain. *Nat Genet* 21: 70-1

282. Zincarelli C, Soltys S, Rengo G, Rabinowitz JE. 2008. Analysis of AAV serotypes 1-9 mediated gene expression and tropism in mice after systemic injection. *Mol Ther* 16: 1073-80

283. Cadoret A, Ovejero C, Terris B, Souil E, Lévy L, Lamers WH, Kitajewski J, Kahn A, Perret C. 2002. New targets of beta-catenin signaling in the liver are involved in the glutamine metabolism. *Oncogene* 21: 8293-301

284. Wang EY, Yeh SH, Tsai TF, Huang HP, Jeng YM, Lin WH, Chen WC, Yeh KH, Chen PJ, Chen DS. 2011. Depletion of β-catenin from mature hepatocytes of mice promotes expansion of hepatic progenitor cells and tumor development. *Proc Natl Acad Sci U S A* 108: 18384-9

285. Fabris L, Spirli C, Cadamuro M, Fiorotto R, Strazzabosco M. 2017. Emerging concepts in biliary repair and fibrosis. *Am J Physiol Gastrointest Liver Physiol* 313: G102-G16

286. Xu J, Murphy SL, Kochanek KD, Bastian BA. 2016. Deaths: Final Data for 2013. *Natl Vital Stat Rep* 64: 1-119

287. Blachier M, Leleu H, Peck-Radosavljevic M, Valla DC, Roudot-Thoraval F. 2013. The burden of liver disease in Europe: a review of available epidemiological data. *J Hepatol* 58: 593-608

288. Younossi ZM, Stepanova M, Afendy M, Fang Y, Younossi Y, Mir H, Srishord M. 2011. Changes in the prevalence of the most common causes of chronic liver diseases in the United States from 1988 to 2008. *Clin Gastroenterol Hepatol* 9: 524-30.e1; quiz e60

289. Schuppan D, Schattenberg JM. 2013. Non-alcoholic steatohepatitis: pathogenesis and novel therapeutic approaches. *J Gastroenterol Hepatol* 28 Suppl 1: 68-76

290. Bataller R, Brenner DA. 2005. Liver fibrosis. *J Clin Invest* 115: 209-18

291. Kim WR, Lake JR, Smith JM, Skeans MA, Schladt DP, Edwards EB, Harper AM, Wainright JL, Snyder JJ, Israni AK, Kasiske BL. 2015. OPTN/SRTR 2013 Annual Data Report: liver. *Am J Transplant* 15 Suppl 2: 1-28

292. Demetris AJ, Seaberg EC, Wennerberg A, Ionellie J, Michalopoulos G. 1996. Ductular reaction after submassive necrosis in humans. Special emphasis on analysis of ductular hepatocytes. *Am J Pathol* 149: 439-48

293. Nejak-Bowen K, Monga SP. 2008. Wnt/beta-catenin signaling in hepatic organogenesis. *Organogenesis* 4: 92-9

294. Haegel H, Larue L, Ohsugi M, Fedorov L, Herrenknecht K, Kemler R. 1995. Lack of beta-catenin affects mouse development at gastrulation. *Development* 121: 3529-37

295. Cheng JH, She H, Han YP, Wang J, Xiong S, Asahina K, Tsukamoto H. 2008. Wnt antagonism inhibits hepatic stellate cell activation and liver fibrosis. *Am J Physiol Gastrointest Liver Physiol* 294: G39-49

296. Ge WS, Wang YJ, Wu JX, Fan JG, Chen YW, Zhu L. 2014. β-catenin is overexpressed in hepatic fibrosis and blockage of Wnt/β-catenin signaling inhibits hepatic stellate cell activation. *Mol Med Rep* 9: 2145-51

297. Lin Y, Fang ZP, Liu HJ, Wang LJ, Cheng Z, Tang N, Li T, Liu T, Han HX, Cao G, Liang L, Ding YQ, Zhou WJ. 2017. HGF/R-spondin1 rescues liver dysfunction through the induction of Lgr5. *Nat Commun* 8: 1175

298. Xu J, Tan Y, Shao X, Zhang C, He Y, Wang J, Xi Y. 2018. Evaluation of NCAM and c-Kit as hepatic progenitor cell markers for intrahepatic cholangiocarcinomas. *Pathol Res Pract* 214: 2011-7